The Pennsylvania State University

The Graduate School

Department of Chemistry

HYDROPHOBIC AND HYDROPHILIC CONTROL IN POLYPHOSPHAZENE MATERIALS

A Thesis in

Chemistry

by

Lee Brent Steely

Submitted in Partial Fulfillment
of the Requirements
for the Degree of

Doctor of Philosophy

August 2007

The thesis of Lee Brent Steely was reviewed and approved* by the following:

Harry R. Allcock
Evan Pugh Professor of Chemistry
Thesis Advisor
Chair of Committee

Alan J. Benesi
Senior Lecturer in Chemistry

James P. Runt
Professor of Polymer Science

Mary Beth Williams
Associate Professor of Chemistry

Ayusman Sen
Professor of Chemistry
Head of the Department of Chemistry

*Signatures are on file in the Graduate School

ABSTRACT

This thesis is the culmination of several recent studies focused on the surface characterization of polyphosphazenes specifically the properties of water repellency or hydrophobicity. Chapter 1 is a background account of polyphosphazene chemistry and the hydrophobicity of polyphosphazenes.

Chapter 2 provides an examination of the role of surface morphology on hydrophobicity. This study deals in depth with the electrospinning of poly[bis(2,2,2-trifluoroethoxy)phosphazene] in tetrahydrofuran. This process yields fiber mats or bead and fiber mats which exhibit roughness in continuous contact with the water droplet (fiber mats) or discontinuous contact (bead and fiber mats). These surface roughness types are compared to spun cast films using water contact angles to measure the air-water-polymer interface.

The influence of aromatic moieties and fluorine content on the air-water-polymer interface is examined in Chapter 3. This study examines the influence of fluorine content and aryloxy groups on the hydrophobicity of a polyphosphazene surface via static water contact angle measurements on a goniometer. Polymer surfaces of spun cast and electrospun mats were probed with advancing, receeding, and static water contact angle and dip coated slides of the same materials were also examined with a Langmuir-Blogett trough.

Chapter 4 is a description of the environmental plasma surface treatments of polyphosphazenes as a method of functionalizing solid polymer surfaces. The treatment procedure of functionalizing spun cast and electrospun poly[bis(2,2,2-

trifluoroethoxy)phosphazene] surfaces with plasma gases of oxygen, nitrogen, methane, and tetrafluoromethane is detailed. The resulting functionalization of the surface is examined with XPS and water contact angle data.

In Chapter 5 fluoroalkoxy polyphosphazenes were processed with liquid carbon dioxide into foams. The foams were then tested for flame retardance and hydrophobicity.

Appendixes A-C contain studies on moisture sensitive phosphoranimine monomer storage, micelle formation in water from triblock copolymers, and single ion conductive membranes with increased hydrophobicity respectively. Although the appendixes examine polyphosphazene hydrophobic relationships they are not specific to surface hydrophobicity of solids and were not placed in the main text. Appendix A involves the optimization of storage conditions for a phosphoranimine monomer. Conditions examined include room temperature to -80 ºC and dilution with a variety of organic solvents. The micelle formation of A-B-A triblock copolymer of poly[bis(2,2,2-trifluoroethoxy)phosphazene]-poly(propylene-glycol)-poly[bis(2,2,2-trifluoroethoxy)phosphazene] was explored in appendix B. It was determined with light scattering and TEM that hairpin folding of our triblock copolymer allowed micelle formation with the two hydrophobic poly[bis(2,2,2-trifluoroethoxy)phosphazene] blocks facing the hydrophobic core of the micelle. Appendix C details the lithium ion conductivity of poly[norbornene-pendent-cyclotriphosphazene] with sulfonimide and methoxyethoxyethoxy groups attached. These results are then compared with unbound lithium counter ion systems.

TABLE OF CONTENTS

List of Figures…….xi

List of Schemes…….xiv

List of Tables…….xv

Preface……..xvi

Acknowledgements…….xvii

Chapter 1. Introduction……1

A. Synthesis of Polyphosphazenes…….1

B. Enhanced Hydrophobicity Via Surface Modification……2

C. Origins of Hydrophobicity……5

D. Specific Examples of Hydrophobic Polyphosphazenes……7

E. Superhydrophobic Nanofibers……..10

F. Applications of Hydrophobic Polyphosphazenes…….11

G. Advantages of Polyphosphazenes……14

H. References……15

Chapter 2. Poly[bis(2,2,2-trifluoroethoxy)phosphazene] Superhydrophobic Nanofibers…….19

A. Introduction……..19

1. Nanofiber Mats…….19

2. Potential Applications……...20

3. Comparison to Other Superhydrophobic Materials……..……20

B. Results and discussion…….…….23

1. Solvent and Fiber Diameter……..23

2. Formation of Bead Morphology……..……..24

3. Probing the Surface with XPS and WCA…….……26

4. Models of Superhydrophobicity…….……..26

5. Superhydrophobicity of Poly[bis(2,2,2-trifluoroethoxy)phosphazene]……...28

C. Conclusions……..28

D. Experimental……31

1. Reagents ……..31

2. Characterization Equipment……..…31

3. Electrospinning Processing……..……32

4. Synthesis of Poly[bis(2,2,2-trifluoroethoxy)phosphazene]**(3)**…….33

E. References……33

Chapter 3. Hydrophobic Behavior of Aryloxy, Fluoroaryloxy, and Fluoroalkoxy Polyphosphazenes……....36

A. Introduction……..36

B. Results and Discussion…….....38

1. Static Water Contact Angle Data and Fluorine Placement……..……38

2. Dynamic Water Contact Angle (DCA) Data……..…….41

C. Conclusions……..42

D. Experimental……42

1. Reagent and Characterization Equipment…….42

2. Polymer Synthesis and Purification……..43

3. Spin Casting Processing……47

4. Silanation of Glass Coverslips……..47

4. Dip-Coating Processing……48

5. Electrospinning Processing……...48

6. Static Water Contact Angle (WCA) Analysis……..49

7. Dynamic Contact Angle (DCA) Analysis……49

E. References……50

Chapter 4. Plasma Surface Functionalization of Poly[bis(2,2,2-trifluoroethoxy)phosphazene] Films and Nanofibers……...52

A. Introduction……..52

B. Results and Discussion……55

1. Morphology and Hydrophobicity…….55

2. Change in Surface Chemistry……...55

3. Processing Influence on Hydrophobicity……..58

C. Conclusions……..63

D. Experimental……63

1. Reagents……63

2. Characterization Equipment……..66

3. Polymer Synthesis…….70

4. Polymer Purification…….70

5. Spincasting Processing……..70

6. Electrospinning Processing……...71

7. Plasma Treatment of Polymer Surfaces……71

E. References……72

Chapter 5. Foam Formations from Fluorinated Polyphosphazenes by Liquid CO_2 Processing…….73

A. Introduction…….73

B. Results and Discussion……73

1. Films Cast on Glass……..73

2. Free Standing Films……...74

3. Water Absorption and Flame Test……74

C. Conclusions……..77

D. Experimental……78

1. Reagents and Equipment……...78

2. Polymer Synthesis……..…78

3. Polymer Characterization……..….81

4. Foam Formation……..…..81

5. Foam Characterization……..84

6. Flame Test…….84

E. References……85

Appendix A. Spontaneous-polymerization of Trichloro-N-trimethylsilylphosphoranimine……87

A. Introduction……..87

1. Cationic Polyermization……87

2. Monomer Storage……..89

B. Results and Discussion…….91

1. Influence of Reaction Solvent……...91

2. Influence of Glass Surfaces……..94

C. Conclusions……..98

D. Experimental Secion……98

1. Reagents ……...99

2. Characterization Equipment……..99

3. Sample Preparation……...99

E. References……..100

Appendix B. New Amphiphilic Poly[bis(2,2,2-trifluoroethoxy)phosphazene]/ Poly(propylene glycol) Triblock Copolymers: Synthesis and Micellar Characteristics……103

A. Introduction……103

B. Results and Discussion……...106

1. ABA Block Copolymer Synthesis……..106

2. Self-Association of Triblock Copolymers in an Aqueous Phase……110

3. Partitioning of Pyrene in Micellar Solutions……..116

C. Conclusions……118

D. Experimental……..……118

1. Reagents……..118

2. Characterization Equipment……119

3. Synthesis of Bromophosphoranimine 1……..……121

4. Synthesis of Trifluoroethoxyphosphoranimine 3……121

5. Synthesis of Chlorophosphoranimine 4……..……123

6. Synthesis of Triblock Copolymers 6……..……123

7. Micellar Sample Preparation……...……125

8. Fluorescence and Light Scattering Measurements……..……125

E. References……..……126

Appendix C. Ionically Conductive Polynorbornenes with Pendent Sulfonimide/Methoxyethoxyethoxy Bearing Cyclotriphosphazene Units……128

A. Introduction……128

B. Results and Discussion……...130

1. Lithium Ion Conductivity……...…130

2. Influences on Conductivity in a Norbornene/Phosphazene Polymer……...134

3. Role of Glass Transition Temperature……136

4. Advantages of a Single-Ion Conductive Polymer……...139

C. Conclusions……140

D. Experimental……..140

1. Characterization Equipment……141

2. Sulfonimide Synthesis……143

3. Norbornene-Pendent-Pentachlorocyclotriphosphazene Synthesis….143

4. Catalyzed Polymerization of the Monomer……144

5. Chlorine Replacement Reaction…….144

E. References……..146

LIST OF FIGURES

Figure 1-1. Polyphosphazene backbone.……....3

Figure 1-2. Hydrophobic polyphosphazenes (WCA, water contact angle)……9

Figure 1-3. SEM micrograph of electrospun poly[bis(2,2,2 trifluoroethoxy)phosphazene] nanofibers from tetrahydrofurane at a concentration of (a) 5% (wt/v) of the polymer and (b) 0.5% (wt/v) of the polymer……..12

Figure 1-4. Water droplet on electrospun poly[bis(2,2,2trifluoroethoxy)phosphazene] film…….13

Figure 2-1. SEM micrograph of electrospun 3 nanofibers from 10% (wt/v) of polymer from (a) methylethyl ketone, (b) acetone, and (c) tetrahydrofuran……22

Figure 2-2. SEM micrograph of electrospun nanofibers from THF at a concentration of (a) 25% (wt/v) of the polymer, (b) 5% (wt/v) of the polymer, and (c) 0.5% (wt/v) of the polymer……25

Figure 2-3. WCA measurements on spun cast and electrospun poly[bis(2,2,2-trifluoroethoxy)phosphazene] films…….……..27

Figure 2-4. Effect of fiber diameter on static water contact angle……...30

Figure 3-1. Structures of poly(diphenoxyphosphazene) **(1)**, poly[bis(para-fluorophenoxy)phosphazene] **(2)**, poly[bis(meta-trifluoromethylphenoxy)phosphazene] **(3)**, and poly[bis(2,2,2-trifluoroethoxy)phosphazene]**(4).**…….…….37

Figure 3-2. Electrospinning device……...39

Figure 3-3. SEM of 5 wt % (l.) and 0.5 wt % (r.) poly[bis(2,2,2-trifluoroethoxy)phosphazene]……40

Figure 3-4. Average static water contact angle values vs. processing……..……45

Figure 4-1. (a) Atmospheric RF plasma and (b) schematic diagram of plasma generator……53

Figure 4-2. Structure of poly[bis(2,2,2-trifluoroethoxy)phosphazene]……54

Figure 4-3. XPS spectra of methane, nitrogen, and oxygen surface plasma treated poly[bis(2,2,2-trifluoroethoxy)phosphazene] and an untreated reference

……..…….59

Figure 4-4. Electrospinning device……...60

Figure 4-5. (A) CF_4 and (B) N_2 treated poly[bis(2,2,2-trifluoroethoxy)phosphazene] **(1)**……...…62

Figure 4-6. Electrospun bead/fiber mats of polymer **1**…….65

Figure 4-7. Electrospun poly[bis(2,2,2-trifluoroethoxy)phosphazene] **(1)** with plasma treatments……...68

Figure 4-8. Static water contact angle (WCA) of polymer 1 as a function of processing conditions……...……69

Figure 5-1. Structures of polymer (1) poly[bis(2,2,2-trifluoroethoxy)phosphazene] and polymer (2) poly[(2,2,2-trifluoroethoxy)(2,2,3,3,4,4,5,5-octafluoropentoxy)phosphazene]……...75

Figure 5-2. (A) Raman spectrum of polymer **(1)** unpressurized and (B) Raman spectrum of polymer **(1)** infused with CO_2 at 2200 psi…….76

Figure 5-3. SEM of polymer films (A) solution cast **(2)**, (B) CO_2 treated **(2)**, (C) solution cast **(1)**, and (D) CO_2 treated **(1)**……..79

Figure 5-4. (A) Thick film foam of **(2)** (B) thick film foam of **(1)** (C) SEM of **(2)** foam (D) SEM of **(1)** foam……..80

Figure 5-5. Polymer **(1)** foam floating on water……...82

Figure 5-6. Film strip of polymer **(1)** flame test……...83

Figure A-1. Trichloro-*N*-trimethylsilylphosphoranimine monomer remaining unpolymerized at -3 ºC (acidic glass surface)……....90

Figure A-2. Loss of Cl-monomer at 21 ºC (acidic glass)……..…93

Figure A-3. Loss of Cl-monomer 21 ºC (neutral glass)……95

Figure A-4. DSC of trichloro-*N*-trimethylsilylphosphoranimine monomer…….….97

Figure B-1. ^{1}H NMR spectrum of $PN_{0.5}$-$PPG_{1.0}$-$PN_{0.5}$……...109

Figure B-2. Excitation spectra of pyrene as a function of $PN_{0.4}$-$PPG_{1.0}$-$PN_{0.4}$ concentration in water. ……111

Figure B-3. Plot of I_{336}/I_{334} (from pyrene excitation spectra) vs log C for $PN_{0.4}$-$PPG_{1.0}$-$PN_{0.4}$……..…112

Figure B-4. Schematic representation of micelles formed from PN-PPG-PN triblock copolymers……...…115

Figure B-5. TEM micrograph of $PN_{0.5}$-$PPG_{1.0}$-$PN_{0.5}$ micelles……117

Figure B-6. Plots of (F - Fmin)/(Fmax - F) vs concentration of $PN_{0.2}$-$PPG_{1.0}$-$PN_{0.2}$ (circle), $PN_{0.4}$-$PPG_{1.0}$-$PN_{0.4}$ (diamond), $PN_{0.5}$-$PPG_{1.0}$-$PN_{0.5}$ (triangle), and $PN_{0.7}$-$PPG_{1.0}$-$PN_{0.7}$ (square) in water……...120

Figure B-7. Equations B-1, B-2, and B-3……....122

Figure C-1. ^{31}P NMR spectra of (A) the unsubstituted pentachlorocyclophosphazene polymer, (B) 5% sulfonimide substitution, and (C) 5% sulfonimide 95% methoxyethoxyethoxy substituted polymer…….129

Figure C-2. Conductivity of poly$Nb(N_3P_3$-SI/MEE) 50 wt% propylene carbonate…131

Figure C-3. Conductivity of poly$Nb(N_3P_3$-SI/MEE) 30 wt% propylene carbonate....132

Figure C-4. Conductivity of poly$Nb(N_3P_3$-SI/MEE) 10 wt% propylene carbonate…133

Figure C-5. Graph of glass transition temperatures……135

LIST OF SCHEMES

Scheme 1-1. Synthesis and functionalization of polyphosphazenes.……4

Scheme 1-2. Surface modification by the introduction of new polymer side groups at an interface……....6

Scheme 2-1. Synthesis of poly[bis(2,2,2-trifluoroethoxy)phosphazene]……21

Scheme A-1. Cationic polymerization of phosphoranimine……88

Scheme B-1. Phosphoranimine functionalization of PPG…….104

Scheme B-2. Synthesis of PN-PPG-PN block copolymer…….105

Scheme C-1. Norbornene-pendent-pentachlorocyclotriphosphazene monomer synthesis……...137

Scheme C-2. Poly(norbornene-pendent-pentachlorocyclotriphosphazene) synthesis……...138

LIST OF TABLES

Table 2-1. XPS data of spuncast and electrospun poly[bis(2,2,2-trifluoroethoxy)phosphazene] films……...29

Table 3-1. Average static water contact angle average values……....44

Table 3-2. Dynamic contact angle average values…….….46

Table 4-1. Spuncast static water contact angles…….….56

Table 4-2. XPS survey scan atomic ratios……..….57

Table 4-3. WCA of electrospun fiber mats of polymer **1**……64

Table 4-4. WCA data electrospun bead and fiber mats of poly[bis(2,2,2-trifluoroethoxy)phosphazene] **(1)**……..67

Table A-1. Water content of solvents measured by Karl Fisher titration……92

Table B-1. Properties of the triblock copolymers……..…108

Table B-2. Properties of PN-PPG-PN micelles…….…114

Table C-1. Lithium, oxygen, and nitrogen ratios and conductivity of poly(norbornene-pendent-phosphazene) polymers……..…142

PREFACE

Portions of this thesis have been adapted for publication. Chapter 1 was adapted for publication in *Polymer International* and was coauthored by H. R. Allcock and A. Singh. Chapter 2 was adapted for publication in *Langmuir* and was coauthored by H. R. Allcock and A. Singh. Chapter 3 will be adapted for publication and was coauthored by H. R. Allcock, K. Wynne, and A. Mullins. Chapter 4 was adapted for publication in *Langmuir* and was coauthored by H. R. Allcock, S. H. Kim, J. H. Kim, and B. K. Kang. Chapter 5 will be adapted for publication and was coauthored by H. R. Allcock. Appendix 1 will be adapted for publication and was coauthored by H. R. Allcock and R. M. Wood. Appendix 2 was adapted for publication in *Macromolecules* and was coauthored by H. R. Allcock and S. Y. Cho. Appendix 3 will be adapted for publication and was coauthored by H. R. Allcock and D. A. Stone.

ACKNOWLEDGEMENTS

I would like to thank Dr. Allcock for the opportunity of working with him in the field of polyphosphazenes. He helped mold me into the scientist I am today - by challenging me to make the connections between fundamental ideas, development of applications, and communicating my research to others. I especially thank him for his unparalleled editorial skills and professional approach to research which are an inspiration and aid to all of his graduate students. I also thank Noreen Allcock for her work in support of the group. I would also like to thank The Pennsylvania State University and The National Science Foundation for support of my research.

I further thank all the graduate students I worked with while at the University Park campus for insightful discussions, teaching me, and sharing my work. I specifically would like to thank my collaborators on the published work I was involved with – Dr. David Stone, Dr. Rich Wood, Dr. Anurima Singh, and Song-Yun Cho. I would also like to thank Dr. Seong Kim and his graduate student Jeong Kim for collaborative work with the Chemical Engineering department of The Pennsylvania State University. I also thank Dr. Kenneth Wynne and his graduate student Allison Mullins for collaborative research with the Virginia Commonwealth University.

I thank my parents Ken and Ruth Steely for unwaivering emotional, spiritual, and culinary support my entire life. They gave me the confidence and stubbornness to go to college and pursue my doctorate which has led to where I am today.

Chapter 1

Introduction

The hydrophobicity (water repellency) of a polymer surface is an important property that underlies applications that range from waterproof fabrics to cardiovascular implants. Block copolymers that contain a hydrophobic block linked to a hydrophilic block form micelles in water that can serve as vehicles for the delivery of hydrophobic drugs. Hydrophobicity is also a crucial requirement for many types of electrical insulation and for surface coatings that are exposed to the outdoors. The 'non-stick' character of many hydrophobic surfaces and their lubricity are additional properties that are utilized in technology. Classical hydrophobic polymers include silicones [poly(dimethylsiloxane)] and a variety of fluorinated organic polymers such as poly(tetrafluoroethylene) (Teflon®), Viton®, and Kalrez®. However, an entirely different class of hydrophobic polymers is emerging, based on the polyphosphazene platform. These are polymers with a backbone of alternating phosphorus and nitrogen atoms and two organic side groups attached to each phosphorus (Figure 1-1). Polyphosphazenes with fluorinated organic or organosilicon side groups comprise some of the most hydrophobic materials known.

A. Synthesis of Polyphosphazenes

The development of hydrophobic properties in polyphosphazenes is facilitated by the special methods of synthesis that are employed. Fluorinated organic polymers are generally produced by the polymerization of fluorinated monomers. This limits the number of different side groups that can be incorporated, because different polymerization conditions may be needed for different monomers. By contrast, most polyphosphazenes are synthesized by a macromolecular substitution process in which the side groups in a reactive polymer intermediate (**3**) are replaced by selected organic groups. The overall process is illustrated in Scheme 1-1. The reactive macromolecular intermediate is poly(dichlorophosphazene) (**3**), itself produced either by the thermal ring-opening polymerization of the corresponding cyclic trimer (**2**)[1] or via a room temperature living cationic condensation process from a phosphoranimine monomer (**4**).[2] This synthesis protocol allows hydrophobic fluorinated aliphatic side groups, organosilicon or aryloxy groups to be linked to the phosphazene chain. Examples are shown as structures **5**–**14** in Figure 1-2.[3–8] Polyphosphazenes that bear only one type of side group are often crystalline. Those that bear two or more different types of side groups are amorphous, and several of those with fluoroalkoxy side groups (such as **6**) are hydrophobic, high-performance elastomers.

B. Enhanced Hydrophobicity Via Surface Modification

The synthesis protocol just described gives access to hydrophobic polymers through changes at the molecular level. However, an additional approach is to select a polyphosphazene that is optimized for its bulk properties and then introduce different side

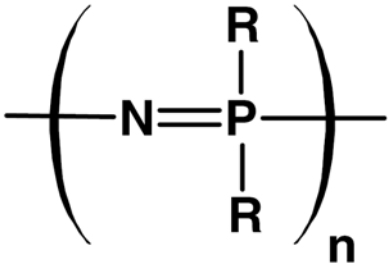

Figure 1-1. Polyphosphazene backbone.

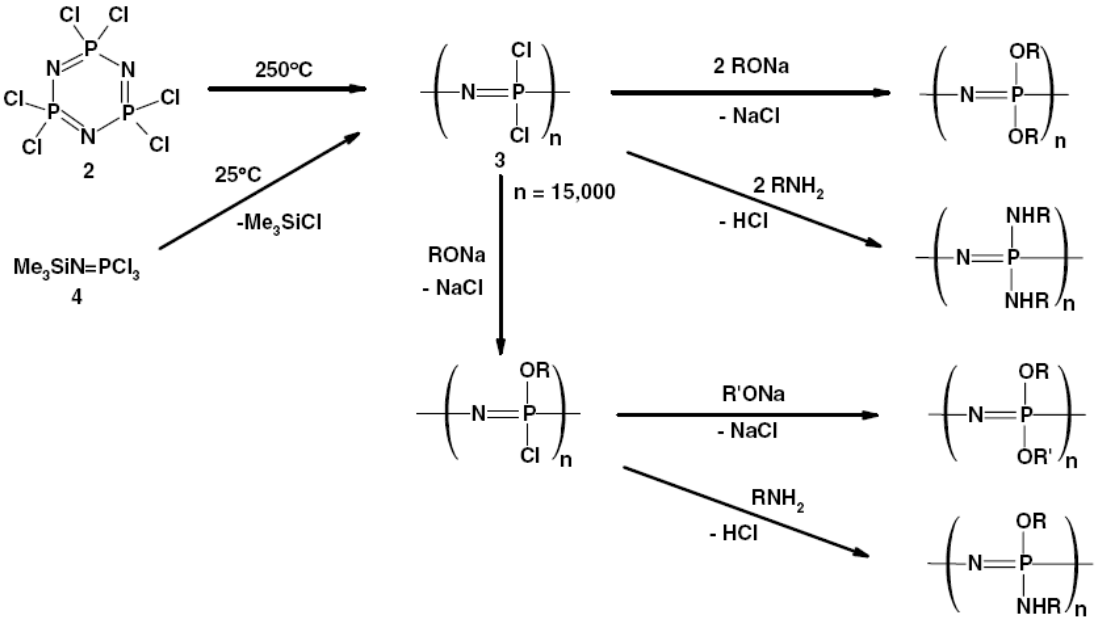

Scheme 1-1. Synthesis and functionalization of polyphosphazenes.

groups by surface reactions.[9] This is possible because side groups that are already present in these polymers can often be replaced by simple metathetical nucleophilic exchange reactions. Trifluoroethoxy side groups are especially suited to replacement reactions because of the electron-withdrawing character of these units and their relatively small size. This allows nucleophilic reagents to replace the trifluoroethoxy groups by other units (Scheme 1-2). In another approach, surface properties of hydrophobic polyphosphazenes have been modified by grafting organic polymers such as polystyrene and poly(ethylene oxide) by photochemical, thermal or γ -radiation techniques.[10] The surface modification method to replace trifluoroethoxy by longer chain fluoroalkoxy units has been used to make the fluoroalkoxyphosphazene elastomer **6** more resistant to hydrocarbons and other fluids.[11] Many of the surface exchange reactions we have reported in the literature[12,13] involve the replacement of trifluoroethoxy groups by hydrophilic or functional units. Surface reactions to introduce hydrophilic units allow one side of a polymer film to become adhesive, while the opposite side remains hydrophobic and resistant to adhesion. It is also possible to alter the hydrophobic or hydrophilic properties of *aryloxy*phosphazene polymers by surface chemistry.[3,14,15] For example, surface hydrosilation chemistry has been used to link organosilicon units to aryloxyphosphazenes to give surface structures of type **14**.[16] These enhance the properties of an already hydrophobic polymer.

C. Origins of Hydrophobicity

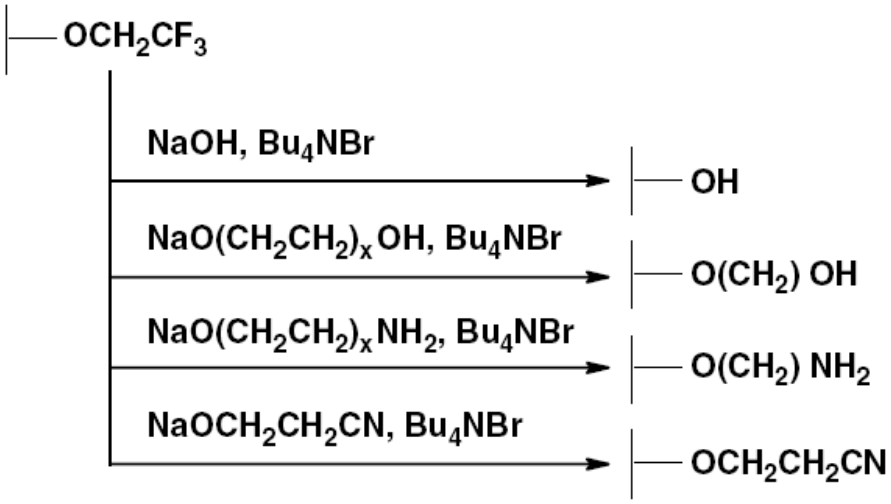

Scheme 1-2. Surface modification by the introduction of new polymer side groups at an interface.

Although the phosphazene backbone is hydrophilic, mainly due to the presence of the nitrogen lone pair electrons, polyphosphazenes can be made hydrophobic by an appropriate choice of side groups. Side groups such as $–OCH_3CF_3$, $–O(CH_2)_xCH_3$, $–OC_6H_5$ or $–Si(CH_3)_3$, which are hydrophobic and large enough to shield the skeleton, generate strong water repellency. The origins of water repellency from C–F, $Si–CH_3$, and aromatic or aliphatic hydrocarbon groups have been debated for many years and are still not fully understood. The bond polarizability and bond lengths of C–F and C–H bonds are different. However, the surface area of the peripheral units is cited as a key factor in determining the hydrophobic properties of a molecule. Two dominant mathematical models for determining the surface area of a molecule are solvent-accessible surface area (SASA) and molecular surface area (MSA).[17,18] Experimentally, terminal CF_3 and CF_2H units differ in hydrophobic behavior but, after correcting for the difference in their hydrophobic surface area with the SASA or the MSA, their hydrophobic character should be almost the same.[19] Within the polyphosphazene series the most dramatic hydrophobic effects are associated with fluorinated or organosilicon side groups or with block or graft copolymers that combine fluoroalkoxyphosphazene units with poly(organosiloxane) components. These may be compared with block copolymers that have both fluoro-organic and poly(dimethylsiloxane) blocks.[20] Hydrophobicity is frequently measured by surface contact angles to water. Water droplets spread out on a hydrophilic surface and retract to a semi-spherical droplet on a hydrophobic interface. Contact angles of 90–100◦ or higher are typical for films of the most hydrophobic materials known.

D. Specific Examples of Hydrophobic Polyphosphazenes

Some of the most hydrophobic polyphosphazenes bear fluorinated side groups such as the trifluoroethoxy groups shown in polymer **5**. Other examples include polymers **6**, **7**, **8** and **12** shown in Figure 1-2, with the contact angles to water given beneath each structure. Polymers that bear side units with terminal $–CF_2H$ groups are less hydrophobic than those with terminal $–CF_3$ groups. Moreover, polymers with $–OCH_2CF_2OCF_2CF_2OCF_2CF_3$ side groups are more hydrophobic than those with $–OCH_2CH_2OCH_2CH_2OCH_2CF_3$ units. Clearly, the density of C–F bonds in the side group system is an important factor that determines the overall surface behavior. Moreover, a low density of C–H bonds and relatively few exposed oxygen atoms that can hydrogen bond to the water are critical factors for high hydrophobicity in these systems.

The inherent flexibility of the polyphosphazene backbone also plays an important role by allowing the hydrophobic side groups to orient toward the surface and dominate the interfacial properties of the polymer.[21–23] This flexibility must be taken into account when designing new low surface energy materials. Organosilicon side groups also play a role in generating hydrophobicity. Examples are shown as structures **7**, **8**, **9**, **13** and **14** in Figure 1-2. These polymers can be synthesized in three ways: (1) through the polymerization of small-molecule cyclophosphazenes that bear organosilicon side groups; (2) by the reactions of organosilicon nucleophiles with polymer **3** to give species such as **8**, **9** or **13**; or (3) by surface reactions that replace one type of side group at the interface with another (structure **14**). A further variation of structure is via the formation of block copolymers that contain both fluoroalkoxyphosphazene and

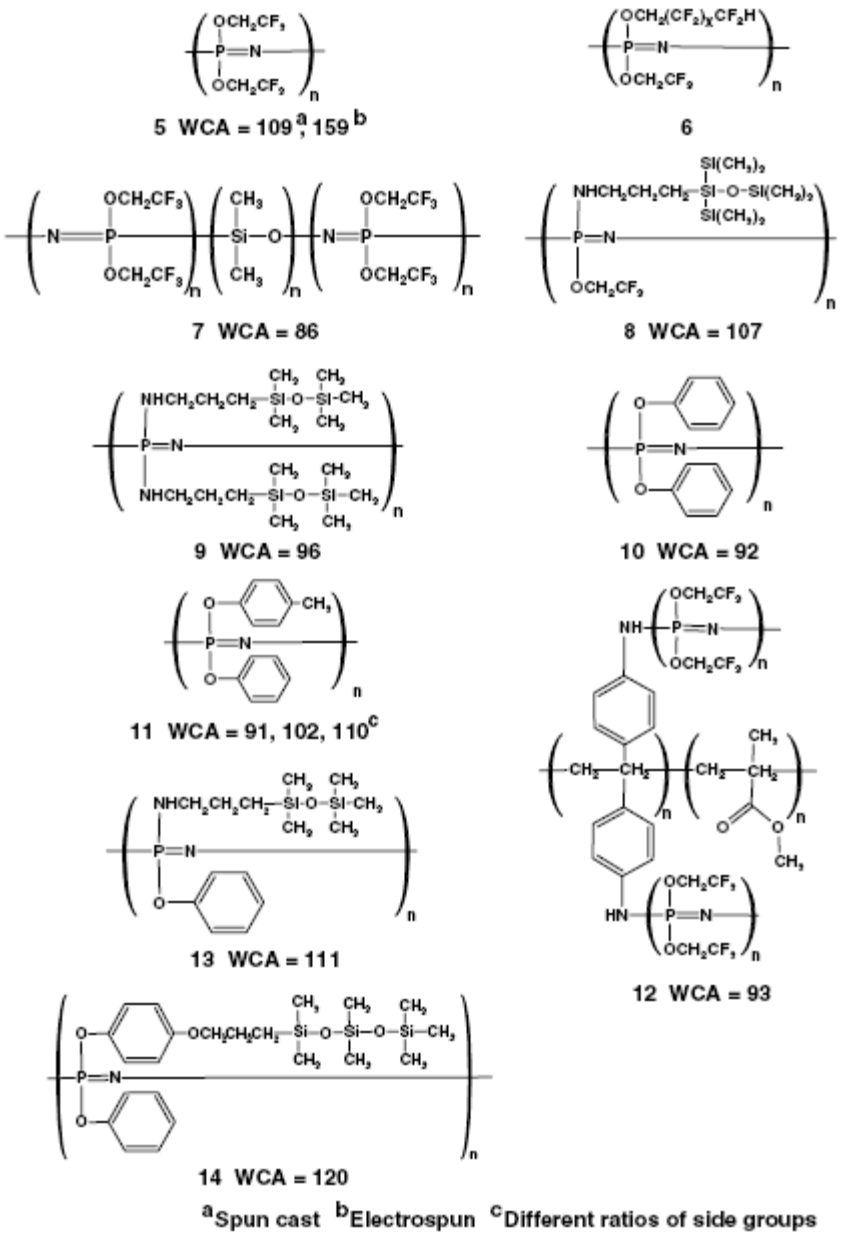

Figure 1-2. Hydrophobic polyphosphazenes (WCA, water contact angle).[3–8]

poly(dimethylsiloxane) blocks (structure **7**). Hydrophobicity at a milder level is also generated by the use of aryloxy side groups, as illustrated by structures **10** and **11**. Fluorinated aryloxy groups or those with fluoroalkyl substituents generate a more impressive hydrophobicity. In all of these polymers the steric size of the side groups prevents hydrogen bonding between water and the backbone nitrogen atoms. Given the dimensions of most of these side units it is perhaps surprising that the relatively small trifluoroethoxy side group is so effective at shielding the backbone. Several different polyphosphazene skeletal architecture types in addition to linear macromolecules have been utilized to generate hydrophobic materials. These include star, block and graft copolymers.[11] High polymers are not the only hydrophobic phosphazene systems known. Low molecular weight oils and waxes can be produced with any of the above side groups by using the living cationic polymerization of **4** to control the molecular weight of the phosphazene or by using the cyclic trimer (**2**) as a reaction substrate.

E. Superhydrophobic Nanofibers

Superhydrophobic surfaces are characterized by a high water contact angle (>150◦) and a low sliding angle (the angle to which a surface must be tilted to cause mobility of a droplet of water). These types of surfaces, with their high water repellency and self-cleaning properties have attracted considerable interest over the past few years for their potential uses in applications such as stain and dust resistant fabrics, self-cleaning windows, microfluidic devices and biomaterials.[24–27] Superhydrophobicity is generated either by increasing the surface roughness of a hydrophobic material or by

applying a hydrophobic material to an inherently rough surface. Thus, both surface chemistry and surface roughness play an important role.[26,28,29] Techniques such as plasma etching, lithography and controlled crystallization have been used to create inherently rough surfaces.[30–32] Recently, electrospinning has emerged as a convenient alternative to generate highly porous polymer mats with high surface roughness.[27,33,34] Electrospinning is a rather simple technique that can produce submicron size fibers of polymers from an electrically charged polymer solution.[35] Variations in the electrospinning conditions yield fiber or fiber-bead morphology (Fig. 1-3), which drastically alters the surface wetting properties. Recently we have electrospun superhydrophobic surfaces from poly[bis(2,2,2-trifluoroethoxy)phosphazene] (**5**).[6] The maximum contact angle observed for *films* of this polymers was 104◦. However, electrospun mats (with the appearance of tissue paper) showed contact angles as high as 159◦. This 55◦ increase is a dramatic illustration of the role played by surface morphology. Poly[bis(2,2,2-trifluoroethoxy)phosphazene] nanofibers can be electrospun readily from common organic solvents like tetrahydrofuran, methyl ethyl ketone or acetone (Figs 1-3 and 1-4). A decrease in fiber diameter increases the hydrophobicity of these mats to give contact angles in the range of 135–159◦. Superhydrophobic properties were most obvious for polymer mats that had a predominantly fiber-bead morphology (Fig. 1-3). Polymer **11** can also be electrospun, and a range of other hydrophobic polyphosphazenes are also being electrospun in our laboratories.

F. Applications of Hydrophobic Polyphosphazenes

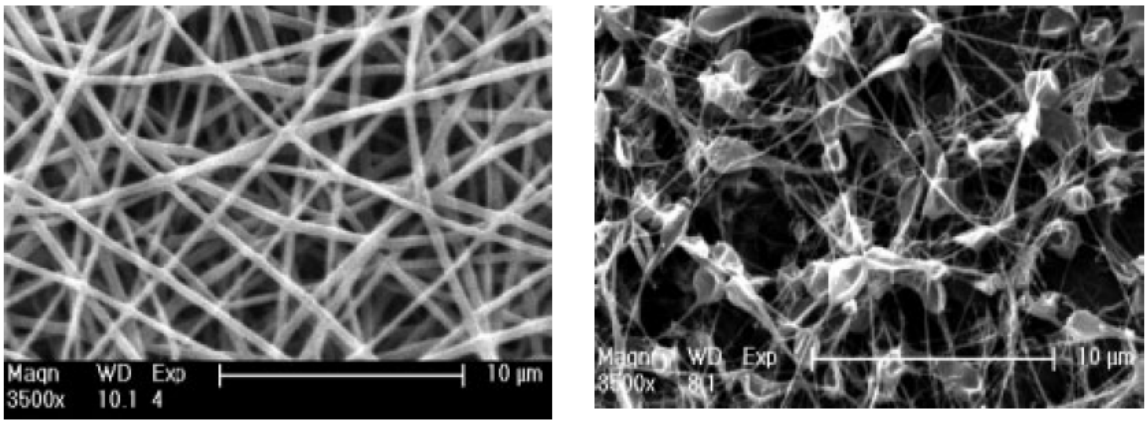

Figure 1-3. SEM micrograph of electrospun poly[bis(2,2,2 trifluoroethoxy)phosphazene] nanofibers from tetrahydrofurane at a concentration of (a) 5% (wt/v) of the polymer and (b) 0.5% (wt/v) of the polymer.

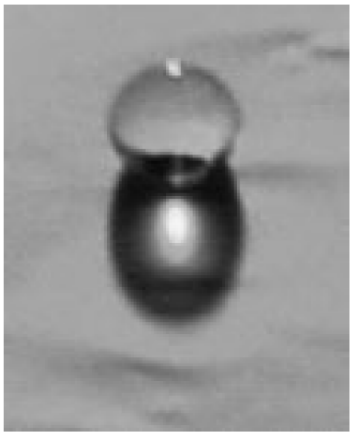

Figure 1-4. Water droplet on electrospun poly[bis(2,2,2trifluoroethoxy)phosphazene] film.

Hydrophobic materials are used in a variety of high performance applications. Hydrophobic elastomers, especially if they are also oil-resistant, are employed as seals in aircraft and marine applications, oil drilling, gas pipelines, fabrics and surface coatings.[36] The mixed-substituent fluoroalkoxy phosphazene polymers such as **6** described earlier have been developed extensively as seals and gaskets for severe use applications.[37,38] Superhydrophobic surfaces, with contact angles of 150◦ or higher, are of special interest as self-cleaning windows, biomedical implants or protective coatings for masonry or metals.[6,39] One hydrophobic small-molecule cyclic phosphazene $N_3P_3(OPhF)_2(OPhCF_3)_4$ is used as a component in hard drive lubricants.[40,41] The *p*-fluoroaryloxy groups provide coordination to an aluminum surface and the *m*-trifluoromethylaryloxy groups provide a hydrophobic protective coating for the hydrophilic aluminum substrate. Other oligomeric hydrophobic polyphosphazenes have been patented as lubricants and hydraulic fluids. Textile fibers can also be coated with hydrophobic polyphosphazenes to produce water repellent fabrics.[37] Micelles with hydrophobic cores are under development for the controlled release of hydrophobic drugs and have been considered for the encapsulation of hydrophobic dyes in water based inkjet media.[42] Poly(diphenoxyphosphazene) (**10**) has been employed as a hydrophobic liquid separation membrane to remove methylene chloride from water.[43]

G. Advantages of Polyphosphazenes

Classical hydrophobic organic fluoropolymers are some of the most useful macromolecules known. Their utility stems from their general inertness to aqueous media, their radiation resistance, and especially their hydrophobicity. Polyphosphazenes with fluorinated organic side groups possess these same properties, supplemented by ease of fabrication due to their solubility in some organic media and, in certain cases, their elasticity at low, normal and high temperatures. It is also possible to modify the surfaces of fluorinated polyphosphazenes in ways that are not possible for fluorocarbon polymers. Hydrophobic properties in these polymers can also be generated by the presence of aryloxy or organosilicon units, and by the electrospinning of nanofibers to yield superhydrophobic surfaces. These developments widen the opportunities for producing interfaces with a broad range of uses in science and technology.

H. References

(1) Allcock, H.R.; Kugel, R.L. *J. Am. Chem. Soc.* **1965**, *87*, 4216-4217.

(2) Allcock, H.R.; Crane, C.A.; Morrissey, C.T.; Nelson, J.M.; Reeves, S.D.; Honeyman, C.H.; Manner, I. *Macromolecules* **1996**, *29*, 7740-7747.

(3) Allcock, H.R.; Morrissey, C.T.; Way, W.K.; Winograd, N. *Chem. Mater.* **1996**, *8*, 2730-2738.

(4) Allcock, H.R.; Powell, E.S.; Maher, A.E.; Berda, E.B. *Macromolecules* **2004**, *37,* 5824-5829.

(5) Allcock, H.R.; Coggio, W.D. *Macromolecules* **1990**, *23*, 1626-1635.

(6) Singh, A.; Steely, L.B.; Allcock, H.R. *Langmuir* **2005**, *21*, 11604-11607.

(7) Allcock, H.R.; Smith, D.E. *Chem. Mater.* **1995**, *7*, 1469-1474.

(8) Allcock, H.R.; Prange, R. *Macromolecules* **2001**, *34*, 6858-6865.

(9) Allcock, H.R. *Applied Organometallic Chemistry* **1998**, *12*, 659-666.

(10) Gleria, M.; Bertani, R.; Jaeger, R.D.; Lora, S.; *Journal of Fluorine Chemistry* **2004**, *125*, 329-337.

(11) Kolich, C.H.; Klobucar, W.D.; Books, J.T. US Patent US 4945139, 1990.

(12) Allcock, H.R.; Rutt, J.S.; Fitzpatrick, R.J.; *Chemistry of Materials* **1991**, *3*, 442-449.

(13) Allcock, H.R.; Fitzpatrick, R.J.; Salvati, L. *Chemistry of Materials* **1991**, *3*, 450-454.

(14) Allcock, H.R.; Fitzpatrick, R.J.; Salvati, L. *Chemistry of Materials* **1991**, *3*, 1120-1132.

(15) Allcock, H.R.; Kwon, S. *Macromolecules* **1986**, *19*, 1502-1508.

(16) Wisian-Neilson, P.; Johnson, R.S.; Zhang, H.; Jung, J.H.; Neilson, R.H.; Ji, J. Watson, W. H.; Krawiec, M. *Inorg. Chem.* **2002**, *41*, 4775-4779.

(17) Lee, B.; Richards, F.M.; *J. Mol. Biol.* **1971**, *55*, 379-400.

(18) Richards, F.M. *Ann. Rev. Biophys. Bioeng.* **1977**, *6*, 151-176.

(19) Gao, J.; Qiao, S.; Whitesides, G.M. *J. Med. Chem.* **1995**, *38*, 2292-2301.

(20) Bertolucci, M.; Galli, G.; Chiellini, E.; Wynne, K.J.; *Macromolecules* **2004**, *37*, 3666-3672.

(21) Sun, H. *J. Am. Chem. Soc.* **1997**, *119*, 3611-3618.

(22) Simonutti, R.; Veeman, W.S.; Ruhnau, F.C.; Gallazzi, M.C.; Sozzani, P. *Macromolecules* **1996**, *29*, 4958-4962.

(23) Jaeger, R.; Lagowski, J.B.; Manners, I.; Vancso, G.J. *Macromolecules* **1995**, *28*, 539-546.

(24) Nakajima, A.; Hashimoto, K.; Watanabe, T.; Takai, K.; Yamauchi, G.; Fujishima, A. *Langmuir* **2000**, *16*, 7044-7047.

(25) Sun, T.; Tan, H.; Han, D.; Fu, Q.; Jiang, L. *Small* **2005**, *1*, 959-963.

(26) Blossey, R. *Nature Materials***2003**, *2*, 301-306.

(27) Acatay, K.; Simsek, E.; Yang, C.O.; Menceloglu, Y.Z. *Angewandte Chemie International Edition* **2004**, *43*, 5210-5213.

(28) Patankar, N.A. *Langmuir* **2004**, *20*, 8209-8213.

(29) Lafuma, A.; Quere, D. *Nature Materials* **2003**, *2*, 457-460.

(30) Miwa, M.; Nakajima, A.; Fujishima, A.; Hashimoto, K.; Watanabe, T. *Langmuir* **2000**, *16*, 5754-5760.

(31) McCarthy, T.J.; Oner, D. *Langmuir* **2000**, *16*, 7777-7782.

(32) Chen, W.; Fadeev, A.Y.; Hsieh, M.C.; Oner, D.; Younghblood, J.; McCarthy, T.J. *Langmuir* **1999**, *15*, 3395-3399.

(33) Demir, M.M.; Yilgor, I.; Yilgor, E.; Erman, B. *Polymer* **2002**, *43*, 3303-3309.

(34) Ma, M.; Hill, R.M.; Lowery, J.L.; Fridrikh, S.V.; Rutledge, G.C. *Langmuir* **2005**, *21*, 5549-5554.

(35) Li, D.; Xia, Y. *Advanced Materials* **2004**, *16*, 1151-1170.

(36) Mark, J.E.; Allcock, H.R.; West, R. *Inorganic Polymers* 2nd edition.; Oxford University Press: New York, 2005.

(37) Allcock, H.R. *Chemistry and Applications of Polyphosphazenes*. Wiley-Interscience: New Jersey, 2003.

(38) Penton, H.R. *Inorganic and Organometallic Polymers*, ed. by Zeldin, M.; Wynne, K.J.; Allcock, H.R. *ACS Symposium Series* no. 360. American Chemical Society: Washington, DC, 1988; pp. 277–282.

(39) Penton, H.R.; Kucsma, M.E.; Pettigrew, F.A. Eur Patent Application 205349, 1986. US Patent Application US 743524, 1996.

(40) Waltman, R.J.; Lengsfield, B.; Pacansky, J. *Chem.Mater.***1997**, *9*, 2185-2196.

(41) Singler, R.E.; Bieberich, M.J. in *Synthetic Lubricants and High Performance Functional Fluids* ed. by Shubkin, R.L. Dekker: New York, 1992; pp. 215–227.

(42) Chang, Y.; Lee, S.C.; Kim, K.T.; Reeves, S.D.; Allcock, H.R. *Macromolecules* **2001**, *34*, 269-274.

(43) Peterson, E.S.; Stene, M.L.; Cummings, D.G.; McCaffrey, R.R. *Sep. Sci. Technol.* **1993**, *28*, 271-.

Chapter 2

Poly[bis(2,2,2-trifluoroethoxy)phosphazene] Superhydrophobic Nanofibers

A. Introduction

1. Nanofiber Mats

In this study, we report the electrospinning of a highly fluorinated polymer, poly[bis(2,2,2-trifluoroethoxy)phosphazene] (**3**), to form nonwoven mats with high surface hydrophobicity. Nanofibers of polymer **3** were readily produced by electrospinning solutions in tetrahydrofuran, methylethyl ketone, or acetone. The degree of hydrophobicity was tuned by fiber diameter and surface morphology, with contact angles to water being in the range of 135°-159°. Electrospinning has emerged as a versatile tool for producing submicron size fibers of polymers.[1-3] In a typical electrospinning process, the surface of a polymer droplet, suspended at the tip of a needle, is charged by application of an electric field. As mutual charge repulsion on the drop surface overcomes surface tension, a charged polymer jet is ejected, travels a certain distance in air, and is collected as a fiber mat on a grounded collector screen. Evaporation of solvent and electrostatic repulsion between the surface charges causes continuous stretching of the polymer jet which results in the formation of submicron size fibers. In cases where the surface tension of the solution exceeds the surface charges, beads or fiber bead morphology is obtained.

2. Potential Applications

Electrospun fibers have a large specific surface area and high porosity with potential uses in filters, membranes, and protective fabric applications.[2,4] Other potential uses include tissue engineering scaffolds, drug delivery matrices and other biomedical applications[2,5,6] as well as nanoelectronics.[2,7,8] Hydrophobicity of a material is a key property that depends on both surface chemistry and surface roughness.[9-11] Hydrophobic polymers (with water contact angle above 90°) are useful in many applications such as inert biomaterials, environmentally resistant coatings, and low friction devices, whereas superhydrophobic materials (with water contact angles above 150°) are of special interest as self-cleaning surfaces and stain-resistant textiles.[12,13]

3. Comparison to Other Superhydrophobic Materials

Actay et al. reported superhydrophobic surfaces by electrospinning low molecular weight poly-(acrylonitrile-*co*-R,R-dimethyl-m-isopropenylbenzyl isocyanate) with a perfluorinated linear diol.[14] A contact angle of 167° was observed for a polymer film with predominantly bead morphology. Jiang et al. report a contact angle of 160° for an electrospun composite film of polystyrene and porous polystyrene microspheres.[15] The advantage of our system over the previously studied approaches is its simplicity. We have taken a highly hydrophobic fluorinated organic-soluble polymer and used electrospinning to further enhance its surface hydrophobicity. The high hydrophobicity of fluorinated

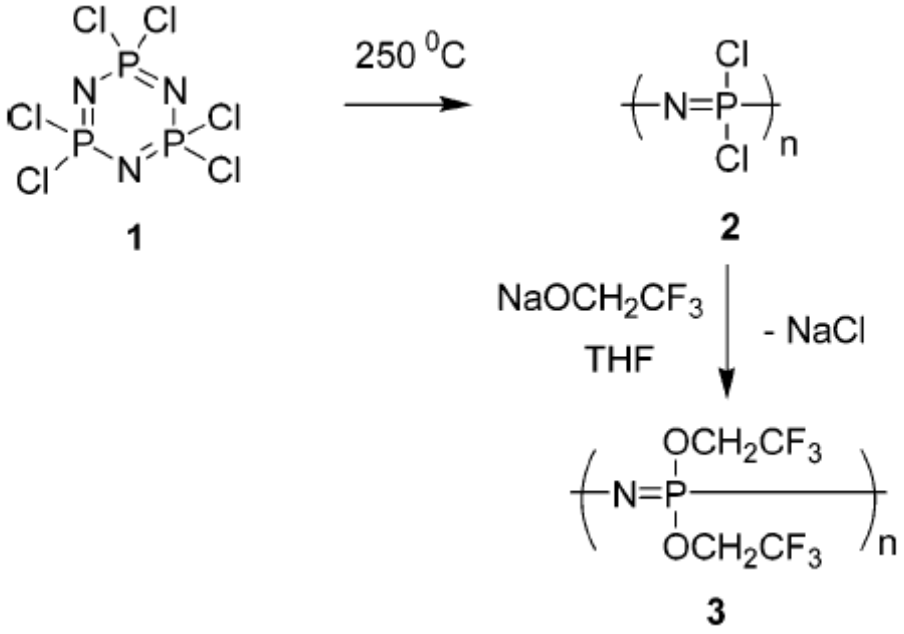

1 **2** **3**

Scheme 2-1. Synthesis of poly[bis(2,2,2-trifluoroethoxy)phosphazene].

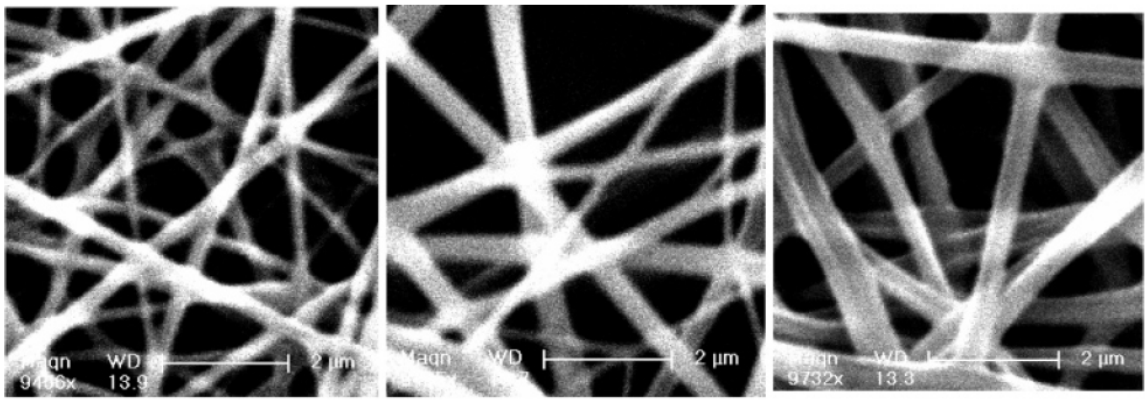

(a) (b) (c)

Figure 2-1. SEM micrograph of electrospun **3** nanofibers from 10% (wt/v) of polymer from (a) methylethyl ketone, (b) acetone, and (c) tetrahydrofuran.

polymers is due to the unique surface activity of fluorine-containing groups, which tend to concentrate at the polymer surface and minimize the surface free energy.[16-18] The advantage of using a fluorinated phosphazene, rather than, for example, poly(tetrafluoroethylene), is its solubility in common organic solvents such as tetrahydrofuran, acetone, or methylethyl ketone. The basic structure of this polymer consists of trifluoroethoxy side groups linked to a backbone of alternating phosphorus and nitrogen atoms (**3**). The combination of fluorinated side groups with an inorganic backbone generates a number of interesting properties many of which are specific to fluorinated polyphosphazenes. For example, coherent films of **3** are hydrophobic, are resistant to many chemicals, are bioinert, and have a high fire resistance and radiation stability. They are also easy to fabricate into microfibers and films. The unique properties of poly[bis(2,2,2-trifluoroethoxy)phosphazene] and related polymers are the reason for their use in membrane research, biomedicine, surface coatings, and elastomers.[19-21] However, this is the first report of superhydrophobicity generated by these polymers. The significance of this approach is that it yields polymer mats with either hydrophobic or superhydrophobic surfaces. Moreover, this work is one of the few examples in which nanofibers of a highly fluorinated polymer have been produced because most hydrophobic fluoropolymers are too insoluble to allow electrospinning to be used.

B. Results and Discussion

1. Solvent and Fiber Diameter

Electrospinning of polymers can be achieved with use of a variety of common organic solvents. The nature of the solvent plays a significant role because solution properties such as dielectric constant, boiling point, viscosity, and surface tension affect the morphology and diameter of the resulting fibers.[24] Thus electrospinning of poly[bis(2,2,2-trifluoroethoxy)phosphazene] was attempted from three solvents: methylethyl ketone (MEK), acetone, and tetrahydrofuran (THF). Fibers could be produced from all three solvents (Figure 1). The average diameter of fibers produced from different solvents was: MEK, 256 ±102 nm; acetone, 397 ±80 nm; and THF, 498 ±51 nm. Electrospinning from THF gave the most regular fibers with a narrow size distribution. By electrospinning from THF solution, the average fiber diameter could be varied from 80 nm to 1.4 μm by variations in the concentration of the polymer. The fiber diameter decreased with decreases in solution concentration.

2. Formation of Bead Morphology

As the concentration decreased, both fibers and beads strung along the fiber morphology were formed. Several studies in the literature have reported the effect of solution concentration on fiber morphology during electrospinning.[4,25] Low concentration solutions, due to a reduced solution viscosity, tend to form beaded fibers due to surface tension effects. Figure 2-2 illustrates the effect of solution concentration on fiber morphology. At higher concentrations, ≥15 wt %, a broad distribution of fiber size was obtained, with the fiber diameter in the range of ±555 nm. However, below this

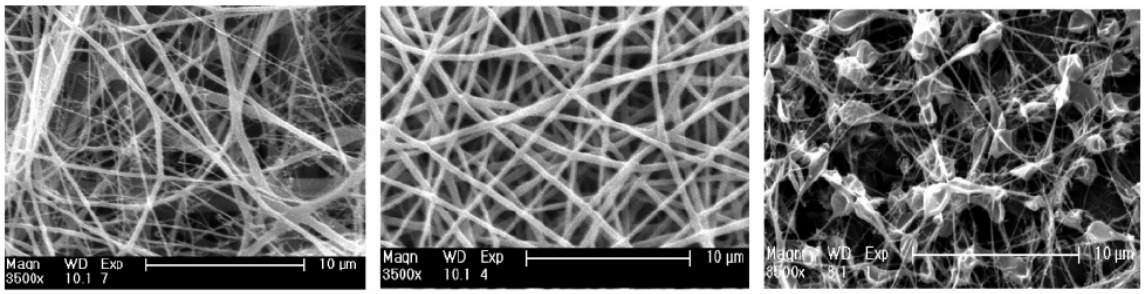

(a) (b) (c)

Figure 2-2. SEM micrograph of electrospun nanofibers from THF at a concentration of (a) 25% (wt/v) of the polymer, (b) 5% (wt/v) of the polymer, and (c) 0.5% (wt/v) of the polymer.

concentration, a drastic improvement in size distribution was achieved with fiber diameters in the range of ±52 nm.

3. Probing the Surface with XPS and WCA

The surface properties of electrospun mats were analyzed by XPS and static water contact angle (WCA) measurements. XPS analysis showed no change in fluorine content on an electrospun surface when compared to a spun cast film (Table 2-1). However, WCA meausurements showed a marked increase in hydrophobicity of the electrospun mats. The WCA on a spun cast film was 104°. However, electrospun fiber mats showed WCA values in the range of 135°-159 ° (Figure 2-3). The contact angle increased with a decrease in fiber diameter and reached a "superhydrophobic state" as both beads and fibers were formed on the surface of the spun mats (Figure 2-4).

4. Models of Superhydrophobicity

Superhydrophobic surfaces, with high water repellency and self-cleaning properties have attracted considerable interest over the past few years. These surfaces have a contact angle to water above 150° and a low sliding angle.[9-11] In most cases, hydrophobic materials with high surface roughness show superhydrophobic properties. Two different models, Wenzel and Cassie, have been proposed for explaining the wetting behavior of rough surfaces.[10] The Wenzel model hypothesizes that an increase in surface roughness causes an increase in surface area which leads to enhanced hydrophobicity.

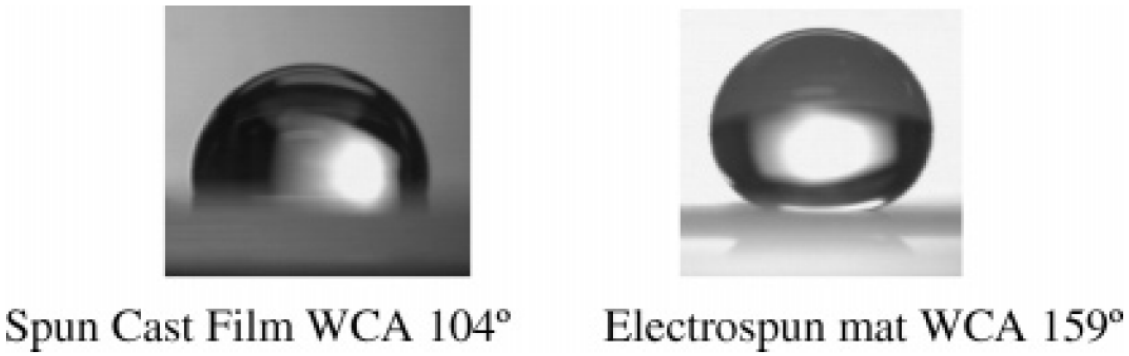

Figure 2-3. WCA measurements on spun cast and electrospun poly[bis(2,2,2-trifluoroethoxy)phosphazene] films.

Since the liquid fills up the spaces on the rough surface leading to a better spinning, these types of surfaces show a high hysteresis (the difference between advancing and receding contact angles). The Cassie model suggests that a rough surface will lead to the creation of grooves with trapped air. Liquid droplets remain suspended on these air trapped grooves and thus are not pinned to the surface leading to a low hysteresis.

5. Superhydrophobicity of Poly[bis(2,2,2-trifluoroethoxy)phosphazene]

Poly[bis(2,2,2-trifluoroethoxy)phosphazene] mats electrospun from 1 wt % and 0.5 wt % THF solution showed a contact angles of 152° ± 2.6°and 155° ± 2.6°, respectively. The advancing and receding contact angles were 149° and 145°, respectively, for a mat spun from 1 wt % solution and 150° and 147°, respectively, for a mat spun from 0.5 wt % solution. An electrospun mat has a higher degree of surface roughness, compared to a spun cast film.[14,26] This roughness is further enhanced by the formation of micron size beads on the surface.[14] Thus, poly[bis(2,2,2-trifluoroethoxy) phosphazene] mats electrospun from 1 wt % and 0.5 wt % THF solutions showed "superhydrophobic properties" as the WCA on these films was over 150° and a low value for contact angle hysteresis (<4°)was recorded.

C. Conclusions

Highly hydrophobic, nanostructured mats of poly[bis(2,2,2-trifluoroethoxy)phosphazene] were produced via electrospinning. Fibers with average

sample	F%	O%	N%	C%	P%
spun cast film	43.2	14.3	7.1	28.2	7.1
electrospun mat	43.3	14.2	7.3	28.0	7.3

Table 2-1. XPS data of spuncast and electrospun poly[bis(2,2,2-trifluoroethoxy)phosphazene] films.

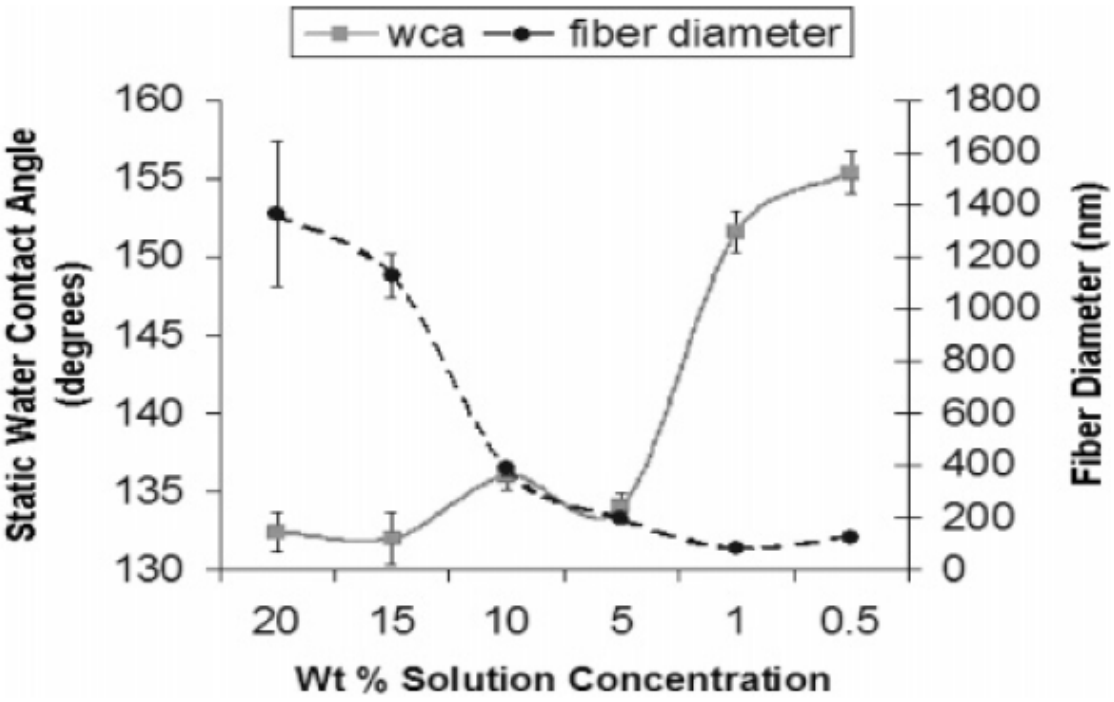

Figure 2-4. Effect of fiber diameter on static water contact angle.

diameters in the range of 80 nm to 1.4 μm were fabricated. The hydrophobicity of the electrospun mats varied with fiber diameter and surface morphology, with contact angles to water being in the range of 135°-159°. The extremely high hydrophobicity of these surfaces is a combined result of surface enrichment with fluorinated units together with the inherent surface roughness associated with an electrospun mat. The development of electropsun mats from polymer **3** constitutes a significant advance for fluorinated polymers that may eventually be utilized in membranes and filters as well as in fabric technology.

D. Experimental

1. Reagents

Polymer synthesis was carried out under an atmosphere of dry argon using standard Schlenk line techniques. Hexachlorocyclotriphosphazene (**1**) (Ethyl Corp. and PCS) was obtained from a trimer-tetramer mixture by sublimation (30 °C/0.2 mmHg). 2,2,2-Trifluorethanol 99.8% (Acros) and sodium hydride 60% (Acros) were used as received. Tetrahydrofuran and acetone were purchased from EM Sciences and were degassed and dried with an alumina bed. Methylethyl ketone was obtained from Aldrich and was used without further purification.

2. Characterization Equipment

Proton and phosphorus NMR characterization was obtained using a BrukerAMX-360 instrument. Molecular weights were determined using a HP1090 liquid chromatograph equipped with Phenomenex columns calibrated against polystyrene standards. Glass transition temperatures were determined from a TA Instruments Q10 differential scanning calorimetry (DSC) apparatus with a heating rate of 10°C/min under an inert atmosphere. SEM was conducted using a FEI-Philips XL-20. XPS data were obtained with use of a Kratos Analytical Axis Ultra instrument and the take off angle for the measurements was 0°. Water contact angle measurements were obtained using a Rame-Hart contact angle goniometer. Water was dispensed from a needle attached to a Gilmont microliter syringe filled with ultra pure water (Millipore system, 18MΩ/cm). Water droplets, 12 μL in size, were placed on the surface and images of the drop silhouette were taken with a video camera and stored for analysis on a computer. For advancing contact angle measurements, 10μL of water was brought in contact with the surface followed by addition of 2 μL of water. For receding contact angle measurements, 2 μL of water was withdrawn from the surface. The reported values are average for five measurements.

3. Electrospinning Processing

Electrospinning was accomplished with the setup described previously.[22] Parameters that were kept constant during spinning were working distance at 20 cm, flow rate of polymer solution at 1 mL/h, and the applied potential at 15 kV. The variable parameters were type of solvent and concentration of the polymer solution.

4. Synthesis of Poly[bis(2,2,2-trifluoroethoxy)phosphazene](3)

Synthesis of polymer **3** was carried out with the use of poly(dichlorophosphazene) prepared by the ring-opening polymerization of hexachlorocyclotriphosphazene (Scheme 2-1).[23] Poly[dichlorophosphazene] (**2**) (20 g, 0.173 mol) was dissolved in THF (2000 mL). The sodium salt of trifluoroethanol (86.32 g, 0.862 mol) was added, and the reaction mixture was stirred for 48 h. A white fibrous polymer was isolated by precipitation of a concentrated solution of the reaction mixture into acidic water. The polymer was further purified by repeated precipitations from THF into water and hexanes. The synthetic route is summarized in Scheme 2-1. ^{1}H NMR (d_8-THF), ppm: δ 4.54 (singlet); ^{31}P (d_8-THF), ppm: δ -5.17 (singlet). *M*n 656 000, *M*w 1 560 000, PDI 2.38; Tg -62 °C, T (1) 64 °C, Tm 241°C.

E. References

(1) Reneker, D. H.; Chun, I. *Nanotechnology* **1996**, *7*, 216-223.

(2) Huang, Z. M.; Zhang Y. Z.; Kotaki, M.; Ramakrishna, S. *Compos. Sci. Technol.* **2003**, *63*, 2223-2253.

(3) Li, D.; Xia, Y. *Adv. Mater.* **2004**, *16*, 1151-1170.

(4) Deitzel, J. M.; Kleinmeyer, D.; Harris, D.; Tan, N. C. B. *Polymer* **2001**, *42*, 261-272.

(5) Subhabrata, B.; Nair, L. S.; Singh, A.; Krogman, N. R.; Bender, J.; Greish, Y. E.; Brown, P. W.; Allcock, H. R.; Laurencin, C. T. *Mater. Res. Soc. Symp. Proc.* **2005**, 845 (Nanoscale Materials Science in Biology and Medicine), 91-96.

(6) Yoshimoto, H.; Shin, Y. M.; Terai, H.; Vacanti, J. P. *Biomaterials* **2003**, *24*, 2077-2082.

(7) MacDiarmid, A. G.; Jones, W. E.; Norris, I. D.; Gao, J.; Johnson, A. T.; Pinto, N. J.; Hone, J.; Han, B.; Ko, F. K.; Okuzaki, H.; Llaguno, M. *Synth. Met.* **2001**, *119*, 27-30.

(8) Dror, Y.; Salalha, W.; Khalfin R. L.; Cohen, Y.; Yarin, A. L.; Zussman, E. *Langmuir* **2003**, *19*, 7012-7020.

(9) Blossey, R. *Nat. Mater.* **2003**, *2*, 301-306.

(10) Lafuma, A.; Quere, D. *Nat. Mater.* **2003**, *2*, 457-460.

(11) Patankar, N. A. *Langmuir* **2004**, *20*, 8209-8213.

(12) Nakajima, A.; Hashimoto, K.; Watanabe, T.; Takai, K.; Yamauchi, G.; Fujishima, A. *Langmuir* **2000**, *16*, 7044-7047.

(13) Furstner, R.; Barthlott, W.; Neinhuis, C.; Walzel, P. *Langmuir* **2005**, *21*, 956-961.

(14) Acatay, K.; Simsek, E.; Yang, C. O.; Menceloglu, Y. Z. *Angew. Chem. Int. Ed.* **2004**, *43*, 5210-5213.

(15) Jiang, L.; Zhao. Y.; Zhai. J. *Angew. Chem. Int. Ed.* **2004**, *43*, 4338-4341.

(16) Deitzel, J. M.; Kosik, W.; McKnight, S. H.; Tan, N. C. B.; DeSimone, J. M.; Crette, S. *Polymer* **2002**, *43*, 1025-1029.

(17) Kassis, C. M.; Steehler, J. K.; Betts, D. E.; Guan, Z.; Romack, T. J.; DeSimone, J. M.; Linton, R. W. *Macromolecules* **1996**, *29*, 3247-3254.

(18) Thomas, R. R.; Anton, D. R.; Graham, W. F.; Darmon, M. J.; Stika, K. M. *Macromolecules* **1998**, *31*, 4595-4604.

(19) Allcock, H. R. In *Chemistry and Applications of Polyphosphazenes*; Wiley-Interscience: Hoboken, NJ, 2003; p 504.

(20) Gleria, M.; Bertani, R.; Jaeger, R. D. *J. Inorg. Organomet. Polym.* **2004**, *14* (1), 1-28.

(21) Gleria, M.; Bertani, R.; Jaeger, R. D.; Lora, S. *J. Fluorine Chem.* **2004**, *125*, 329-337.

(22) Nair, L. S.; Subhabrata, B.; Bender, J.; Greish, Y. E.; Brown, P. W.; Allcock, H. R.; Laurencin, C. T. *Biomacromolecules* **2004**, *5*(6), 2212-2220.

(23) Allcock, H. R.; Kugel, R. L.; Valan, K. J. *Inorg. Chem.* **1966**, *5*(10), 1709-1715.

(24) Lee, K. H.; Kim, H. Y.; Khil, M. S.; Ra, Y. M.; Lee D. R. *Polymer* **2003**, *44*, 1287-1294.

(25) Fong, H.; Chun, I.; Reneker, D. H. *Polymer* **1999**, *40*, 4585-4592.

(26) Demir, M. M.; Yilgor, I.; Yilgor, E.; Erman, B. *Polymer* **2002**, *43*, 3303-3309.

Chapter 3

Hydrophobic Behavior of Aryloxy, Fluoroaryloxy, and Fluoroalkoxy Polyphosphazenes

A. Introduction

Recent development of superhydrophobic polyphosphazene surfaces has renewed interest in probing the surface energy associated with phosphazene surfaces.[1] Relatively little advancing and receding water contact angle work has been reported for phosphazenes in the literature.[2,3] In this work the surfaces of four polyphosphazenes (Figure 3-1) with differing morphologies were probed with sessile drop method and Wilhelmy plate method water contact angle measurements. The sessile drop method employs a single droplet of water to which water is added then removed to obtain advancing and receeding water contact angles. The Wilhelmy plate method uses coated substrates which are dipped into a solvent bath to measure the air-water-polymer interface. Advancing angles are obtained while advancing the substrate into the solvent bath and receeding angles during retraction of the substrate from the bath. Hysteresis is the difference between solvent contact with a dry surface or a previously wetted surface.

In this work four polyphosphazenes were utilized with varied fluorine content to examine the role of fluorine concentration on hydrophobicity. Secondly, different morphologies of each material were produced by electrospinning, spin casting, and dip coating. These morphologies provide relatively flat film surfaces, fiber mats which are

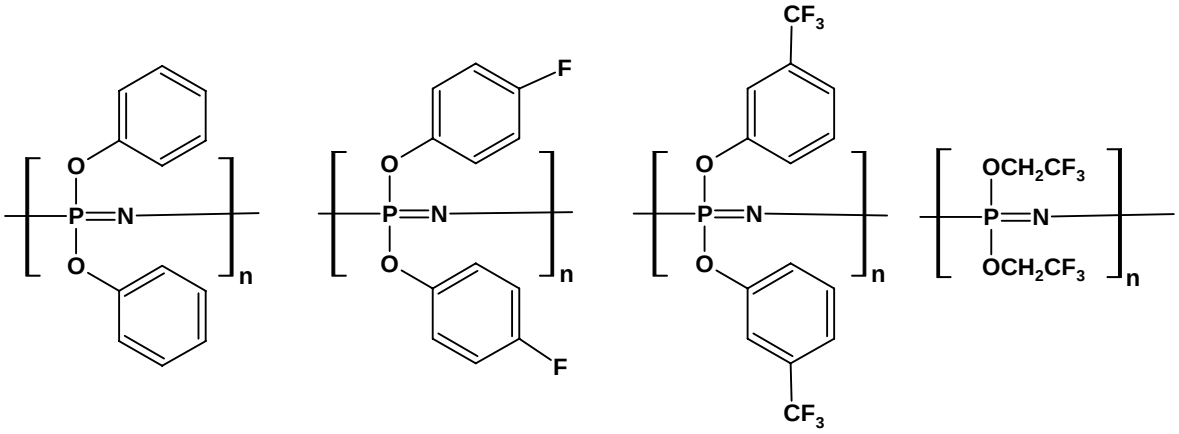

(1) **(2)** **(3)** **(4)**

Figure 3-1. Structures of poly(diphenoxyphosphazene) **(1)**, poly[bis(para-fluorophenoxy)phosphazene] **(2)**, poly[bis(meta-trifluoromethylphenoxy)phosphazene] **(3)**, and poly[bis(2,2,2-trifluoroethoxy)phosphazene] **(4).**

porous yet provide continuous contact with the water droplet, and bead mats which produce discontinuous contact with the water droplet as described by McCarthy.[4]

B. Results and Discussion

1. Static Water Contact Angle Data and Fluorine Placement

Water contact angle measurements show hydrophobic character of polymer surfaces. From previous work by Allcock and others on polyphosphazenes it is known that polyphosphazene side groups control hydrophobic character of the polymer.[5] We wanted to know if in light of current studies on processing and superhydrophobic behavior of poly[bis(2,2,2-trifluoroethoxy)phosphazene] similar dramatic increases in hydrophobic character could be effected by processing other polyphosphazenes.[6] As shown in table 3-1 static water contact angles did increase with similar magnitude by processing. This increase is attributed to differences in surface morphology. The lowest static water contact angle is obtained from the flat spun cast polymer Figure 3-4. When the polymers were electrospun at 5 wt % non-woven fiber mats are formed, 1 wt % and 0.5 wt % produce a mixture of beads and fibers as shown in Figure 3-3. However the 0.5 wt % contained more beads because the Taylor cone was less stable with the lower viscosity solution.[6] Maximum increases in static water contact angles were obtained with the high bead concentration morphology for poly[bis(2,2,2-trifluoroethoxy)phosphazene and poly[bis(meta-trifluoromethylphenoxy)phosphazene we believe that this is caused by the location of the outermost fluorine atoms from the backbone in these two polymers.

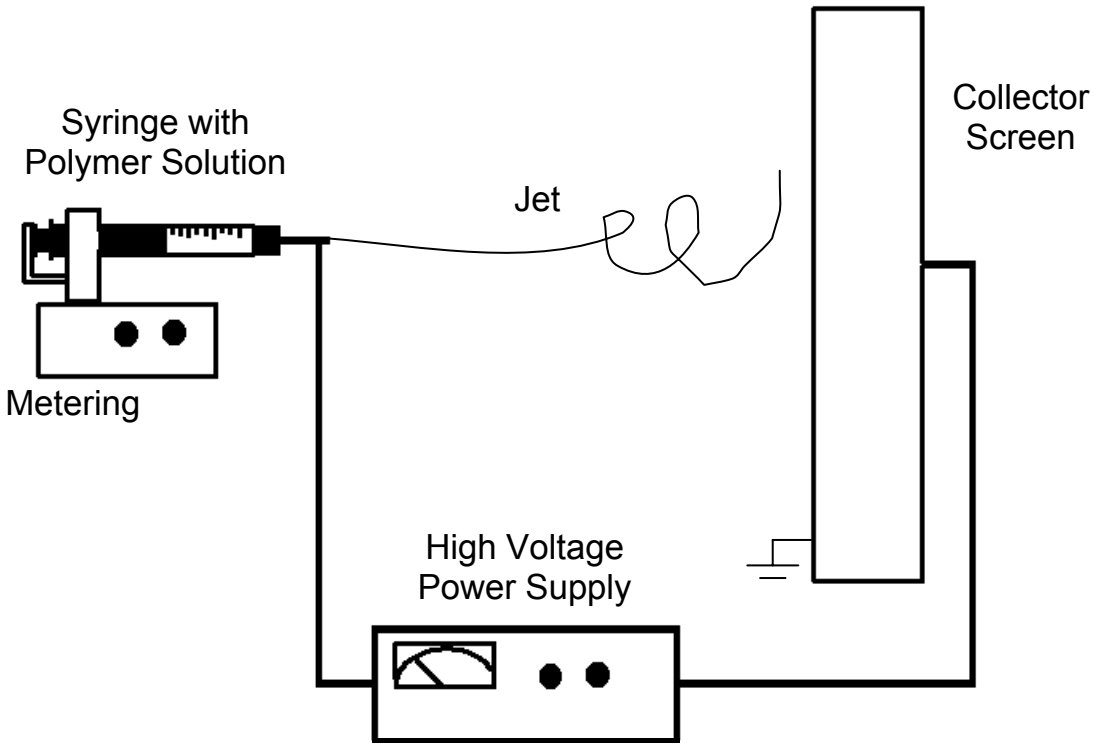

Figure 3-2. Electrospinning device.

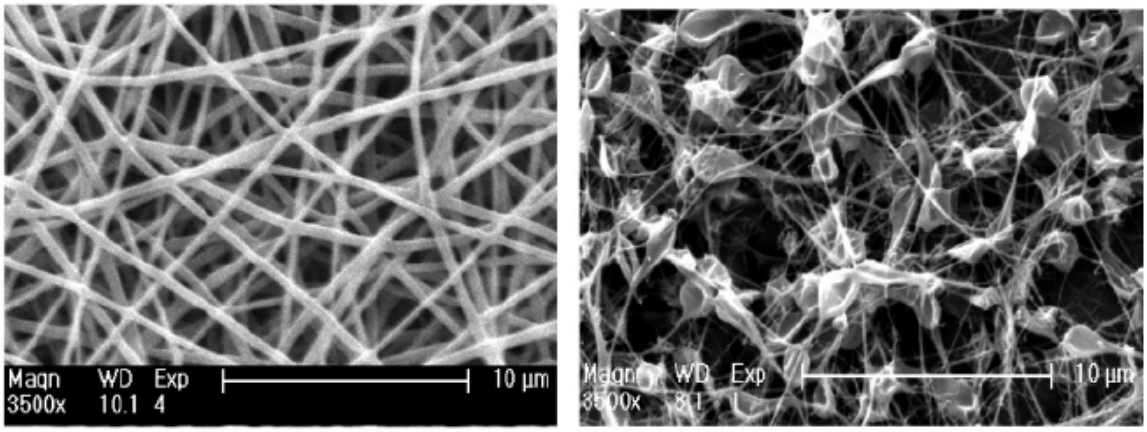

Figure 3-3. SEM of 5 wt % (l.) and 0.5 wt % (r.) poly[bis(2,2,2-trifluoroethoxy)phosphazene].

By reducing the surface area acting on the water droplet, the fluorines on the CF_3 can more effectively repel the water because they stick out from the polymer backbone and more efficiently act on the surface tension of the water droplet. However, poly(diphenoxyphosphazene) and poly[bis(para-fluorophenoxy)phosphazene] contain much less fluorine and the interaction with the surface tension is less repulsive which we believe allows the droplet to sink around the beads and have more surface interaction than the fiber mat analogues of these polymers. All electrospun mats were tested for *n*-hexadecane contact angle, but all samples showed complete spreading over the entire surface.

2. Dynamic Water Contact Angle (DCA) Data

Four polyphosphazenes (Figure 3-1) with varied fluorine content are examined by DCA to determine the role of fluorine concentration on wetting behavior. DCA results show that surface composition is strongly influenced by the extent and nature of semi-fluorinated groups. Decreasing water advancing (θ_{adv}) and receding (θ_{rec}) contact angles with decreasing fluorine contents were observed. Semi-fluorinated polymers (**2-4**) are more hydrophobic than the poly(diphenoxyphosphazene)(**1**), but differentiation of wetting amongst the semifluorinated coatings by water is modest (Table 3-2). Oil (n-hexadecane) contact angles show clear differentiation of surface wetting. High contact angle hysteresis of 29° for **4** reflects a rapid surface rearrangement from a $–CF_3$ to a $–CH_2$ dominated surface. Lack of contact angle hysteresis for aromatic polymers (**2** and **3**) suggests a chemically heterogeneous surface with a composition that is invariant in water

and hexadecane. Semifluorinated polymers (**2-4**) are more oleophobic than the poly(diphenoxyphosphazene) (**1**).

C. Conclusions

The increasing fluorine content of the polymer showed increased hydrophobicity as anticipated. However, the oleophobicity also increased with increasing fluorine content with increasing levels of hysteresis. This shows the chemical resistance associated with fluorinated polyphosphazenes is tied to their fluorine content. The fluorine atoms at the polymer surface reduce the surface energy and allow the surface tension of the non-polar hexadecane and the polar water to dominate the interaction. This effect is magnified for water when surface roughness is induced by various processing methods, as the morphology itself reduces the effective surface acting on the droplet thus further reducing the surface energy. The results were much different with the *n*-hexadecane, the moderate contact angles are quite high when the reduced surface tension of the non-polar testing medium in taken into consideration. The reduced surface tension of the *n*-hexadecane allows it to penetrate the rough morphologies via capillary action.

D. Experimental

1. Reagents and Characterization Equipment

Polymer synthesis was carried out under an atmosphere of dry argon using standard Schlenk line techniques. Hexachlorocyclotriphosphazene (Ethyl Corp. and PCS) was obtained from a trimer-tetramer mixture by sublimation (30 °C/0.2 mmHg). Phenol 99%+ (Aldrich) 4-fluorophenol 99% (Aldrich), meta-trifluoromethylphenol 98%+ (Acros), 2,2,2-trifluorethanol 99.8% (Acros), and sodium stick (Aldrich) were used as received. Tetrahydrofuran was purchased from EM Sciences and was degassed and dried with an alumina bed. Proton and phosphorus NMR characterization was obtained using a Bruker AMX-360 instrument. Molecular weights were determined using a HP1090 liquid chromatograph equipped with Phenomenex columns calibrated against polystyrene standards. Glass transition temperatures were determined from a TA Instruments Q10 differential scanning calorimetry (DSC) apparatus with a heating rate of 10°C/min under an inert atmosphere. Liquids used for DCA analysis were: 18 MΩ/cm water obtained from a Millipore™ filtration system and n-hexadecane 99% (Acros) were used as received.

2. Polymer Synthesis and Purification

Poly(diphenoxyphosphazene) (1), poly[bis(para-fluorophenoxy)phosphazene] **(2)**, poly[bis(meta-trifluoromethylphenoxy)phosphazene] **(3)**, and poly[bis(2,2,2-trifluoroethoxy)phosphazene] **(4)** were synthesized as described previously in the literature.[7] All polymers were made from the same batch of poly(dichlorophosphazene). Sodium phenoxide, sodium para-fluorophenoxide, sodium meta-trifluoromethylphenoxide, and sodium 2,2,2-trifluoroethoxide were made by reacting the

Sample	Static (°)	Advancing (°)	Receeding (°)	Hysteresis (°)
Ph 5 wt %	139	141	139	3
Ph 1 wt %	131	141	139	2
Ph 0.5 wt %	123	139	127	12
Ph Spuncast	78	91	87	4
F-Ph 5 wt %	133	138	138	1
F-Ph 1 wt %	130	140	137	3
F-Ph 0.5 wt %	125	140	137	2
F-Ph Spuncast	97	93	87	6
CF3-Ph 5 wt %	131	147	143	4
CF3-Ph 1 wt %	142	139	137	3
CF3-Ph 0.5 wt %	148	148	146	2
CF3-Ph Spuncast	98	94	93	1
TFE 5 wt %	134	151	143	8
TFE 1 wt %	152	149	145	4
TFE 0.5 wt %	155	150	147	3
TFE Spuncast	104	109	99	10

Table 3-1. Average static water contact angle average values.

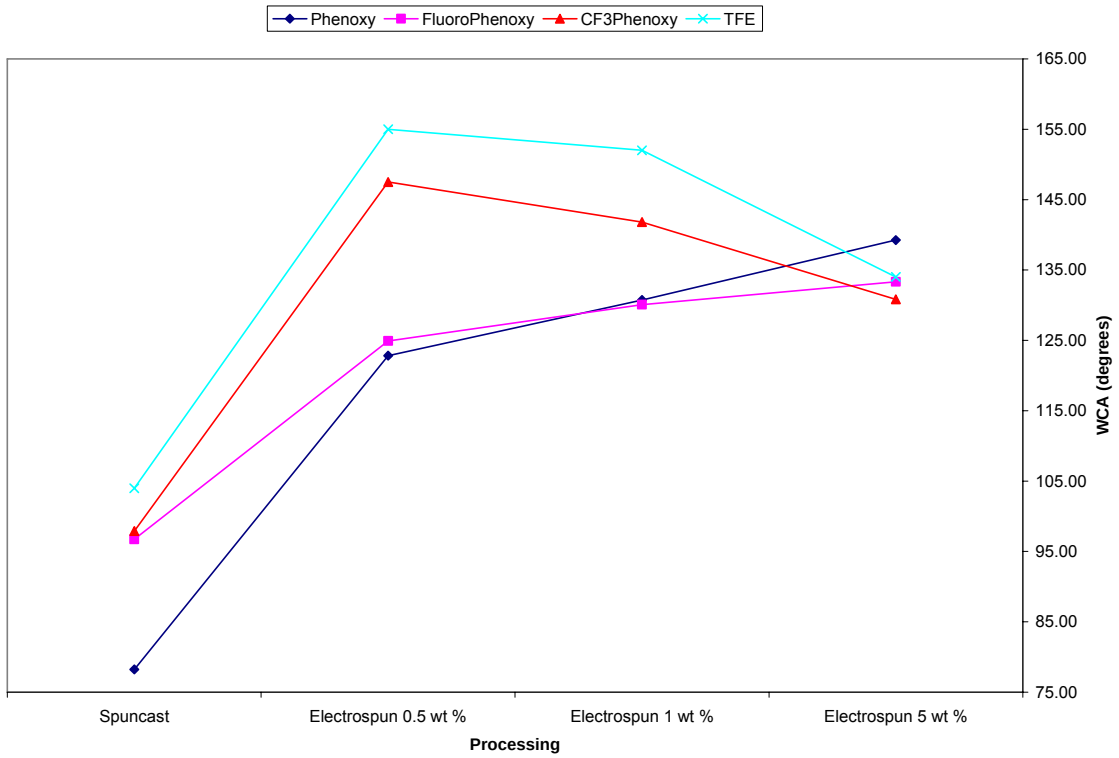

Figure 3-4. Average static water contact angle values vs. processing.

Surface	Water (º)			n-Hexadecane (º)		
	Θ_{ADV}	Θ_{REC}	Hysteresis	Θ_{ADV}	Θ_{REC}	Hysteresis
Polymer (4)	123	78	45	73	44	29
Polymer (3)	119	77	42	43	44	-1
Polymer (2)	106	52	54	27	32	-5
Polymer (1)	103	69	34	27	27	0

Table 3-2. Dynamic contact angle average values.

respective alcohol with dry sodium stick in THF. Individual salt solutions were then cannulated into stirring solutions of poly(dichlorophosphazene) in THF. The reactions of poly(diphenoxyphosphazene) and poly[bis(2,2,2-trifluoroethoxy)phosphazene] were stirred at 40 ºC under nitrogen for 72 hours. Poly[bis(para-fluorophenoxy)phosphazene] and poly[bis(meta-trifluoromethylphenoxy)phosphazene] reaction solutions were heated in an autoclave at reflux with a pressure of 3 atmospheres for 24 hours to increase the rate of substitution.

All polymers were centrifuged (5000 rpm, 30 min.) to remove salts from the reaction solution. The decanted solution was then concentrated on a rotovap and precipitated repeatedly from THF into water to remove trace salt and from THF into hexanes to remove residual cyclic trimer.

3. Spin Casting Processing

Solutions of 2.5 wt % (wt/v) of polymer in dry uninhibited THF were stirred in sealed beakers for 24 hours ensure uniform distribution of the polymers in the solutions and avoid THF evaporation. Cleaned glass slides were coated by spin casting the polymer solution at 5K rpm for 20 sec, three coats were applied to one side of each slide to avoid any pinholes from evaporating solvent. Spun cast samples were then dried in a room temperature vacuum oven with a liquid nitrogen cold trap.

4. Silanation of Glass Coverslips

In order to overcome poor adhesion, silanation of the glass coverslips (Corning, 24 x 40 x 1.2 mm) was employed. Coverslips were flame dried for 5 seconds, cooled for 60 seconds, and then immersed in a 2 wt.% solution of 3-aminopropyltriethoxysilane 99%(Sigma-Aldrich) in acetone 99.9% (Sigma-Aldrich) for 45 seconds. Excess reagent was rinsed off with DI water for 60 seconds and then allowed to dry overnight in a covered beaker.

5. Dip-Coating Processing

Sample films were prepared using the 3-aminopropyltriethoxysilane treated coverslips and dip-coated using 2.5 wt % solutions of polymer in THF. Coverslips were inverted and covered to ensure slow evaporation and even distribution of the polymer coating. The cover was removed after ~ 60 minutes and then coverslips were dried in a vertical position for 2-3 hours. Resulting sample films were placed in a vacuum oven (30º C with a liquid nitrogen cold trap attached) for 12 hours to remove any residual solvent and then allowed to dry overnight in a covered beaker.

6. Electrospinning Processing

Polymers were dissolved in dry uninhibited THF and solutions of varied concentrations were electrospun at 15kV ± 2kV using a syringe pump with a flow rate of 1mL/hr. The distance from needle tip to the aluminum foil covered grounding plate was 20 cm as described previously and shown in Figure 3-2.[6]

7. Static Water Contact Angle (WCA) Analysis

Static water contact angle measurements were obtained using a Rame-Hart contact angle goniometer. Water was dispensed from a needle attached to a Gilmont microliter syringe filled with ultrapure water (Millipore system, 18MΩ/cm). Water droplets, 12 μL in size, were placed on the surface and digital images of the drop silhouette were recorded with a video camera and analyzed on a computer. For advancing contact angle measurements, 10μL of water was brought in contact with the surface followed by addition of 2 μL of water. For receding contact angle measurements, 2 μL of water was withdrawn from the surface. Reported water contact angle values are the average of five measurements.

8. Dynamic Contact Angle (DCA) Analysis

Force-distance curves were obtained and advancing and receding contact angles were subsequently determined by the Wilhelmy Plate method using a Cahn 312 contact angle analyzer (Cerritos, CA.)

The 50 mL beaker used for DCA analysis was flame dried for 60 seconds and then cooled for 3 minutes prior to adding the interrogating liquid. Surface tension checks were performed to check for glassware contamination before sample immersion. If a particular beaker was contaminated for more than three runs, it was soaked in a 2-propanol /potassium hydroxide base bath overnight, rinsed with Millipore^{TM} water for 30

seconds, and then flamed for 60 seconds prior to use. In order to check for hydrophibicity and oliophobicity, three interrogating liquids were used. Hydrophobicity was investigated using Millipore^{TM} water; n-hexadecane (Acros) and isopropanol (Acros) for oliophobicity. Interrogating liquid surface tensions were checked prior to and after each sample immersion to detect contamination. Typical values were: 72.6 ±0.5 dynes/cm for water and 27.5 ± 1.0 dynes/cm for n-hexadecane.

For DCA analysis, a coated coverslip was hung from the electrobalance by utilizing a small clip. The beaker of the interrogating liquid was placed on the stage and the stage was automatically raised and lowered to let the interrogating liquid impinge upon the slide. Force-Distance curves (fdc) were generated and analyses of these curves yielded advancing (θ_{adv}) and receding (θ_{rec}) contact angles. With DCA analysis, apparent negative net force readings are a result of hydrophobic surfaces, while apparent positive net force readings are indicative of hydrophilic surfaces. Stage speeds were 100 μm/s and dwell times between advancing and receding contact angles were 10 s. Beakers were re-flamed, washed with Millipore water, and filled with fresh interrogating liquid prior to subsequent analyses.

E. References

(1) Singh, A.; Steely, L.; Allcock, H. R. *Langmuir*; **2005**; *21*(25); 11604-11607.

(2) Mack, L. L.; Fitzpatrick, R. J.; Allcock, H. R. *Langmuir*; **1997**; *13*(7); 2123-2132.

(3) Tian, Y.; Ng, Q. Y.; Fendler, J. H. *Langmuir*; **1998**; *14*(11); 3067-3070.

(4) Chen, W.; Fadeev, A. Y.; Hsieh, M. C.; Oner, D.; Youngblood, J.; McCarthy, T. J. *Langmuir*; **1999**; *15*(10); 3395-3399.

(6) Singh, A.; Steely, L.; Allcock, H.R. *Langmuir* **2005**, *21*(25); 11604-11607.

(5) Allcock, H. R.; Steely, L. B.; Singh, A. *Polymer International* **2006**, (55) 621-625.

(7) Allcock, H. R. Chemistry and Applications of Polyphosphazenes. *John Wiley & Sons*, **2003**, 725pages

Chapter 4

Plasma Surface Functionalization of Poly[bis(2,2,2-trifluoroethoxy)phosphazene] Films and Nanofibers

A. Introduction

Many applications are limited by a lack of materials that allow precise tuning of the surface characteristics. Controlled hydrophobic or hydrophilic surfaces are important in biomedicine, adhesion, and general technology. Such properties are already possible using well known high performance polymers, but the degree of surface property tuning is limited because it is closely coupled to the bulk properties. Polyphosphazenes are particularly well suited for a variety of surface applications because of their thermo-oxidative and radiation stability and controllable chemical properties via different side groups linked to the polymer chain. One of the keys to generating and understanding hydrophobic character is the chemical structure of the polymer surface, especially when fluorine is present.[1,2] We focus here on the fluorinated polyphosphazene, poly[bis(2,2,2-trifluorethoxy)phosphazene] **(1)** because of its high fluorine content and good solubility in common organic solvents. By plasma treatment of the polymer surface we have changed the native static water contact angle of 101º from the superhydrophilic range of 5º to the superhydrophobic range of 153º. This was accomplished by using a high throughput atmospheric plasma treatment device which does not require high vacuum to create the plasma field. Instead, this device relies on the gas flow between the charging

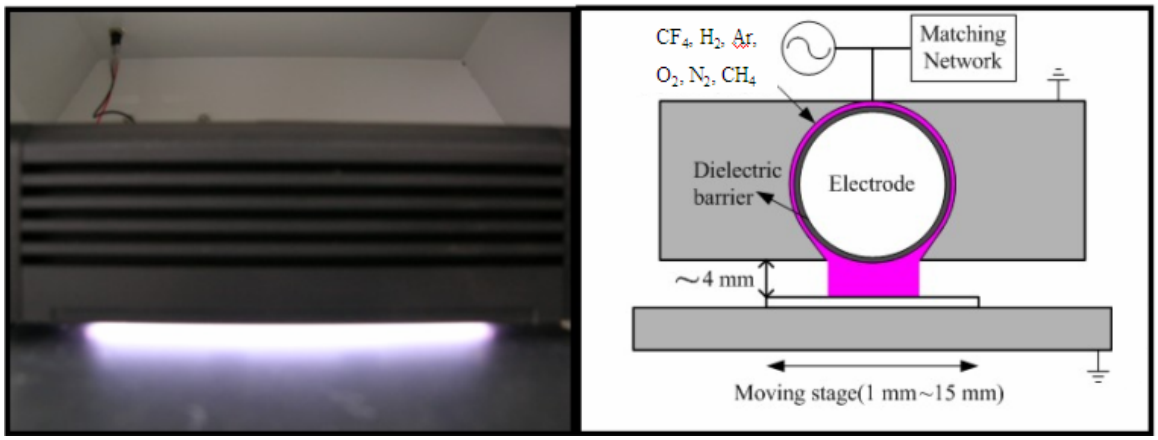

(a) **(b)**

Figure 4-1. (a) Atmospheric RF plasma and (b) schematic diagram of plasma generator.

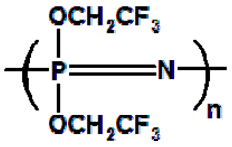

(1)

Figure 4-2. Structure of poly[bis(2,2,2-trifluoroethoxy)phosphazene].

head and the treatment surface to maintain the gas ratio required to create the plasma.[3,4] Surface plasma treatment is especially important for tuning the surface properties of polyphosphazenes because it provides access to high performance materials that have useful mechanical behavior combined with controllable surface characteristics.

B. Results and Discussion

1. Morphology and Hydrophobicity

Plasma treated spuncast films showed no signs of melting, cratering, or defects either macroscopically or under SEM analysis. However, the static water contact angles shown in Table 4-1 revealed that significant changes in the surface chemistry had occurred. The oxygen plasma treated polymer showed the lowest contact angle of 5º. Nitrogen and methane plasma treatments yielded water contact angles of 39º and 68º respectively, which are considered to be hydrophilic and amphiphilic respectively. The CF_4 treatment gave the highest water contact angle of any spuncast polyphosphazene tested, with a value of 151º.

2. Change in Surface Chemistry

XPS analysis revealed large changes in the ratio of surface elements as shown in Table 4-2. The methane plasma treatment appeared to coat the surface with a thin film of carbon. New nitrogen and oxygen signals in the XPS spectra from the oxygen and

Spuncast	Watts	100	100	200	250
Morphology	Rate	10mm/sec	10mm/sec	10mm/sec	10mm/sec
Treatment	Untreated	O_2	N_2	CH_4	CF_4/H_2
WCA	103.42	5.29	39.45	67.65	151.02

Table 4-1. Spuncast static water contact angles.

Atomic %	Bulk	Untreated	100 W 10mm/sec O_2	200 W 10mm/sec CH_4	100 W 10mm/sec N_2
C	28.57	28.25	21.90	84.64	<0.01
N	7.14	7.05	7.71	4.82	11.65
O	14.29	14.90	26.46	9.61	51.46
F	42.86	43.07	34.38	0.92	20.71
P	7.14	6.72	9.54	<0.01	16.18

Table 4-2. XPS survey scan atomic ratios.

nitrogen plasma treatments were readily detected while signals from other elements in the polymer were slightly reduced. This produced a functionalized surface instead of a coating film. The high resolution scans shown in Figure 4-3 illustrate that the methane treatment totally obscured the carbon signal from the polymer side units. Nitrogen and oxygen plasma treatments induced the growth of new peaks associated with the regions where amine and carbonyl groups are found. These peaks were not present in the untreated polymer. We believe that depending on the plasma gas, these new surfaces are comprised of alkyl chains, amino groups, or oxygenated species on the surface of the polymer. It seems likely that these new units are formed by reaction with or displacement of $–OCH_2CF_3$ groups. Reactions with the phosphorus-nitrogen backbone are also possible.

3. Processing Influence on Hydrophobicity

The electrospun fiber mats showed some change in water contact angle after plasma treatment. However, the contact angle changes were less pronounced than in the spuncast films. The lower sensitivity of the nanofibers can be explained by the presence of porous voids filled with air. Each water droplet is mainly in contact with the fiber surface and does not experience the highest levels of hydrophobicity possible. The filaments of the fiber mat provide unbroken lines of contact at the interface of the water droplet.[5] The *beaded* mat morphology provides a discontinuous surface in contact with the water droplet, thus higher hydrophobicity values are generated.[5] The SEM pictures

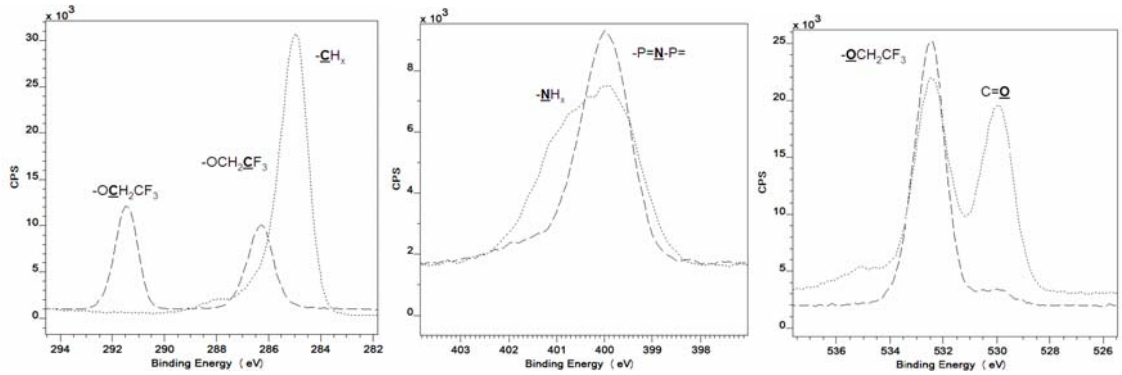

Figure 4-3. XPS spectra of methane, nitrogen, and oxygen surface plasma treated poly[bis(2,2,2-trifluoroethoxy)phosphazene] and an untreated reference (large dash).

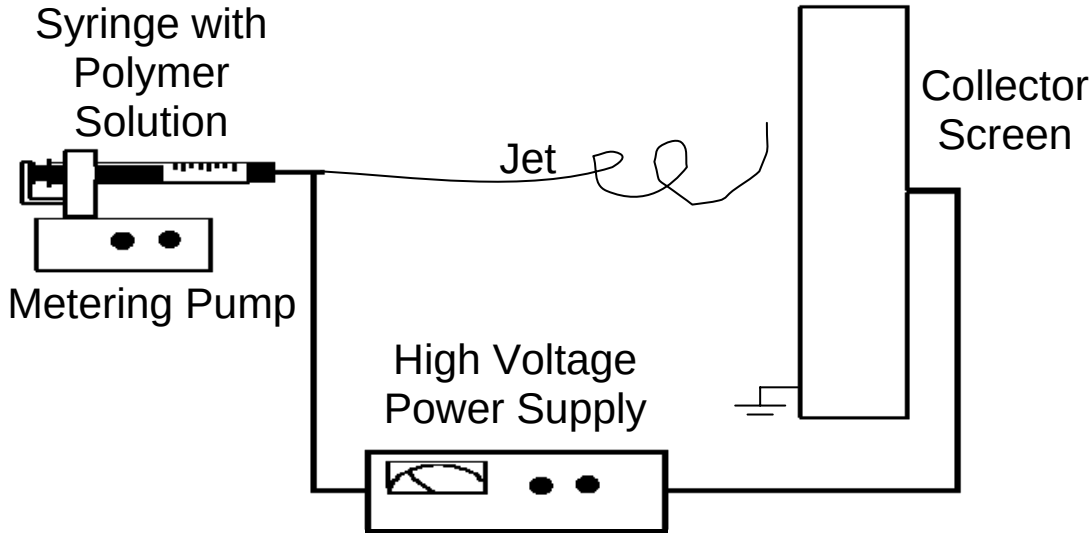

Figure 4-4. Electrospinning device.

illustrate that no fiber melting or damage occurred. Thus, the plasma can modify either flat or rough surfaces without melting or damage to the morphology of the surface.

The fiber mats without beads are considered to have "nanometer-scale roughness" because the surface is a mesh of non-woven fibers. These generate only small differences in mat height where a number of fibers are overlapped. The surface of the fiber mat provides continuous shallow contact with the droplets. As a droplet presses on the outermost fibers of the mat and enters the porous areas, the lower fibers within the pores then come into contact with the droplet.

Electrosprayed bead mats of **(1)** introduced micrometer scale roughness to the system. The bead structure generates a near superhydrophobic surface even before plasma treatment because the beads act as discrete points on the surface tension of the water droplet. This situation was not changed by a CF_4/H_2 or CH_4 plasma because these treatments form a thin coating on the surface of **1,** which hides the native surface. The relationship between types of roughness and the chemical nature of the surface is important for achieving a high water contact angle. However, roughness reduces the changes brought about by surface treatments compared to the films because less surface area acts on the water droplet. Thus, when an ideal discontinuous surface contact morphology is reached, the chemical nature of the rough material has little influence on the surface of a water droplet because roughness allows only the tips of the discrete points to apply tension to the water droplet. As shown in Figure 4-8, the range of water contact angles is largest for the plasma-treated *spuncast* films, which have the highest surface area in contact with the water droplet. The rough surfaces of *fiber mats*, and *bead*

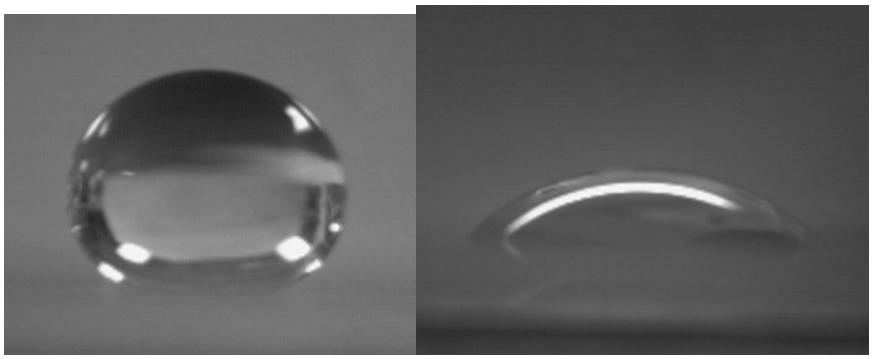

(A) **(B)**

Figure 4-5. (A) CF_4 and (B) N_2 treated poly[bis(2,2,2-trifluoroethoxy)phosphazene] **(1).**

mats generate narrower ranges of water contact angles after plasma treatment due to the decreased influence of chemical surface properties relative to surface roughness.

C. Conclusions

Plasma treatment of polymeric materials derived from polymer **1** generates a variety of hydrophobicity levels from one initial material. The variations in water contact angle that can be obtained from one polymer— poly[bis(2,2,2-trifluoroethoxy)phosphazene] by plasma treatment of films ranged from 5º to 150º in surface water contact angle. The plasma method has some advantages over solution-based surface side group exchange reactions, because no solvent is required and no significant surface morphological changes were detected by SEM.[6,7] The atmospheric plasma method provides a rapid, simple route to enhance the utility of polyphosphazene for surface application, including those required for biomedical materials.

D. Experimental

1. Reagents

The polymer was synthesized under an atmosphere of dry argon using standard Schlenk line techniques. Hexachlorocyclotriphosphazene (Fushimi Pharmaceutical or PCS) was obtained from a trimer-tetramer mixture by sublimation (30 ºC/0.2 mmHg). 2,2,2-Trifluorethanol 99.8% (Acros) and dry sodium stick (Aldrich) were used as

Fiber	Watts	100	100	200	250
Morphology	Rate	10mm/sec	10mm/sec	10mm/sec	10mm/sec
Treatment	untreated	O_2	N_2	CH_4	CF_4/H_2
WCA	132.65	101.80	133.92	145.35	130.28

Table 4-3. WCA of electrospun fiber mats of polymer **1.**

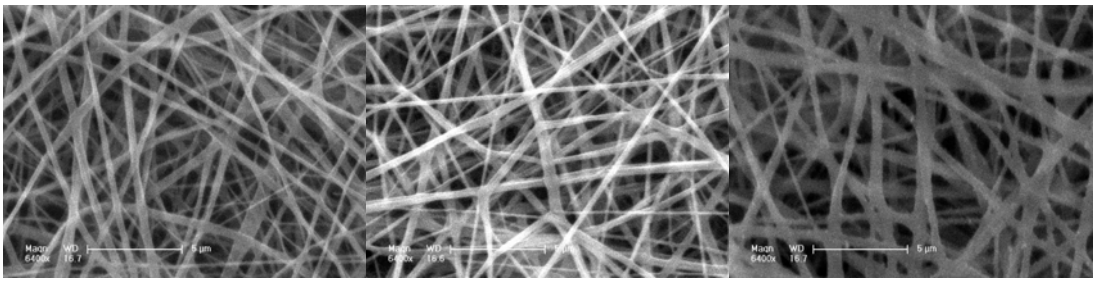

Untreated CH_4 CF_4

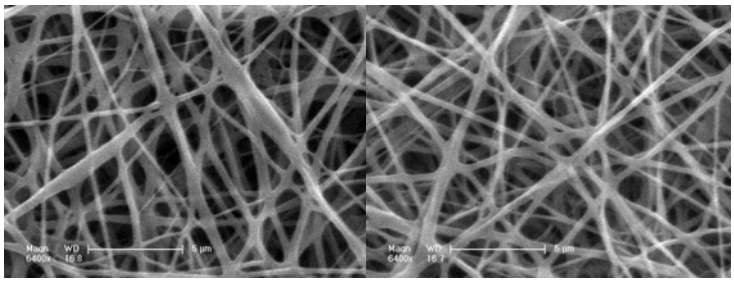

O_2 N_2

Figure 4-6. Electrospun bead/fiber mats of polymer **1.**

received. Tetrahydrofuran was purchased from EM Sciences and was degassed and dried with an alumina bed. Argon, hydrogen, tetrafluoromethane, methane, nitrogen, and oxygen gases were used as received from GT&S Inc.

2. Characterization Equipment

Proton and phosphorus NMR spectra were obtained using a Bruker AMX-360 instrument. Molecular weights were determined using a HP 1090 liquid chromatograph equipped with Phenomenex columns calibrated against polystyrene standards. Glass transition temperatures were determined using a TA Instruments Q10 differential scanning calorimetry (DSC) apparatus with a heating rate of 10 ºC/min under an inert atmosphere. Electrospinning was accomplished with the equipment described previously.[1] The parameters for electrospinning were: a needle tip to ground distance of 20 cm, a flow rate of polymer solution of 1 mL/h, and an applied potential of 15 kV. SEM was conducted using a FEI-Philips XL-20 instrument. XPS spectra were obtained with use of a Kratos Analytical Axis Ultra instrument and the detector was set normal to the surface at 0º. The x-ray gun power was 280 watts. Anode voltage was 14 keV and anode current was 20 mA. The source was monochromatic Al kα X-rays. High resolution scans were taken at a pass energy of 20 eV, with a step size was 0.1 eV. Survey scans were taken at a pass energy of 80 eV, with a step size of 1 eV. Water contact angle measurements were obtained using a Ramé-Hart contact angle goniometer. Water was dispensed from a needle attached to a Gilmont microliter syringe filled with

Bead	Watts	300	300	200	250
Morphology	Rate	10mm/sec	10mm/sec	10mm/sec	10mm/sec
Treatment	Untreated	O_2	N_2	CH_4	CF_4/H_2
WCA	147.14	83.59	128.09	138.19	153.76

Table 4-4. WCA data electrospun bead and fiber mats of poly[bis(2,2,2-trifluoroethoxy)phosphazene] **(1).**

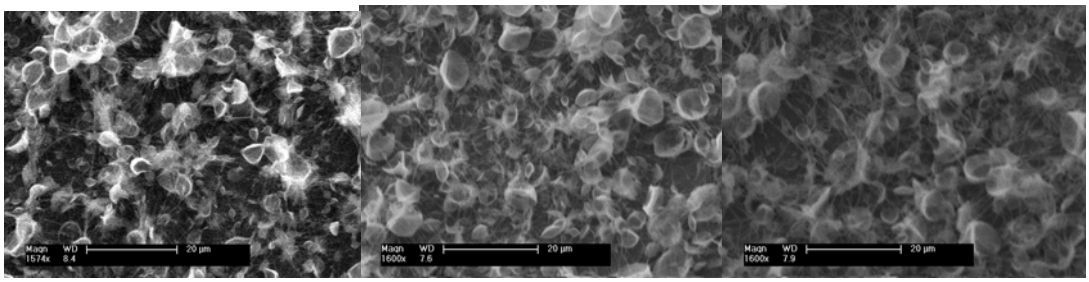

Untreated CH_4 CF_4

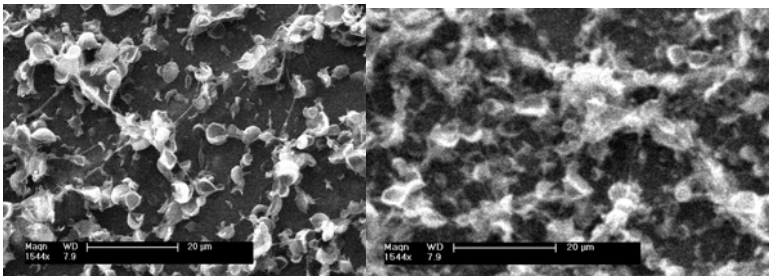

O_2 N_2

Figure 4-7. Electrospun poly[bis(2,2,2-trifluoroethoxy)phosphazene] **(1)** with plasma treatments.

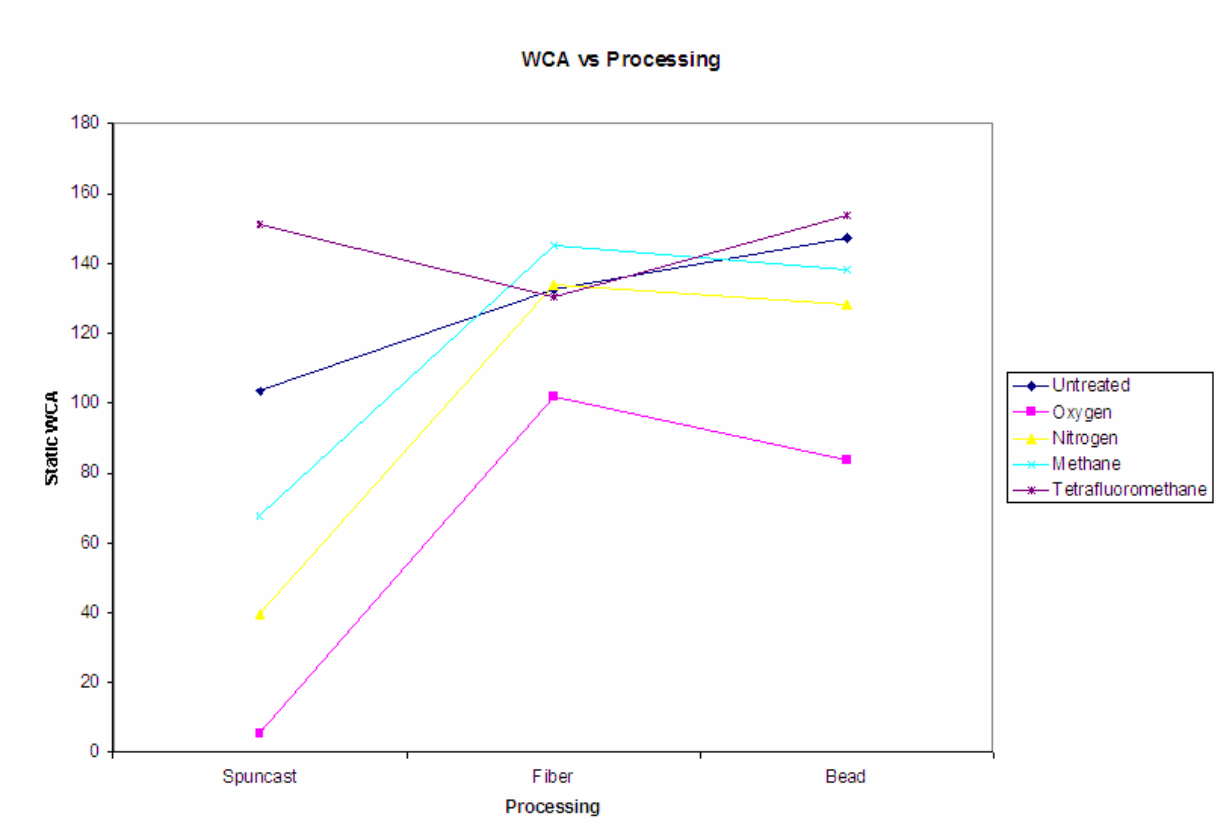

Figure 4-8. Static water contact angle (WCA) of polymer **1** as a function of processing conditions.

ultrapure water (Millipore system, 18 MΩ/cm). Water droplets, 12 μL in size, were placed on the surface and images of the drop silhouette were recorded with a video camera and were stored for analysis on a computer. For static water contact angle measurements, a 10 μL droplet of water was dropped on the surface. The needle was adjusted to allow minimal falling distance for the droplet after detachment from the needle tip via the force of gravity. The reported values are the average of five measurements.

3. Polymer Synthesis

Poly[bis(2,2,2-trifluoroethoxy)phosphazene] **(1)** Sodium 2,2,2 trifluoroethoxide was prepared by the reaction of sodium with 2,2,2-trifluoroethanoxide in THF. This solution was then added to poly(dichlorophosphazene) in THF and the mixture was refluxed for 24 hours.

4. Polymer purification

The insoluble salts were removed from the reaction solution by filtration. The polymer was then isolated by precipitation of a concentrated viscous solution in THF into hexanes. Purification of the polymer was accomplished by repeated, alternating precipitations from THF into hexanes and deionized water (3 times each). ^{1}H NMR (d_8-THF), ppm: δ 4.54 (singlet); ^{31}P (d_8-THF), ppm: δ -5.17 (singlet). Mn 656 000, Mw 1 560 000, PDI 2.38; Tg -62 °C, T (1) 64 °C, Tm 241°C.

5. Spincasting Processing

The polymer was spuncast at 1000 rpm for 60 seconds using dry, uninhibited tetrahydrofuran solutions (2 wt % (wt/v) concentration). Films were allowed to dry at room temperature for 48 hours prior to characterization.

6. Electrospinning Processing

The polymer was electrospun using dry, uninhibited THF solutions (1 wt % (wt/v) concentration) for beaded mats or 5 wt % (wt/v) for fiber only mats. The grounding plate was located 20 cm from the syringe needle tip, and voltages between 13KV-17KV were used as described previously.[1]

7. Plasma Treatment of Polymer Surfaces

The atmospheric RF plasma generator model MyPL-100 (Atmospheric Process Plasma Co, Ltd., Korea) and a 13.56 MHz RF power supply with an L-C matching unit (SEREN Industrial Power System). A representation of the atmospheric RF plasma and a schematic diagram of the plasma generator are shown in Fig. 4-1. The atmospheric RF plasma was generated under glow discharge condition and an arc or streamer was not formed. The usable plasma area is 10 mm wide and 100 mm long. Argon or helium was used as a carrier gas (4 L/min) and O_2, N_2, CH_4, or CF_4/H_2 were used as a reactive gas

(10-20 sccm). The RF power was controlled in the range of 100-250 W. Samples were mounted on a moving stage that traveled about 0.1-0.5 cm below the plasma source along a direction orthogonal to the plasma source head. In this work, the substrate was passed only once across the glow-discharge plasma region at a speed 10 mm/sec.

E. References

(1) Singh, A.; Steely, L.; Allcock, H. R. *Langmuir* **2005**, *21*, 11604.

(2) Allcock, H. R., Steely, L. B., Singh, A. *Polymer International* **2006**, *55*, 621.

(3) Kim, S. H.; Kim, J. H.; Kang, B. K.; Uhm, H. S. *Langmuir* **2005**, *21*, 12213.

(4) Kim, J. H.; Liu, G.; Kim, S. H.; *J. Mater. Chem.* **2006**, *16*, 977.

(5) Chen, W.; Fadeev, A. Y.; Hsieh, M. C.; Oner, D.; Youngblood, J.; McCarthy, T. J. *Langmuir* **1999**, *15*, 3395

(6) Allcock, H. R. *Chemistry and Applications of Polyphosphazenes***;** John Wiley & Sons: Hoboken, New Jersey, 2003.

(7) Allcock, H. R.; Maher, A. E.; Ambler, C. M. *Macromolecules* **2003**, *36*, 5566.

Chapter 5

Foam Formation from Fluorinated Polyphosphazenes by Liquid CO_2 Processing

A. Introduction

Polyurethane foams are currently utilized in many aerospace, automotive, and garment applications. Although inexpensive, many classical urethane based foams are flammable and hydrophilic.[1] We have produced foams of two different fluorinated polyphosphazenes which are known to be fire retardants and hydrophobic.[2,3] These polymers were first plasticized with liquid CO_2 at ~2200 psi in a high pressure reactor. The pressure was then released rapidly to vaporize the CO_2 which expanded to form hollow bubbles in the polymer matrix before diffusing from the polymer. The two polymers examined were poly[bis(2,2,2-trifluoroethoxy)phosphazene] **(1)**, a semi-crystalline elastomer, and poly[$(2,2,2\text{-trifluoroethoxy})_{1.4}$(2,2,3,3,4,4,5,5-octafluoropentoxy)$_{.6}$phosphazene], **(2)** known as PNF or Eypel-F which before crosslinking is an adhesive gum.[2-4] After crosslinking it is an elastomer.

B. Results and Discussion

1. Films Cast on Glass

Thin films of polymer **(1)** and **(2)** were first produced to determine the liquid CO_2 conditions required for solvation. Minimal CO_2 solvation was utilized (~1 minute exposure) so that only minimal cell formation occurred which allowed the plasticization and flattening of the rough film of **(1)** to be observed with SEM in Figure 5-3.

2. Free Standing Films

Polymers **(1)** and **(2)** were then cast into thick films and exposed to liquid CO_2 at 22 ºC and 2200 psi. Release of the pressure yielded expanded foams. Foams were measured after removal from the high pressure reactor, and expansion parameters varied from 53% volume increase for **(2)** to 150% volume increase for **(1)**. Surface samples from each foam were examined by SEM to confirm a closed cell foam structure (Figure 5-4). Polymer **(1)** foam contained cells that expanded and then shrank to yield the wrinkled cell structure in Figure 5-4. Foam cells of **(2)** relaxed into the voids created by the CO_2 expansion.

3. Water Absorption and Flame Test

Foams of **(1)** and **(2)** showed no weight change from water absorption after being soaked for 2 hours in a water bath at 22 ºC. Polymer **(1)** floated on the surface of the water bath as illustrated in Figure 5-5, while polymer **(2)** did not float because of a lower void volume. Samples of polymer **(1)** and **(2)** foams were exposed to a methane flame repeatedly and self-extinguished immediately after removal from the ignition source.

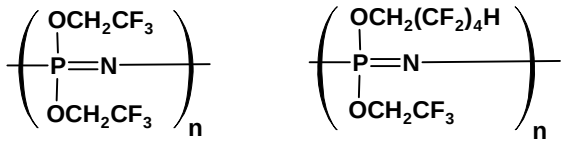

(1) (2)

Figure 5-1. Structures of polymer (1) poly[bis(2,2,2-trifluoroethoxy)phosphazene] and polymer (2) poly[(2,2,2-trifluoroethoxy)(2,2,3,3,4,4,5,5-octafluoropentoxy)phosphazene].

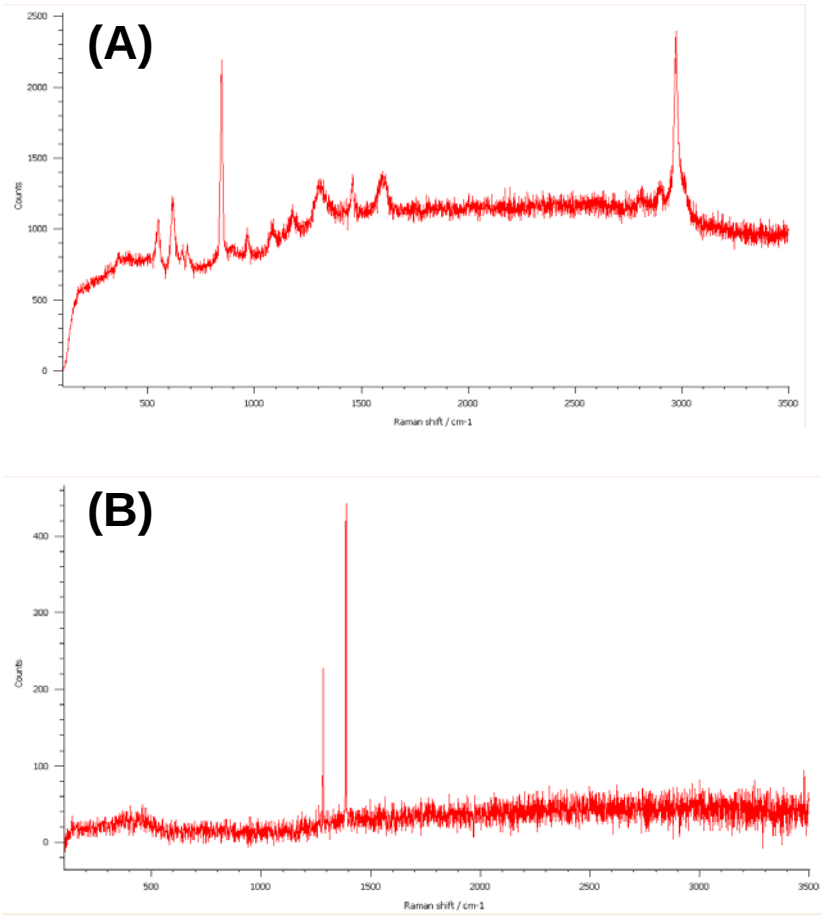

Figure 5-2. (A) Raman spectrum of polymer **(1)** unpressurized and (B) Raman spectrum of polymer **(1)** infused with CO_2 at 2200 psi.

Prolonged exposure for 3-5 seconds melted the surface of the foam to form a waxy coating which dripped from the foam and self-extinguished.

C. Conclusions

The solubility of these polymers in liquid carbon dioxide is almost certainly due to the presence of the fluoroalkoxy side groups, which are readily solvated by the liquid medium. The partial positive charge on the carbon atom of CO_2 is probably attracted to the highly electronegative fluorine atoms in the polymer side groups. In this respect, the behavior of these polyphosphazenes in liquid CO_2 parallels the solubility of other fluorinated macromolecules. This is also consistent with the observation that non-fluorinated polyphosphazenes such as poly(diphenoxyphosphazene) or poly(diethoxyphosphazene) are not swollen by carbon dioxide.

Polymer **1** is a semi-crystalline thermoplastic, with a T_g at -66 ^oC and various T_{LC} transitions at 90 ^oC and a T_m transition near 242 ^oC. Thus, from an applications viewpoint, the white, tough, lightweight foams from polymer **1** could be utilized in non-flammable hydrophobic flotation devices, or in thermal or electrical insulation.[7,8]

The gum-like, adhesive character and absence of crystallinity in polymer **2** means that foams prepared from this polymer must be crosslinked immediately after expansion in order to maximize the useful properties. Free radical crosslinking techniques for this polymer are well developed and could in principle be utilized. To optimize the material for fire-resistance, sound- and vibration-reducing properties, coupled with hydrophobicity.[9,10]

D. Experimental

1. Reagents and Equipment

The polymers were synthesized under an atmosphere of dry argon using standard Schlenk line techniques. Hexachlorocyclotriphosphazene (Fushimi Pharmaceutical or PCS) was obtained from a trimer-tetramer mixture by sublimation (30 ºC/0.2 mmHg). 2,2,2-Trifluorethanol 99.8% (Acros) and dry sodium metal (Aldrich) were used as received. Tetrahydrofuran was purchased from EM Sciences and was degassed and dried with an alumina bed. Dry carbon dioxide gas was used as received. Proton and phosphorus NMR spectra were obtained using a Bruker AMX-360 instrument. Molecular weights were determined using a HP 1090 liquid chromatograph equipped with Phenomenex columns calibrated against polystyrene standards. Raman scattering spectra were collected at room temperature using a Renishaw inVia Raman Microscope (Gloucestershire, GL12 8JR, U.K.) with a CCD detector. SEM was conducted using a FEI-Philips XL-20 instrument.

2. Polymer Synthesis

Poly[bis(2,2,2-trifluoroethoxy)phosphazene] **(1)** was synthesized from sodium 2,2,2 trifluoroethoxide, prepared by the reaction of sodium with 2,2,2-trifluoroethanol in THF. The synthesis of polymer **(2)** utilized the same reagent plus sodium

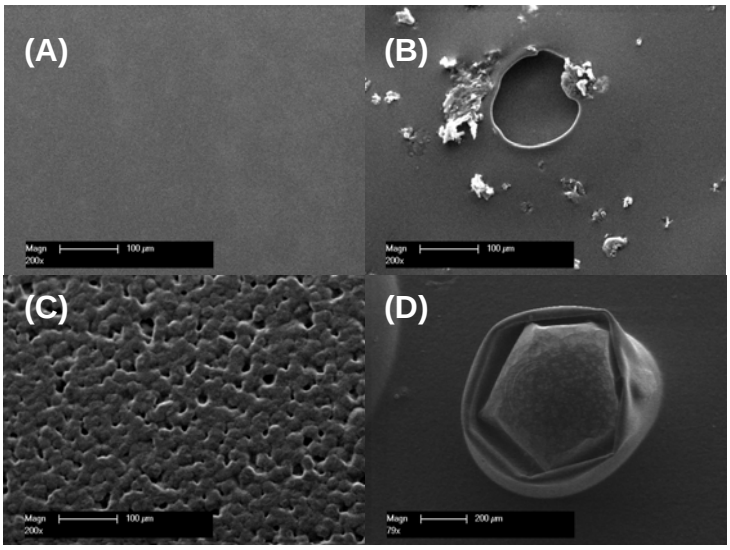

Figure 5-3. SEM of polymer films (A) solution cast **(2)**, (B) CO_2 treated **(2)**, (C) solution cast **(1)**, and (D) CO_2 treated **(1).**

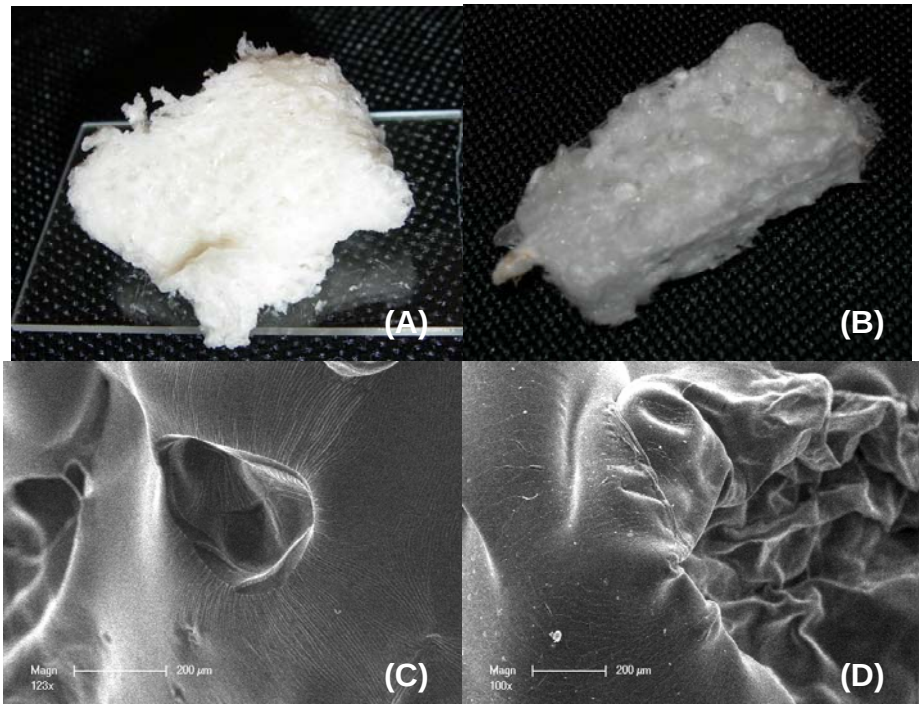

Figure 5-4. (A) Thick film foam of **(2)** (B) thick film foam of **(1)** (C) SEM of **(2)** foam (D) SEM of **(1)** foam.

2,2,3,3,4,4,5,5-octafluoropentoxide prepared by the reaction of sodium with 2,2,3,3,4,4,5,5-octafluoropentanol in THF. The solution of the two salts was then added to poly(dichlorophosphazene) dissolved in THF and the mixture was refluxed for 24 hours. The insoluble sodium chloride was removed from the reaction solution by filtration. The polymer was then isolated by precipitation of a concentrated, viscous solution in THF into hexanes. Purification of the polymer was accomplished by repeated, alternating precipitations from THF into hexanes and deionized water (3 times each).

3. Polymer Characterization

Poly[bis(2,2,2-trifluoroethoxy)phosphazene] **(1)** ^{1}H NMR (d_8-THF), ppm: δ 4.54 (singlet); ^{31}P (d_8-THF), ppm: δ -5.17 (singlet). Mn 656 000, Mw 1 560 000, PDI 2.38. Poly[(2,2,2-trifluoroethoxy)(2,2,3,3,4,4,5,5-octafluoropentoxy)phosphazene] **(2)** with 69.41% of the side groups are 2,2,2-trifluoroethoxy by proton NMR ^{1}H NMR (d_8-THF), ppm: δ 3.85 (2H singlet), δ 4.05 (2H doublet), δ 5.69 (1H singlet); ^{31}P (d_8-THF), ppm: δ -9.62 (singlet). Mn 526 000, Mw 1 317 000, PDI 2.50.

4. Foam Formation

Thin films of polymer **(1)** and **(2)** on 18 mm diameter glass cover slips were placed in a high pressure reactor, which was then filled with liquid CO_2 (2200 psi at 22 ºC). After 1 minute the pressure was released. Bubbles formed in the polymer film as gaseous CO_2 escaped from the plasticized film. Films dimensions were measured before

Figure 5-5. Polymer **(1)** foam floating on water.

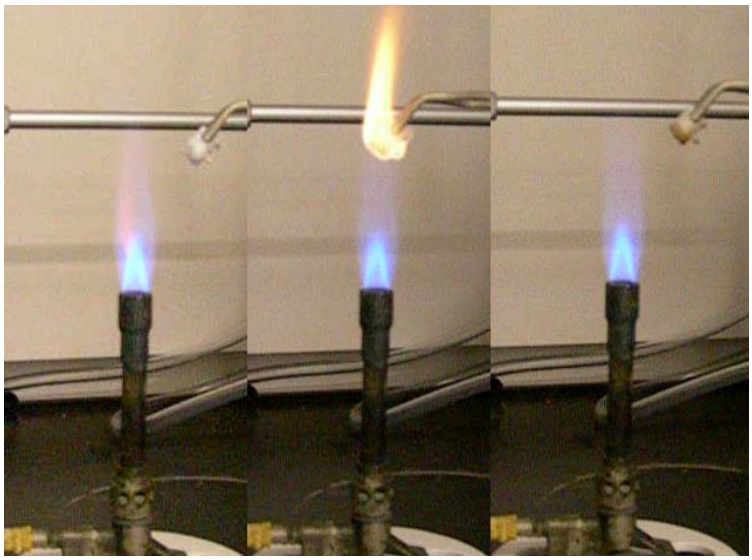

Figure 5-6. Film strip of polymer **(1)** flame test.

and after CO_2 exposure. Thick films were free standing with the dimensions of 2cm x 2cm x 0.5cm before exposure to CO_2. Thick films were exposed to liquid CO_2 (2200 psi at 22 ºC) in a high pressure reactor for 60 minutes before the pressure was released to allow the liquid CO_2 to vaporize.

5. Foam Characterization

Raman spectroscopy was used first to examine **(1)** before CO_2 exposure as seen in Figure 5-2.A. The pressurized Raman spectroscopy sample was contained in a quartz capillary attached to a small pressure chamber with a pressure meter attached. This allowed Raman spectroscopy to be conducted on polymer **(1)** solvated in the CO_2 at 2200 psi. The spectra indicated that the CO_2 signal had diluted the signal from polymer **(1)** (Figure 5-2.B). The bending mode of P-N combined with a P-O mode at 625 cm^{-1} form the only signal associated with the backbone.[5] All other peaks in the Raman spectroscopy of **(1)** are associated with the $–OCH_2CF_3$ group whose assignments were described in detail by Durig, *et al*.[6] After pressure release, SEM revealed that the surface of the resultant foam was smooth in appearance between discreet cavities in the polymer surfaces of both **(1)** and **(2)** (Figure 5-3). Both foams were white and polymer **(2)** showed a volume increase of 53%, while polymer **(1)** showed a volume increase of 150%.

6. Flame Test

A piece from each foam was repeatedly exposed (~1sec per exposure) directly above the blue section of a methane-fueled Bunsen burner flame as shown in Figure 5-6. The foams self-extinguished immediately after removal from the ignition source. After several cycles the surface of the foams melted and dripped from the foam structure. Small droplets burned while in the ignition source then self-extinguished after falling free of the burner flame.

E. References

(1) Hedrick, Glen W.; Green, Acy J. *Ind. Eng. Chem. Prod. Res. Dev.* **1973**, *12*(4), 319-321.

(2) Pike, J. K.; Ho, T.; Wynne, K. J. *Chem. Mater.* **1996**, *8*(4), 856-860.

(3) Allcock, H. R. In *Chemistry and Applications of Polyphosphazenes*; Wiley-Interscience: Hoboken, NJ, 2003;

(4) Singler, Robert E. *Journal of Inorganic and Organometallic Polymers and Materials* **2006**, 16(4), 307-309.

(5) Luther, T. A.; Stewart, F. F.; Budzien, J. L.; LaViolette, R. A.; Bauer, W. F.; Harrup, M. K.; Allen, C. W.; Elayan, A. *J. Phys. Chem. B* **2003**, 107, 3168-3176.

(6) Li, Y. S.; Cox, F. O.; Durig, J. R. *J. Phys. Chem.* **1987**, 91, 1334-1344.

(7) Allcock, H. R.; Maher, A. E.; Ambler, C. M. *Macromolecules* **2003**, 36(15), 5566-5572.

(8) Maher, A. E.; Allcock, H. R. *Macromolecules* **2005**, 38(2), 641-642.

(9) Godfrey, Lenard E. A.; Schappel, Joseph W. *Ind. Eng. Chem. Prod. Res. Dev.* **1970**,

9(4), 426-436.

(10) Reed, C. S.; Taylor, J. P.; Guigley, K. S.; Coleman, M. M.; Allcock, H. R. *Polymer Engineering & Science* **2000**, 40(2), 465-472.

Appendix A

Spontaneous-polymerization of Trichloro-*N*-trimethylsilylphosphoranimine

A. Introduction

1. Cationic Polymerization

A major advantage of polyphosphazenes compared to most other macromolecular systems is the ease with which their properties can be customized by side group substitution reactions.[1] This makes them attractive candidates for numerous applications as biomaterials, flame retardants, high performance elastomers, and energy-related materials.

The traditional access route to polyphosphazenes depends on the reaction of organic or organometallic nucleophiles with the macromolecular intermediate poly(dichlorophosphazene). The use of this methodology has yielded over 700 different polyphosphazenes.[1] The most widely utilized synthesis of poly(dichlorophosphazene) is accomplished by the thermal ring-opening polymerization (at 250ºC) of hexachlorocyclotriphosphazene, although alternative processes have been researched.[2-4] The ring-opening method yields high molecular weight poly(dichlorophosphazene), with degrees of polymerization typically around 15,000 (molecular weights in the range of 1-2

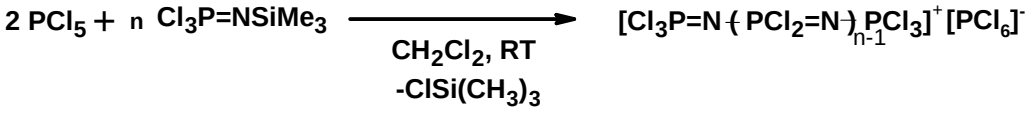

Scheme A-1. Cationic polymerization of phosphoranimine.

x 10^6). This process allows limited control over molecular weight, and the degree of linearity or branching is difficult to control. However, the molecular weight of poly(dichlorophosphazene) produced by this method can be controlled through the use of a Lewis acid initator[5-7], but there is still little control over the molecular weight distribution, and the polydispersities are typically broad.

For these reasons, a room temperature controlled living polymerization method was developed which allows precise control of molecular weights and the possibility of producing several different macromolecule architectures, such as block, comb, and graft copolymers[8-25]. This method involves the cationic polymerization of trichloro-*N*-trimethylsilylphosphoranimine (Scheme A-1).

2. Monomer Storage

The development of this room temperature cationic polymerization has provided improved molecular weight control, low thermal energy input, and both subtle and major architectural control, and makes this process one of the most promising routes for the large-scale production of polyphosphazenes. However, the chlorophosphoranimine monomer undergoes spontaneous self-polymerization during storage for moderate lengths of time, even at -25 ^{o}C under an inert atmosphere. The products of this spontaneous polymerization include both poly(dichlorophosphazene) and hexachlorocyclotriphosphazene.

We have examined the behavior of the phosphoranimine monomer in the liquid state and in a variety of solvents, at two different temperatures (21 ^{o}C and -3 ^{o}C) in an

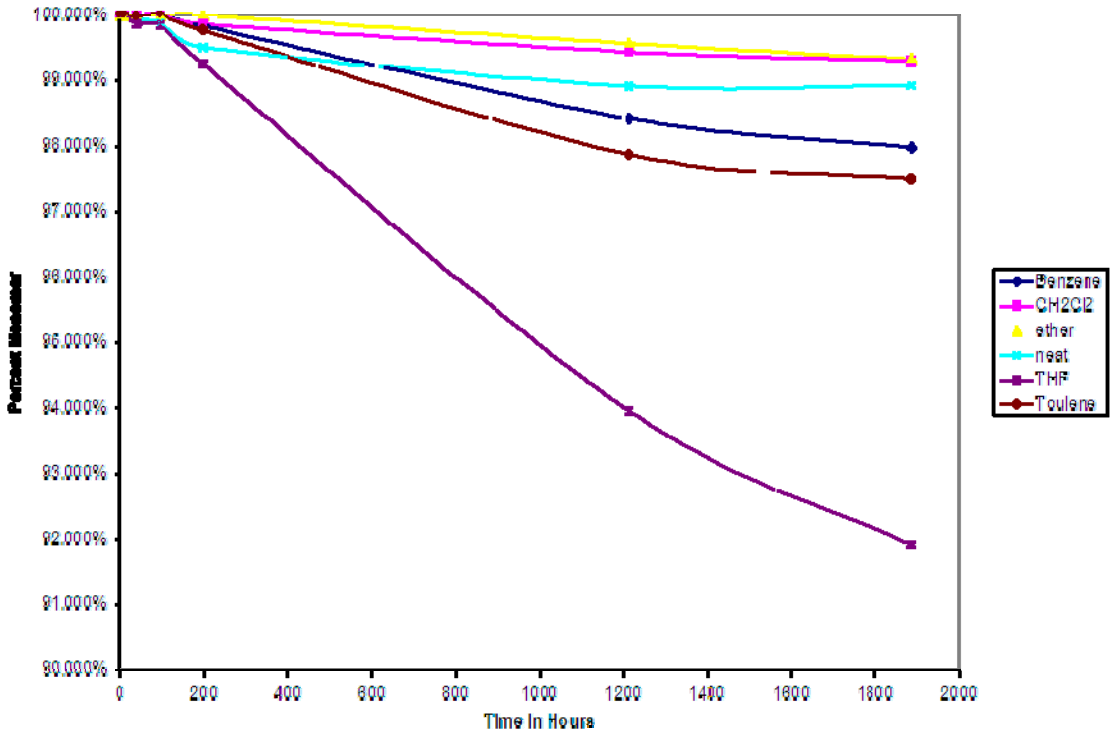

Figure A-1. Trichloro-*N*-trimethylsilylphosphoranimine monomer remaining unpolymerized at -3 ºC (acidic glass surface).

attempt to understand the reaction and prevent spontaneous polymerization during long-term storage. The formation of poly(dichlorophosphazene) and hexachlorocyclotriphosphazene was monitored as a function of time by ^{31}P NMR spectroscopy.

B. Results and Discussion

1. Influence of Reaction Solvent

For samples maintained at -3 ºC (Figure A-1), polymerization of the monomer was fastest in THF, and slowest in dichloromethane or diethyl ether. This suggests that more polar solvents promote the polymerization. It is interesting to note that at low temperature, the undiluted monomer spontaneously-polymerized at the same rate as when it was dissolved in diethyl ether or dichloromethane. Benzene and toluene solvents gave similar reaction rates, which were faster than those in diethyl ether or dichloromethane. Thus, aromatic solvents are effective at inhibiting the polymerization than solvents with more or less polarity that are not aromatic. The water contents of the solvents as measured by Karl Fischer titrimetry (Table A-1) show no relationship between trace water content and rate of polymerization.

The samples at 21 ^{o}C (Figure A-2), polymerized at a much faster rate of reaction than did the samples at -3 ^{o}C. The solvent-free sample polymerized 5% of monomer in 600 hours, and toluene showed the highest conversion on monomer after 600 hours. The

Solvent	Water content (ppm)
Benzene	0.60
CH_2Cl_2	0.63
Ether	2.54
THF	1.48
Toluene	0.27

Table A-1. Water content of solvents measured by Karl Fisher titration.

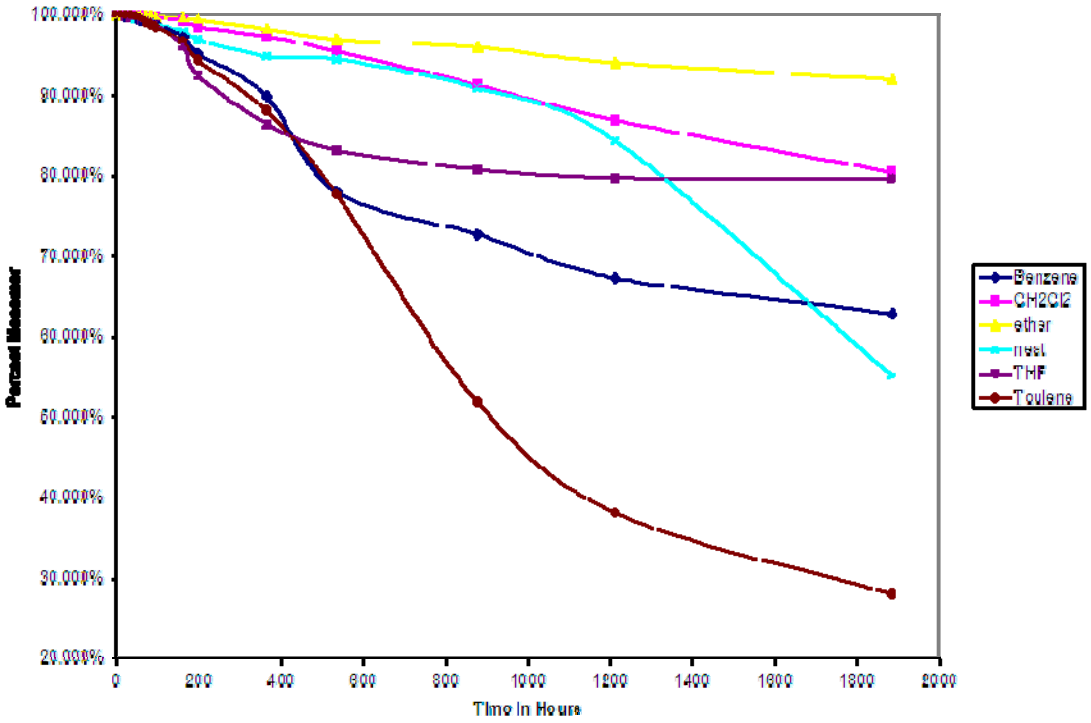

Figure A-2. Loss of Cl-monomer at 21 ºC (acidic glass).

rates of reaction in benzene and toluene were again the highest, and this is consistent with the above postulate that the electronic environment in these solvents promote the polymerization reaction. The solvents in which the rate of reaction was slowest were again dichloromethane and diethyl ether.

The polymerzations in solution all followed the same basic profile, with the rate of reaction slowing as monomer is consumed. The rate of reaction of the solvent-free monomer appears also to follow this profile, but is offset by a slower initial rate of reaction. The reaction rate of the self-polymerization is faster in the solvent-free sample due to the high concentration of the monomer.

In all samples, the formation of linear oligomers were detected with ^{31}P NMR at -17 ppm similar to that of poly(dichlorophosphazene) before the formation of cyclic trimer at 20 ppm. An explanation for this phenomenon is that monomer reacts first to form oligomers with living chain ends. The living chain ends can then react either with more monomer to form polymers, or undergo an intramolecular reaction and cyclize to form the cyclic trimer. As the monomer is consumed, the probability of the cyclization verses linear chain growth increases. This can only happen if the rate of the polymerization reaction is slow – in reactions where the polymerization is catalyzed with PCl_5, the formation of cyclic trimer was not detected. The uncatalyzed, thermal polymerization reaction, however, appear to be slow enough to allow this to happen.

2. Influence of Glass Surfaces

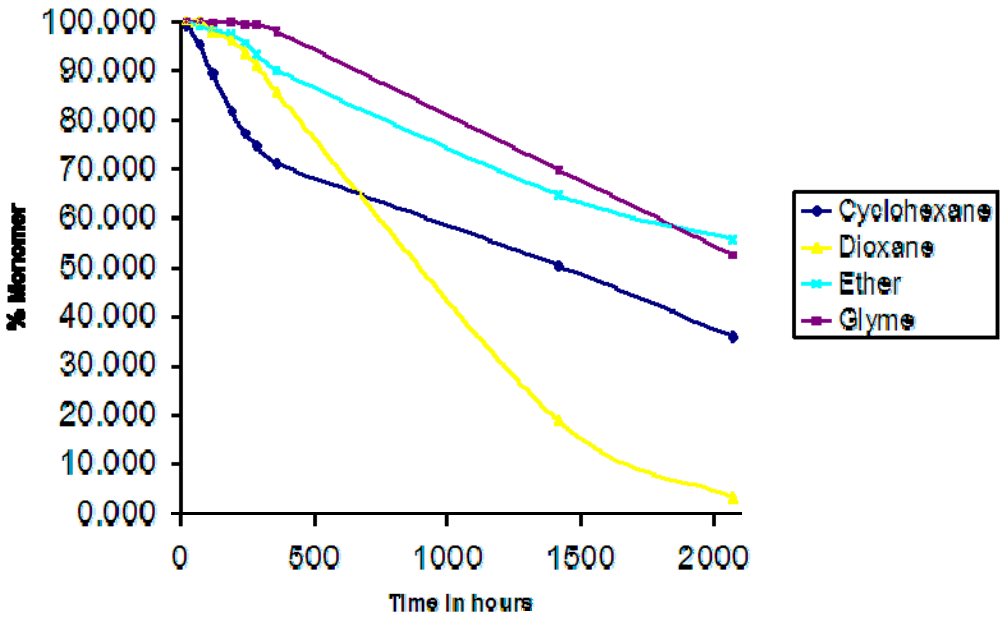

Figure A-3. Loss of Cl-monomer 21 ºC (neutral glass).

In a further study, the solvents that showed increased polymerization rates (benzene, methylene chloride, tetrahydrofuran, and toluene) were replaced, and samples with glyme, dioxane, and cyclohexane as the solvents were prepared. These solvents have been used historically for reactions and storage of

poly(dichlorophosphazene). To eliminate the acidic surface of the glass NMR tubes, the tubes were functionalized with trimethylsilyl groups. Chlorotrimethylsilane was poured in the NMR tube and allowed to react under an inert atmosphere for 30 minutes. The tubes were then dried in a vacuum oven overnight to remove any residual chlorotrimethylsilane or water. It was found that glyme and ether showed the strongest ability to inhibit the spontaneous-polymerization (Figure A-3). The trimethylsilyl functionalized glass NMR tubes did not inhibit the self-polymerization as well as the acidic glass NMR tubes. After 2000 hours in the functionalized NMR tubes, the sample in ether contained approximately 60% of the initial monomer, in comparison to the sample in the non-functionalized NMR tubes, which retained over 90% of the monomer. Consequently, it is postulated that a slightly acidic environment can improve the storage life of the monomer.

Storage of the phosphoranimine in the solid state was investigated. The freezing point of trichloro-*N*-trimethylsilylphosphoranimine was determined by DSC (Figure A-4) to be -55 ^{o}C. This temperature was considered too low to be a viable method for the medium to long term storage of the phosphoranimine. However, in the frozen state in an inert atmosphere it is highly unlikely that any detectable self-polymerization would take place. Any possible initiation step would be slowed as would the following

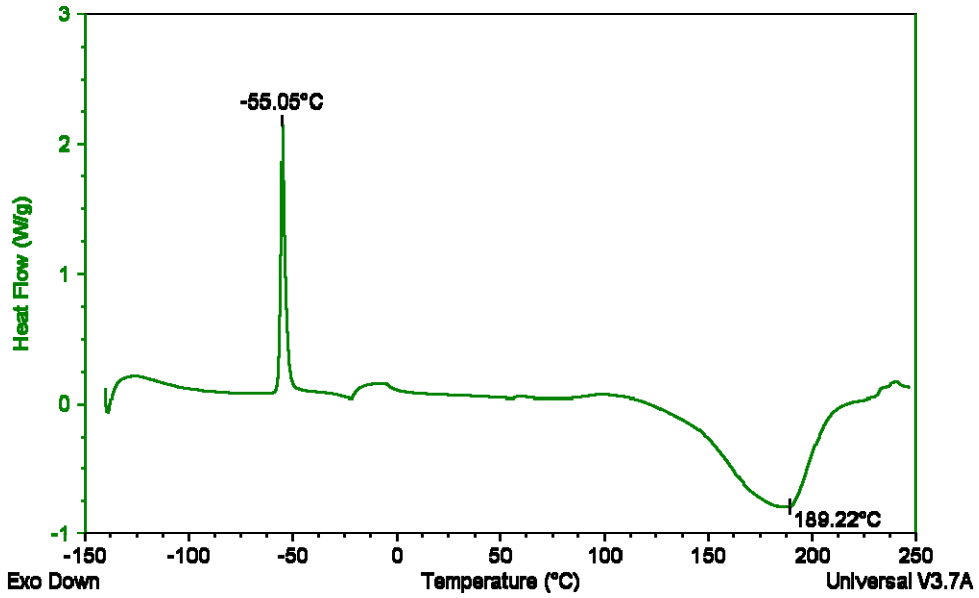

Figure A-4. DSC of trichloro-*N*-trimethylsilylphosphoranimine monomer.

polymerization. Data from the DSC also indicated a broad exothermic transition that peaks at ca. 189 ^{o}C, which is attributed to the thermal polymerization of the phosphoranimine to poly(dichlorophosphazene).

C. Conclusions

The ability to store trichloro-*N*-trimethylsilylphosphoranimine for intermediate lengths of time is a crucial step toward the wider commercialization of polyphosphazenes. Thus, conditions under which trichloro-*N*-trimethylsilylphosphoranimine can be stored were investigated. Several solvents and two different temperatures were examined. It was found that storage of the phosphoranimine at -3 ^{o}C in a typical acidified glass vessel diluted with ether were reasonable storage conditions, under which only 1.2% of the phosphoranimine had been consumed after ~2000 hours. The most likely cause for initiation of polymerization is the deprotection of trimethylsilyl groups from the monomer by attack of HCl. The HCl is produced by reaction of traces of water or hydroxyl groups on the surface of the glass with chlorotrimethylsilane, which is a byproduct of the monomer synthesis. The protected glass test showed earlier polymerization in all solvents. We attribute this to the presence of HCl in the NMR tubes which was not removed by the vacuum oven after protection of the hydroxyl groups with chlorotrimethylsilane. Harsher thermal conditions would have deprotected the glass surface or warped the nmr tubes making them unusable. Further experiments will be needed to investigate possible inhibitors that could be employed for

phosphoranimines as well as the required complimentary synthetic techniques for their removal from the monomer.

D. Experimental Section

1. Reagents

Lithium bis(trimethylsilyl)amide (Aldrich, 97%), phosphorus trichloride (Aldrich, 99%), sulfuryl chloride (Aldrich, 97%), and d_6-acetone (Cambridge Isotope Laboratories, 99.9%) were used as received. Tetrahydrofuran (EMD, 99.99%), diethyl ether (EMD, 99%), dichloromethane (EMD, 99.8%), benzene (EMD, ACS reagent grade), and toluene (EMD, ACS reagent grade) were dried by passage through Glass Contour alumina drying columns before use.[26] The water content of each solvent was evaluated via Karl Fischer titrimetry before use and water concentrations below 3 ppm were found. All chemicals were manipulated in an argon atmosphere drybox.

2. Characterization Equipment

High field ^{1}H (360.14 MHz) and ^{31}P (145.79 MHz) NMR spectra were recorded by use of a Bruker Avance-360 NMR spectrometer, and spectra were referenced to external tetramethylsilane and 85% phosphoric acid respectively. Karl Fischer titrations were performed by use of a Mettler Toledo DL32 Karl Fischer coulometer. Thermal

analysis was performed on a TA Instruments Q10 differential scanning calorimeter calibrated with indium, water, and cyclohexane standards.

3. Sample Preparation

Trichloro-*N*-trimethylsilylphosphoranimine was prepared from PCl_3, $LiN(TMS)_2$, and SO_2Cl_2 according to literature procedures.[27] After several distillations under reduced pressure, the ^{31}P NMR spectrum showed one singlet at -54.74 ppm and the ^{1}H NMR spectrum consisted of one singlet at 0 ppm. Deuterated acetone capillaries were prepared and oven dried under vacuum to remove water from the surface of the glass and ensure an air tight seal of the capillary. NMR tubes were heated and placed under vacuum to remove trace water on the surface of the glass. In an argon filled glovebox each sample was assembled with one acetone capillary inside the NMR tube, chlorophosphoranimine (0.16 mL), and solvent (0.50 mL); except in the case of the solvent free sample where 0.66 mL of chlorophosphoranimine was used in each NMR tube. The tubes containing solutions were capped in the glovebox, then sealed with an oxygen/methane torch. Samples were then stored at -3 ^{o}C ± 0.5 ^{o}C or at 21 ^{o}C ± 1 ^{o}C. Liquid type sample pans were sealed in an argon atmosphere glovebox and tested immediately on a DSC thermal analyzer.

E. References

(1) Allcock, H. R. *Chemistry and Applications of Polyphosphazenes*; Wiley-Interscience: Hoboken, NJ, 2003.

(2) Neilson, R. H.; Wisian-Neilson, P. *Chem. Rev.* **1988**, *88*(3), 541-562.

(3) Neilson, R. H.; Hani, R.; Wisian-Neilson, P.; Meister, J. J.; Roy, A. K.; Hagnauer, G. L. *Macromolecules* **1987**, *20*(5), 910-916.

(4) D'Halluin, G.; De Jaeger, R.; Chambrette, J. P.; Potin, P. *Macromolecules* **1992**, *25*(4), 1254-1258.

(5) Reynard, K. A.; Gerber, A. H. *U. S. Patent 4,005,171*.

(6) Snyder, D. L.; Stayer, M. L.; Kang, J. W. *U. S. Patent 4,123,503*.

(7) Fieldhouse, J. W.; Graves, D. F. *U. S. Patent 4,226,840*.

(8) Sohn, Y. S.; Cho, Y. H.; Baek, H.; Jung, O.-S. *Macromolecules* **1995**, *28*, 7566-7568.

(9) Honeyman, C. H.; Morrissey, C. T.; Manners, I.; Allcock, H. R. *J. Am. Chem. Soc*. **1995**, *117*, 7035-7036.

(10) Allcock, H. R.; Crane, C. A.; Morrissey, C. T.; Nelson, J. M.; Reeves, S. D.; Honeyman, C. H.; Manners, I. *Macromolecules* **1996**, *29*, 7740-7747.

(11) Allcock, H. R.; Nelson, J. M.; Prange, R.; Crane, C. A.; deDenus, C. R. *Macromolecules* **1999**, *32*, 5736-5743.

(12) Prange, R.; Allcock, H. R. *Macromolecules* **1999**, *32*, 6390-6392.

(13) Prange, R.; Reeves, S. D.; Allcock, H. R. *Macromolecules* **2000**, *33*, 5763-5765.

(14) Allcock, H. R.; Cho, S. Y.; Steely, L. B. *Macromolecules* **2006**, *39*(24), 8334-8338.

(15) Allcock, H. R.; Powell, E. S.; Chang, Y.; Kim, C. *Macromolecules* **2004**, *37*(19), 7163-7167.

(16) Allcock, H. R.; Powell, E. S.; Maher, A. E.; Berda, E. B. *Macromolecules* **2004**, *37*(15), 5824-5829.

(17) Allcock, H. R.; Powell, E. S.; Maher, A. E.; Prange, R. L.; de Denus, C. R. *Macromolecules,* **2004**, *37*(10), 3635-3641.

(18) Chang, Y.; Powell, E. S.; Allcock, H. R.; Park, S. M.; Kim, C. *Macromolecules,* **2003**, *36*(7), 2568-2570.

(19) Chang, Y.; Bender, J. D.; Phelps, M. V. B.; Allcock, H. R. *Biomacromolecules,* **2002**, *3*(6), 1364-1369.

(20) Chang, Y.; Prange, R.; Allcock, H. R.; Lee, S. C.; Kim, C. *Macromolecules,* **2002**, *35*(22), 8556-8559.

(21) Allcock, H. R.; Prange, R. *Macromolecules,* **2001**, *34*(20), 6858-6865.

(22) Allcock, H. R.; Prange, R.; Hartle, T. J. *Macromolecules,* **2001**, *34*(16), 5463-5470.

(23) Chang, Y.; Lee, S. C.; Kim, K. T.; Kim, C.; Reeves, S. D.; Allcock, H. R. *Macromolecules,* **2001**, *34*(2), 269-274.

(24) Allcock, H. R.; Reeves, S. D.; Nelson, J. M.; Manners, I. *Macromolecules,* **2000**, *33*(11), 3999-4007.

(25) Prange, R.; Allcock, H. R. *Macromolecules,* **1999**, *32*(19), 6390-6392.

(26) Pangborn, A. B.; Giardello, M. A.; Grubbs, R. H.; Rosen, R. K.; Timmers, F. J. *Organometallics* **1996**, *15*, 1518-1520.

(27) Wang, B.; Rivard, E.; Manners, I. *Inorg. Chem*. **2002**, *41(7)*, 1690-1691.

Appendix B

New Amphiphilic Poly[bis(2,2,2-trifluoroethoxy)phosphazene]/ Poly(propylene glycol) Triblock Copolymers: Synthesis and Micellar Characteristics

A. Introduction

The amphiphilic character of a block copolymer can lead to self-assembly behavior similar to that of low molecular weight ionic surfactants, and this opens numerous avenues for the generation of new properties and uses.[1] Typical micelles have a core comprised of a hydrophobic polymer block and a corona of a hydrophilic polymer block. The simplest material to form this shape is a diblock copolymer with one hydrophobic and one hydrophilic component. More complex and less common micelles utilize triblock copolymers with a single hydrophobic block and two flanking hydrophilic blocks, or vice versa. The micellar characteristics of amphiphilic triblock copolymers depend on the nature of each hydrophilic and hydrophobic block. In principle, the surface properties of self-organized micelles should be highly dependent on the structure of the hydrophilic block. For example, a poly(propylene glycol) (PPG) block would provide more hydrophobicity for micellar aggregates than a poly(ethylene glycol) (PEG) block. On the other hand, the micellar core characteristics would be determined by the structure of the hydrophobic blocks.[2-4] Polyphosphazenes possess an inorganic backbone with two organic groups connected to each phosphorus. These macromolecules generate many

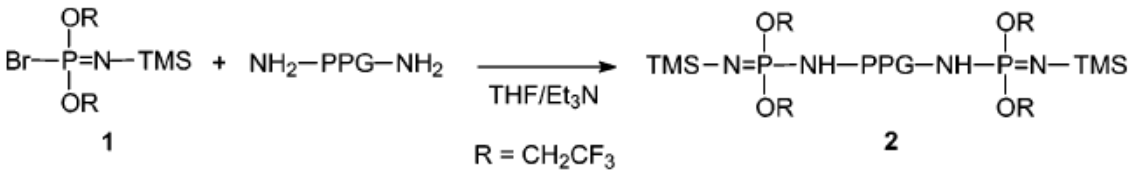

Scheme B-1. Phosphoranimine functionalization of PPG.

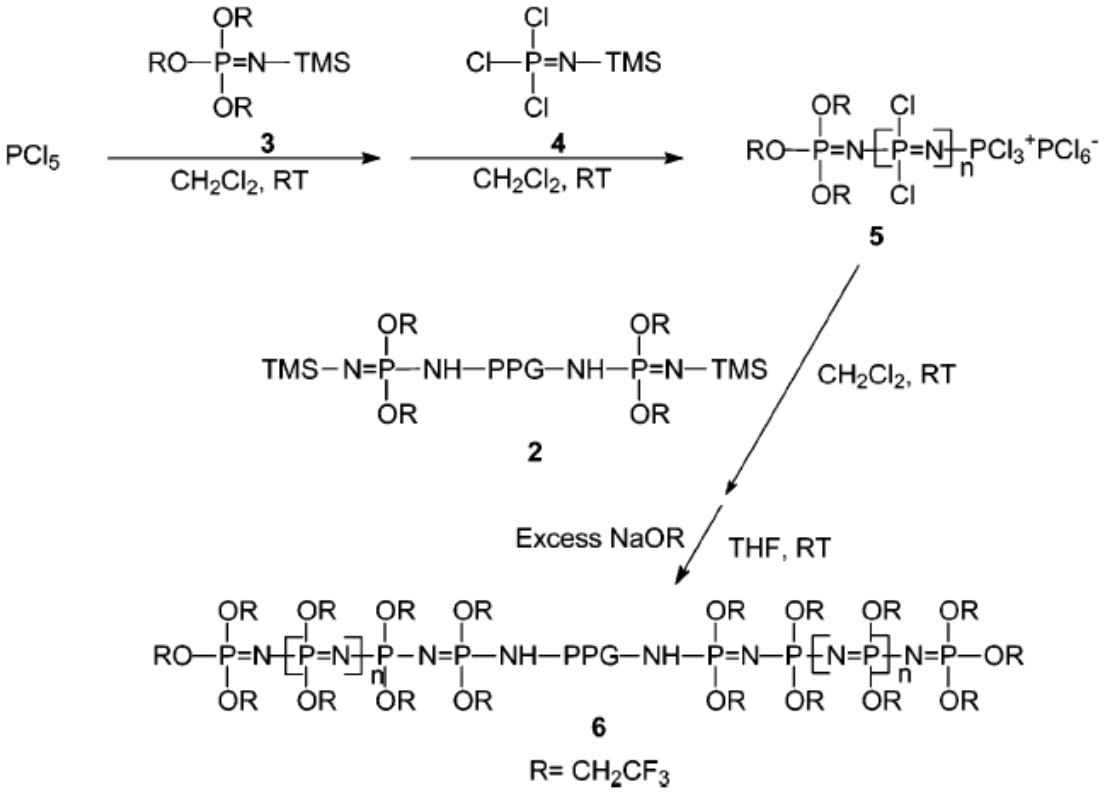

Scheme B-2. Synthesis of PN-PPG-PN block copolymer.

different chemical and physical properties depending on the structure of the side groups. In particular, polyphosphazenes that bear bioinert or biodegradable side groups have attracted much attention as potential biomaterials.[5] An ambient-temperature condensation route for the synthesis of polyphosphazenes via the controlled cationic polymerization of phosphoranimines has been reported.[6-8] This PCl_5-induced polymerization allows the production of a variety of polymeric phosphazene architectures with controlled molecular weights and architectures, including block copolymers.[8] The formation of block copolymers allows fine-tuning of the physical properties through the side-group systems. This present study was focused on a triblock copolymer system with a central organic amphiphilic block of poly-(propylene glycol) flanked by two outer organic/inorganic blocks of hydrophobic polyphosphazenes. The objective was to examine the feasibility that such a polymer might form micelles. PPG was chosen over PEO because of its more amphiphilic characteristics.[9] This work demonstrates that micelles can indeed be formed from such a system and that the micelles vary in size according to the length of the hydrophobic block. These materials are excellent candidates for nanoscale carrier applications such as for hydrophobic dye or pigment incorporation into water-based inks or surface coatings.

B. Results and Discussion

1. ABA Block Copolymer Synthesis

A series of new ABA triblock copolymers of a polyphosphazene and poly(propylene glycol) were prepared by the synthetic procedure illustrated in Schemes B-1 and B-2. Phosphoranimines such as $(CF_3CH_2O)_2BrP{=}NSiMe_3$ (**1**) readily undergo bromine replacement reactions in the presence of amines to produce phosphoranimines such as $RNH(CF_3CH_2O)_2P{=}NSiMe_3$.[6,7] These species can then be utilized as initiators and/or terminators in the cationic living polymerization of $Cl_3P{=}NSiMe_3$. Stoichiometric amounts of amine-terminated poly-(propylene glycol), such as H_2N-PPG-NH_2 were allowed to react with **1** in THF in the presence of triethylamine (Scheme B-1). This process produced the phosphoranimine-terminated poly-(propylene glycol), $Me_3SiN{=}P(OCH_2CF_3)_2NH$-PPG-$NH(CF_3CH_2O)_2P{=}NSiMe_3$ (**2**). Living polyphosphazene **5** can be terminated with triorganophosphoranimines, which allows the controlled introduction of two functional units at the termini of the polyphosphazene chain.[11,12] Thus, compound **2** was employed as a PPG macromolecular terminator for the living polymerization of polyphosphazenes. As illustrated in Scheme B-2, triblock copolymers were prepared by the addition of **2** to **5**. Following termination, the chlorine atoms were replaced by reaction with $NaOCH_2CF_3$ to give PN-PPG-PN triblock copolymer **6**. The molar composition ratios of the repeating units of PPG to polyphosphazene block (*x*:*y*:*z*) in **6** were 0.2:1:0.2 for $PN_{0.2}$-$PPG_{1.0}$-$PN_{0.2}$, 0.4:1:0.4 for $PN_{0.4}$-$PPG_{1.0}$-$PN_{0.4}$, 0.5:1:0.5 for $PN_{0.5}$-$PPG_{1.0}$-$PN_{0.5}$, and 0.7:1:0.7 for $PN_{0.7}$-$PPG_{1.0}$-$PN_{0.7}$. The number average molecular weights of copolymers **6** were estimated by comparing the ^{1}H NMR peak integration ratio of the trifluoroethoxy protons at 4.55 ppm and the methyl protons of PPG at 1.13 ppm (Table B-1). The difference between the conclusions from the GPC and ^{1}H NMR estimates can probably be attributed to the inherent approximations in the GPC analysis.

triblock copolymer[a]	M_n (^{1}H NMR)	block ratio (PN/PPO/PN) feed	block ratio (PN/PPO/PN) found[b]	wt % of hydrophobic block[d]	M_n (M_w/M_n)[c]
$PN_{0.2}$−$PPG_{1.0}$−$PN_{0.2}$	7 600	0.2:1:0.2	0.1:1:0.1	0.09	26 000 (1.32)
$PN_{0.4}$−$PPG_{1.0}$−$PN_{0.4}$	12 000	0.4:1:0.4	0.3:1:0.3	0.55	38 000 (1.33)
$PN_{0.5}$−$PPG_{1.0}$−$PN_{0.5}$	18 000	0.5:1:0.5	0.4:1:0.4	0.74	34 000 (1.35)
$PN_{0.7}$−$PPG_{1.0}$−$PN_{0.7}$	27 000	0.7:1:0.7	0.7:1:0.7	0.89	55 000 (1.25)

[a] All the samples were prepared by using PPG with M_n of 4000 as specified by Aldrich. [b] Calculated from ^{1}H NMR spectra, by comparison of peaks at 4.55 ppm (−OCH_2CF$_3$) to peaks at 1.13 ppm (−OCH$_2$CH(CH_3)−). [c] Measured by GPC. [d] Weight percentage of the hydrophobic PN block in the triblock copolymer.

Table B-1. Properties of the triblock copolymers.

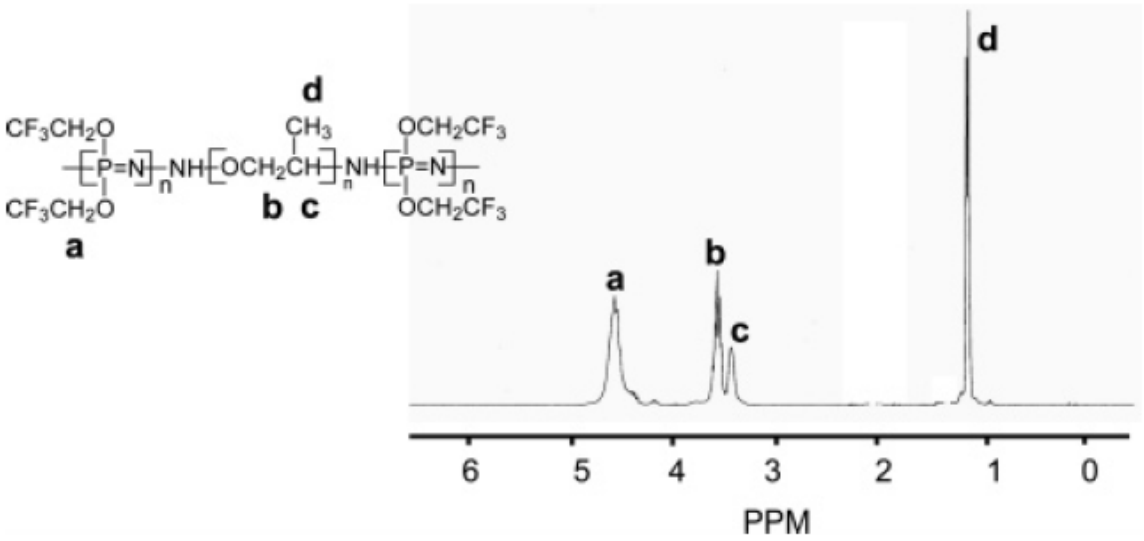

Figure B-1. ^{1}H NMR spectrum of $PN_{0.5}$-$PPG_{1.0}$-$PN_{0.5}$.

The ^{1}H NMR spectrum of $PN_{0.5}$-$PPG_{1.0}$-$PN_{0.5}$ in Figure B-1, as a representative example, shows the characteristic resonance peaks of a PN-PPG-PN triblock copolymer. The PN-PPG-PN triblock copolymers were soluble in THF, acetone, methanol, and DMF but were insoluble in chloroform and *n*-hexane.

2. Self-Association of Triblock Copolymers in an Aqueous Phase

The amphiphilic nature of the triblock copolymers, consisting of PPG flanked by hydrophobic fluoroalkoxyphosphazene blocks, provides an opportunity to form micelles in water. The characteristics of the triblock copolymer micelles in an aqueous phase were investigated by fluorescence techniques, dynamic light scattering, and TEM. The critical micelle concentrations (cmcs) of the triblock copolymers in an aqueous phase were determined by a fluorescence technique using pyrene as a probe.[13-17] In Figure B-2, the excitation spectra of pyrene are shown at various concentrations of $PN_{0.4}$-$PPG_{1.0}$-$PN_{0.4}$. The characteristic feature of the pyrene excitation spectra, the symmetry-forbidden (0,0) band shift from 334 to 336 nm following pyrene partition into the micellar hydrophobic core, was utilized to determine the cmc values of PN-PPG-PN triblock copolymers. For the PN-PPG-PN triblock copolymers, a red shift of (0,0) band from 334 to 336 nm was detected and was utilized to determine the cmc values. Figure B-3 shows the intensity ratios (I_{336}/I_{334}) of the pyrene excitation spectra vs the logarithm of $PN_{0.4}$-$PPG_{1.0}$-$PN_{0.4}$ triblock copolymer concentration. A negligible change of intensity ratios (I_{336}/I_{334}) was detected within a low concentration range, but at a certain concentration, the intensity ratios showed a substantial increase, reflecting the incorporation of pyrene into the

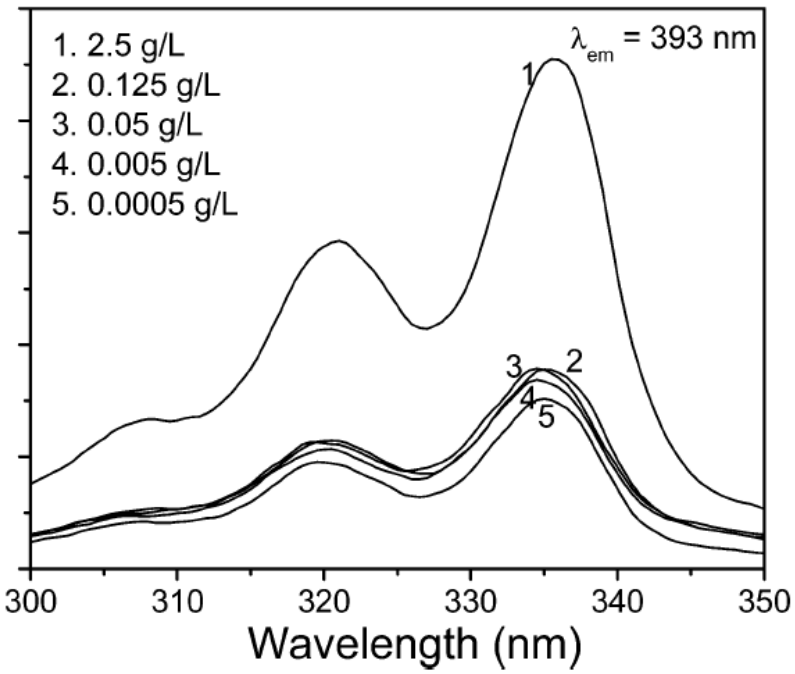

Figure B-2. Excitation spectra of pyrene as a function of $PN_{0.4}$-$PPG_{1.0}$-$PN_{0.4}$ concentration in water. The spectrum of pyrene in pure water is identical to those of the low concentration samples in the figure.

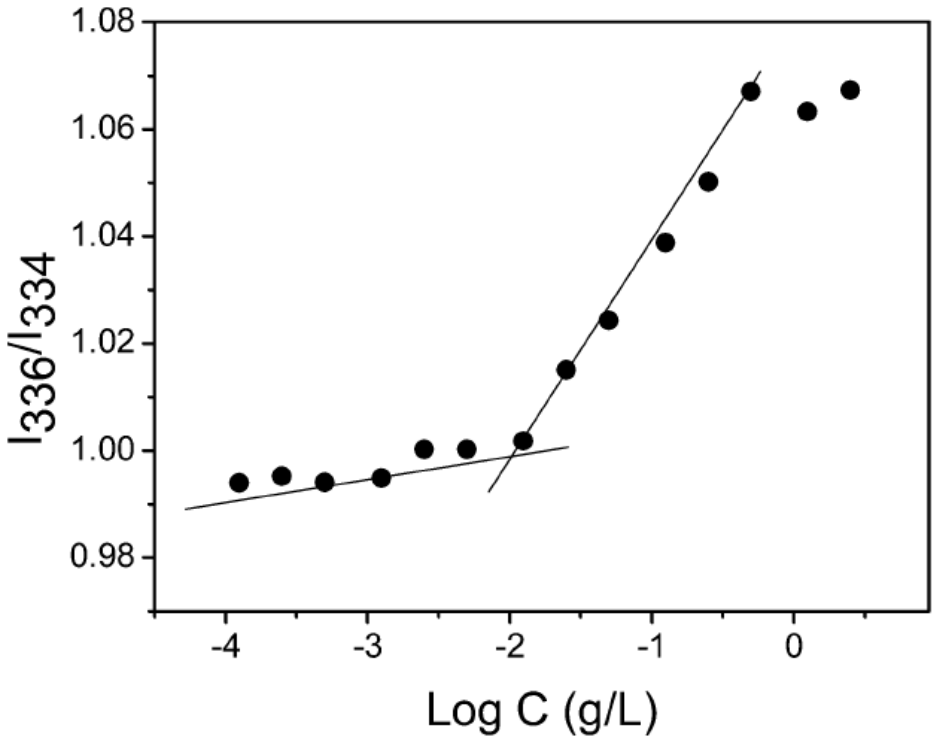

Figure B-3. Plot of I_{336}/I_{334} (from pyrene excitation spectra) vs log C for $PN_{0.4}$-$PPG_{1.0}$-$PN_{0.4}$.

hydrophobic core region of the micelles. Therefore, the cmc was determined from the crossover point at the low concentration range in Figure B-3. The cmc values of the block copolymers were in the range of 9.5-12.4 mg/L depending on the block composition (Table B-2). These values are much lower than those of low molecular weight surfactants (e.g., 2.3 g/L for sodium dodecyl sulfate) but comparable with those of other polymeric amphiphiles.[14-16,18] As the proportion of the hydrophobic phosphazene component became higher, lower cmc values were generated. The mean diameters (*d*) of the block copolymer micelles, measured by dynamic light scattering, were in the range 197-364 nm (Table B-2). The mean diameters of the micelles were not significantly affected by the change in the length of the hydrophobic PN block. Considering the block length in the PN-PPG-PN copolymers and the assumption of a folded triblock copolymer structure in the micelles, this system appears not to generate micelles with *d* values as large as 197-364 nm in an aqueous phase. Therefore, it is suggested that the micelles of PN-PPG-PN are folded in half to maintain the hydrophobic core and a hydrophilic corona (Figure B-4). Larger structures are then formed by association of individual micelles rather than via an enlarged core-shell structure. The polydispersity factors ($\mu_2/\acute{\Gamma}^2$) of the micelles, estimated by the cumulant method, were fairly low (0.11-0.47), which suggests a narrow size distribution.[14,19,20] The size and shape of the micelles formed from PN-PPG-PN triblock copolymers were examined by TEM. Figure B-5 shows micelles formed from a 0.25 g/L solution of $PN_{0.5}$-$PPG_{1.0}$-$PN_{0.5}$. The micelles have a spherical shape, and the estimated diameters are in good agreement with the mean diameters measured using dynamic light scattering.

triblock copolymer	cmc[a] (mg/L)	d^b (nm)	$\mu_2/\Gamma^{2\,c}$	K_v ($\times 10^{-5}$)
$PN_{0.2}$–$PPG_{1.0}$–$PN_{0.2}$	12.4	364	0.26	0.3
$PN_{0.4}$–$PPG_{1.0}$–$PN_{0.4}$	10.8	197	0.47	1.5
$PN_{0.5}$–$PPG_{1.0}$–$PN_{0.5}$	9.8	395	0.11	1.5
$PN_{0.7}$–$PPG_{1.0}$–$PN_{0.7}$	9.5	314	0.15	3.3

[a] Measured at 25 °C. [b] Mean diameters by dynamic light scattering at 25 °C. [c] Polydispersity factor.

Table B-2. Properties of PN-PPG-PN micelles.

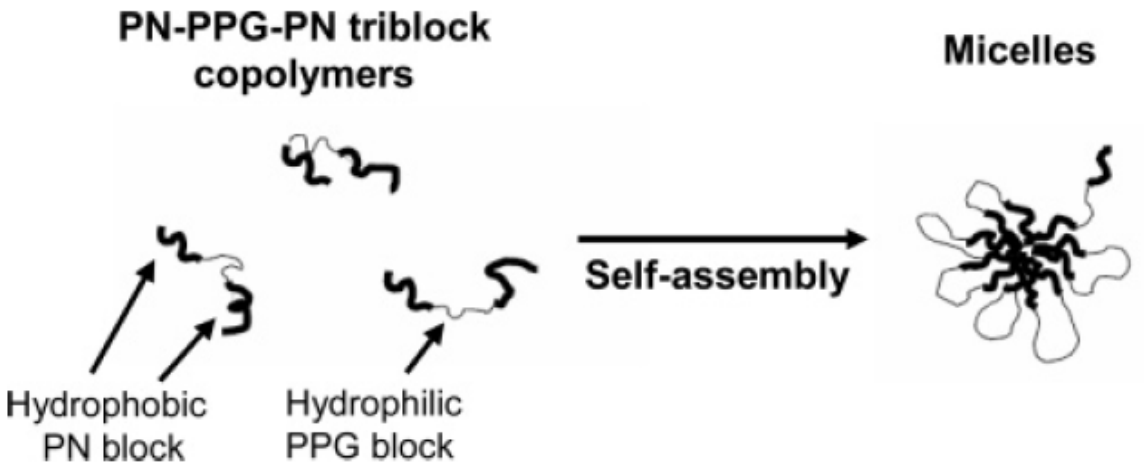

Figure B-4. Schematic representation of micelles formed from PN-PPG-PN triblock copolymers.

3. Partitioning of Pyrene in Micellar Solutions

The hydrophobicity of the micellar core was estimated by measuring the partition equilibrium constant K_v of pyrene, a hydrophobic probe, in the micellar solutions of the triblock copolymers PN-PPG-PNs. In this work, the equilibrium constant K_v was calculated following the method suggested by Wilhelm et al.[13] In this method, pyrene binding to the micelles is considered in terms of a simple equilibrium distribution between a micellar (PN) phase and the water phase. The ratio of the pyrene concentration in the micellar phase to the water phase ($[Py]_m/[Py]_w$) can be correlated to the ratio of volume of each phase as expressed in eq B-1. Equation B-2 can be rewritten as where x is the weight fraction of PN blocks in the triblock copolymer, c is the concentration of the triblock copolymer, and F is the density of the PN core of micelles, which is assumed to be the bulk density of the polyphosphazene (1.10 g/mL). In the intermediate range of polymer concentrations with substantial increases of intensity ratios (I_{336}/I_{334}), $[Py]_m/[Py]_w$ can be written as where F_{max} and F_{min} correspond to the average magnitude of I_{336}/I_{334} in the flat region of the high and low concentration ranges in Figure B-3, and F is the intensity ratio (I_{336}/I_{334}) in the intermediate concentration range of the triblock copolymers. Combining eqs B-2 and B-3, K_v values of pyrene were determined by using a plot $(F - F_{min})/(F_{max} - F)$ vs PN-PPG-PN concentration, as shown in Figure B-6. The K_v values, as summarized in Table B-2, were in the range from 3.0×10^4 to 3.3×10^5 for the PN-PPG-PN system. As the length of the hydrophobic blocks in the copolymers increases, the K_v value increases, suggesting that the hydrophobicities of the micelles also increase.[16] K_v values in the range 1.79×10^5-5.88×10^5 have been reported

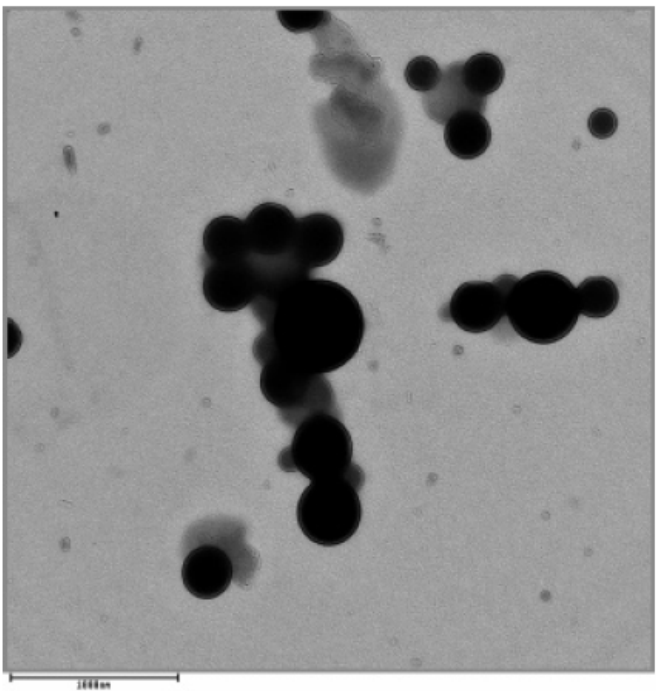

Figure B-5. TEM micrograph of $PN_{0.5}$-$PPG_{1.0}$-$PN_{0.5}$ micelles. The bar indicates 1000 nm.

for poly(2-ethyl-2-oxazoline)-poly(ε-caprolactone) and poly(2-ethyl-2-oxazoline)-poly(L-lactide).[21]

C. Conclusions

Amphiphilic triblock copolymers based on a poly(propylene glycol) as the central block flanked by hydrophobic polyphosphazene blocks were synthesized via the controlled cationic induced polymerization of $Cl_3N{=}PSiMe_3$ at ambient temperature. The block copolymers formed PN-PPG-PN polymeric micelles that self-organized in an aqueous phase. These were examined by using fluorescence techniques, dynamic light scattering, and transmission electron microscopy. The critical micelle concentrations (cmcs) of the PN-PPG-PN polymeric micelles depend on the length of the hydrophobic polyphosphazene block and were in the range 9.5-12.4 mg/L. TEM samples were stained with uranyl acetate From the TEM and dynamic light scattering results, the PN-PPG-PN polymeric micelles were spherically shaped with sizes that ranged between 197 and 364 nm in diameter. The hydrophobicity

of the micellar core was estimated by measurement of the partition equilibrium constant, K_v, of pyrene in the micellar solution of PN-PPG-PN, and the values were in the range from 3.0×10^4 to 3.3×10^5, which were similar to those of other reported polymeric micelles.

D. Experimental

1. Reagents

Poly(propylene glycol)bis(2-aminopropyl ether) ($CH_3CH(NH_2)CH_2$-PPG-NH_2), *M*n 4000) (Aldrich) was used after drying under vacuum. Lithium bis(trimethylsilyl)amide (Aldrich) was used without further purification. Phosphorus pentachloride (Aldrich) was purified by sublimation under vacuum before use. 2,2,2-Trifluoroethanol was dried over calcium hydride and was distilled before use. Tetrahydrofuran and *n*-hexane (Aldrich) were distilled into the reaction flask from sodium benzophenone ketyl under an atmosphere of dry argon. Dichloromethane (Aldrich) was dried by passage through an alumina column. All glassware was flame-dried under vacuum before use. The reactions were performed under an atmosphere of dry argon or nitrogen.

2. Characterization Equipment

^{1}H and ^{31}P spectra were recorded on a Bruker WM-360 NMR spectrometer operated at 360 and 90.27 MHz, respectively. ^{1}H NMR spectra were referenced to solvent signals while ^{31}P NMR chemical shifts are relative to 85% phosphoric acid as an external reference, with positive shift values downfield from the reference. Molecular weights were estimated using a Hewlett-Packard HP 1090 gel permeation chromatograph equipped with an HP-1047A refractive index detector, American Polymer Standards AM gel 10 mm and AM gel 10 mm 104 Å column, and calibrated vs polystyrene standards (Polysciences). The samples were eluted at 40 °C with a 0.1 wt % solution of tetra-*n*-butylammonium nitrate (Aldrich) in THF (OmniSolv).

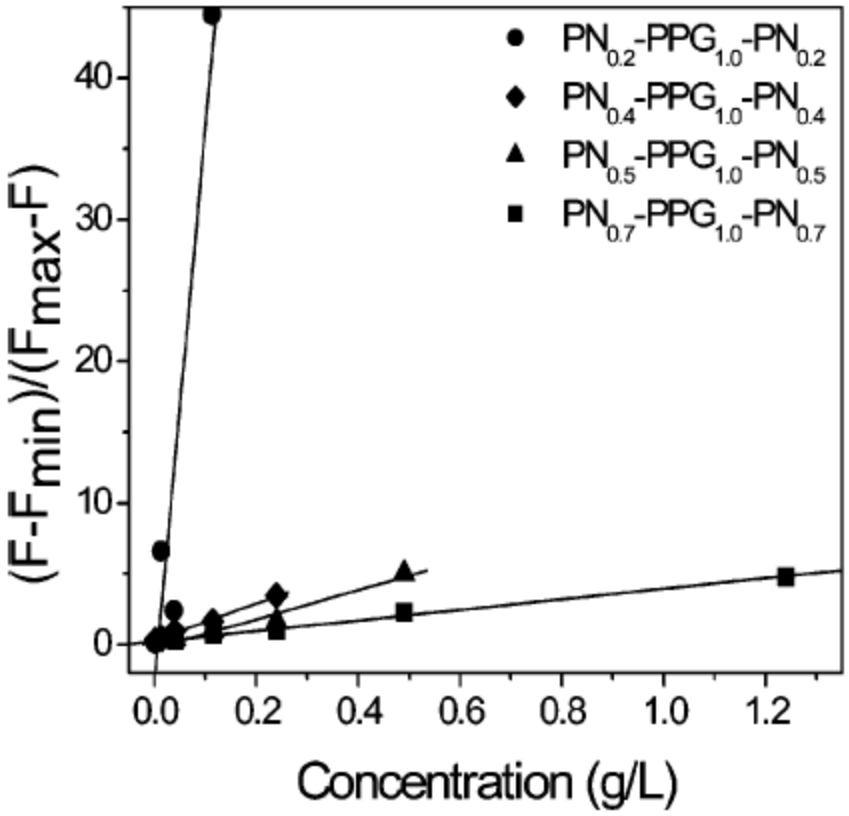

Figure B-6. Plots of (F - Fmin)/(Fmax - F) vs concentration of $PN_{0.2}$-$PPG_{1.0}$-$PN_{0.2}$ (circle), $PN_{0.4}$-$PPG_{1.0}$-$PN_{0.4}$ (diamond), $PN_{0.5}$-$PPG_{1.0}$-$PN_{0.5}$ (triangle), and $PN_{0.7}$-$PPG_{1.0}$-$PN_{0.7}$ (square) in water.

3. Synthesis of Bromophosphoranimine 1

A hexane (700 mL) solution of $LiN(SiMe_3)_2$ (36.55 g, 0.22 mol) was cooled to 0 °C, and PCl_3 (30.00 g, 0.22 mol) was added slowly over 30 min. The reaction mixture was stirred at 0 °C for 1 h and allowed to warm to room temperature followed by stirring for 2 h. Then, a stock solution prepared from $NaOCH_2CF_3$ (0.44 mol; 43.62 g of $HOCH_2CF_3$ and 10.02 g of Na metal) was transferred to the reaction mixture at room temperature. Following addition of the salt, the reaction mixture was stirred at room temperature for 12 h. After completion of the reaction, the mixture was centrifuged for 30 min to remove sodium chloride. The solution was transferred to a round-bottom flask, and the solvent was removed at reduced pressure by rotary evaporation. The remaining solution was vacuum distilled to produce a colorless liquid. The product was dissolved in benzene (200 mL) and cooled to 10 °C. To this solution was added bromine (29.61 g) in benzene (50 mL), and the mixture was stirred at 10 °C for 2 h and allowed to warm to room temperature. The solvent was removed at reduced pressure, and the crude product was vacuum distilled at least twice to remove unreacted bromine and produce a colorless liquid (34.86 g, yield 40%). ^{1}H NMR ($CDCl_3$): δ 0 (s, 9H), 4.23 (q, 4H). ^{31}P NMR ($CDCl_3$): δ -33.93.

4. Synthesis of Trifluoroethoxyphosphoranimine 3

To a solution of bromophosphoranimine **1** (11.63 g, 29.36 mmol) in THF (50 mL)

$$[\mathrm{Py}]_\mathrm{m}/[\mathrm{Py}]_\mathrm{w} = K_\mathrm{v} V_\mathrm{m}/V_\mathrm{w}$$

Equation (B-1)

$$[\mathrm{Py}]_\mathrm{m}/[\mathrm{Py}]_\mathrm{w} = K_\mathrm{v} x(c - \mathrm{cmc})/1000\rho$$

Equation (B-2)

$$[\mathrm{Py}]_\mathrm{m}/[\mathrm{Py}]_\mathrm{w} = (F - F_\mathrm{min})/(F_\mathrm{max} - F)$$

Equation (B-3)

Figure B-7. Equations B-1, B-2, and B-3.

was added a solution of sodium trifluoroethoxide (32.30 mmol) at -78 °C. The reaction mixture was stirred at -78 °C for 1 h and allowed to warm to room temperature. After completion of the reaction, the reaction mixture was passed through a pad of Celite to remove precipitated sodium chloride. The filtrate was collected, and the solvent and excess trifluoroethanol were removed at reduced pressure. The crude product was purified by vacuum distillation (at 40 °C) to yield a colorless liquid (6.10 g, yield 50%). ^{1}H NMR ($CDCl_3$): δ 0.00 (s, 9H), 4.23 (q, 6H). ^{31}P NMR ($CDCl_3$): δ -11.90.

5. Synthesis of Chlorophosphoranimine 4[10]

A solution of $LiN(SiMe_3)_2$ (53.53 g, 0.32 mol) in 700 mL of diethyl ether was cooled to 0 °C, and PCl_3 (43.95 g, 0.32 mol) was added dropwise over 30 min. The reaction mixture was allowed to warm to room temperature and was stirred for 2 h. Sulfuryl chloride (43.19 g, 0.32 mol) was added slowly, and the reaction mixture was stirred at 0 °C for 3 h. After completion of the reaction, the salt was removed by filtration. The crude product was purified by vacuum distillation (30 °C, 0.3 mmHg) to yield a colorless liquid (25.15 g, yield 35%). ^{1}H NMR ($CDCl_3$): δ 0.00 (s, 9H). ^{31}P NMR ($CDCl_3$): δ -54.10.

6. Synthesis of Triblock Copolymers 6

A mixture of NH_2-PPG-NH_2 (2.10 g, 0.53 mmol) and triethylamine (0.10 g) in THF (100 mL) was cooled to 0 °C. To this solution was added dropwise $(CF_3CH_2O)_2BrP{=}NSiMe_3$ (0.42 g, 1.05 mmol) over a 30 min period. The reaction mixture was stirred for 12 h at room temperature. All volatiles and solvent were removed under reduced pressure to produce a yellow viscous liquid. This end-functionalized product was dissolved in CH_2Cl_2 for further reaction. In a separate reaction vessel, PCl_5 (0.44 g, 2.10 mmol) was dissolved in 50 mL of distilled CH_2Cl_2 at room temperature. The end-capper reagent $(CF_3CH_2O)_3P{=}NSiMe_3$ (0.44 g, 14.70 mmol) was added to the solution, which was stirred for 1 h at room temperature. The monomer, $Cl_3P{=}NSiMe_3$ (3.30 g, 9.62 mmol), was then added to the reaction mixture which was stirred for 2 h to generate "living" poly(dichlorophosphazene) chains. The solution of PPG-phosphoranimine in CH_2Cl_2 was then added to the polyphosphazene solution, and the mixture was stirred for 10 h at room temperature to terminate the polymerization. The CH_2Cl_2 was removed from the reaction mixture under reduced pressure, and the polymer was redissolved in 25 mL of freshly distilled THF. An excess of $NaOCH_2CF_3$ (34.65 mmol) in THF was added to the polymer solution to replace the labile chlorine atoms in the phosphazene blocks. The reaction mixture was stirred at room temperature until ^{31}P NMR spectroscopy indicated complete replacement of the chlorine atoms. The reaction solution was then concentrated and precipitated repeatedly from THF into deionized water and into hexanes. The polymer was purified again by dialysis against EtOH/H_2O (4/1 vol/vol), followed by drying under reduced pressure to give a viscous yellowish liquid.

7. Micellar Sample Preparation

To prepare micellar solutions, Nanopure water with a conductivity of 18.2 MΩ/cm (10 mL) was added dropwise to a stirred THF solution of the triblock copolymer (10 mL). The THF was removed on a rotary evaporator at 30 °C for 2 h. The micellar solution was diluted with Nanopure water to obtain a concentration range from 5 x 10^{-4} to 1 x 10^{-4} g/L. For the measurement of fluorescence spectra, a pyrene solution in THF (1.2 x 10^{-3} M) was added to Nanopure water to give a pyrene concentration of 12x10^{-7} M, and THF was removed using a rotary evaporator at 30 °C for 2 h. The pyrene solution was mixed with the triblock copolymer solutions to obtain copolymer concentrations from 2.5 x 10^{-4} to 1.25 x 10^{-4} g/L. The pyrene concentration of the samples was 6.0 x 10^{-7} M. All the samples were sonicated for 15 min and were allowed to stand for 2 days before fluorescence measurements.

8. Fluorescence and Light Scattering Measurements

The fluorescence spectra were obtained using a Perkin-Elmer LS 55 spectrofluorometer. For the measurement of pyrene excitation spectra, emission and excitation bandwidths were set at 5 nm each, and the emission wavelength was set at 393 nm.

The sizes and size distributions of the triblock copolymer micelles were evaluated by dynamic light scattering (DLS) using a particle size analyzer (BI-90 Plus, Brookhaven Instruments Corp., Holtsville, NY) with a scattering angle of 90°. Samples were filtered

through a 0.45 μm syringe filter before measurement of particle size for each sample. Measurements were conducted at room temperature (25 °C).

E. References

(1) Edens, M. W. *Surfactant Sci. Ser.* **1996**, *60*, 185.

(2) Kwon, G. S.; Suwa, S.; Yokoyama, M.; Okano, T.; Sakurai, Y.; Kataoka, K. *J. Controlled Release* **1994**, *29*, 17.

(3) Gao, Z.; Varshney, S. K.; Wong, S.; Eisenberg, A. *Macromolecules* **1994**, *27*, 7923.

(4) Yu, K.; Eisenberg, A. *Macromolecules* **1996**, *29*, 6359.

(5) (a) Allcock, H. R.; Pucher, S. R.; Turner, M.; Fitzpatrick, R. *Macromolecules* **1992**, *25*, 5573. (b) Allcock, H. R.; Dudley, G. K. *Macromolecules* **1996**, *29*, 1313.

(6) Honeyman, C. H.; Manners, I.; Morrissey, C. T.; Allcock, H. R. *J. Am. Chem. Soc.* **1995**, *117*, 7035.

(7) Nelson, J. M.; Allcock, H. R.; Manners, I. *Macromolecules* **1997**, *30*, 3191.

(8) (a) Allcock, H. R.; Reeves, S. D.; Nelson, J. M.; Crane, C. A. *Macromolecules* **1997**, *30*, 2213. (b) Nelson, J. M.; Primrose, A. P.; Hartle, T. J.; Allcock, H. R. *Macromolecules* **1998**, *31*, 947.

(9) Schild, H. G.; Tirrell, D. A. *J. Phys. Chem.* **1990**, *94*, 4352.

(10) Wang, B.; Rivard, E.; Manners, I. *Inorg. Chem.* **2002**, *41*, 1690.

(11) Allcock, H. R.; Nelson, J. M.; Prange, R.; Crane, C. A.; de Denus, C. R. *Macromolecules* **1999**, *32*, 5736.

(12) Prange, R.; Allcock, H. R. *Macromolecules* **1999**, *32*, 6390.

(13) Wilhelm, M.; Zhao, C.; Wang, Y.; Xu, R.; Winnik, M. A.; Mura, J.; Riess, G.; Croucher, M. D. *Macromolecules* **1991**, *24*, 1033.

(14) Nagasaki, Y.; Okada, T.; Scholz, C.; Iijima, M.; Kato, M.; Kataoka, K. *Macromolecules* **1998**, *31*, 1473.

(15) Kwon, G. S.; Naito, M.; Yokoyama, M.; Okano, T.; Sakurai, Y.; Kataoka, K. *Langmuir* **1993**, *9*, 945.

(16) Kabanov, A. V.; Nazarova, I. R.; Astafieva, I. V.; Batrakova, E. V.; Alakhov, V. Y.; Yaroslavov, A. A.; Kabanov, V. A. *Macromolecules* **1995**, *28*, 2303.

(17) Astafieva, I.; Zhong, X. F.; Eisenberg, A. *Macromolecules* **1993**, *26*, 7339.

(18) Phillips, J. N. *Trans. Faraday Soc.* **1955**, *51*, 561.

(19) Harada, A.; Kataoka, K. *Macromolecules* **1995**, *28*, 5294.

(20) Harada, A.; Kataoka, K. *Macromolecules* **1998**, *31*, 288.

(21) Chang, Y.; Lee, S. C.; Kim, K. T.; Kim, C.; Reeves, S. D.; Allcock, H. R. *Macromolecules* **2001**, *34*, 269.

Appendix C

Ionically Conductive Polynorbornenes with Pendent Sulfonimide/Methoxyethoxyethoxy Bearing Cyclotriphosphazene Units

A. Introduction

Many polyphosphazene-based materials have been synthesized in an attempt to find an appropriate combination of low glass transition temperature and high ion conductivity. Linear alkyl ether substituted polyphosphazenes with dissolved lithium salts are known to be ionically conductive at least partly through cation transport between the alkyl ether side groups.[1,2] Polynorbornenes with cyclotriphosphazene pendent units that bear methoxyethoxyethoxy side groups have also been synthesized.[3] Previous studies of these systems focused on membranes with non-bound lithium salts in the system (ie. polymers doped with lithium salts). These systems are limited by the solubility of the salts in the polymer matrix, the tendencies for ion aggregation, and the high T_g values that are generated at high salt concentrations. Moreover, for lithium-seawater primary batteries, the possibility exists that the salt may diffuse from the membrane and limit the usefulness of the device. A polymer with the counter anion to lithium covalently bonded to the polymer might allow higher loadings of lithium and thus generate higher conductivities, and should prevent loss of the salt over extended periods of time. In this work the sulfonimide group was chosen as the immobilized anion unit. Cyclotriphosphazene units pendent to a polynorbornene chain were employed to allow a

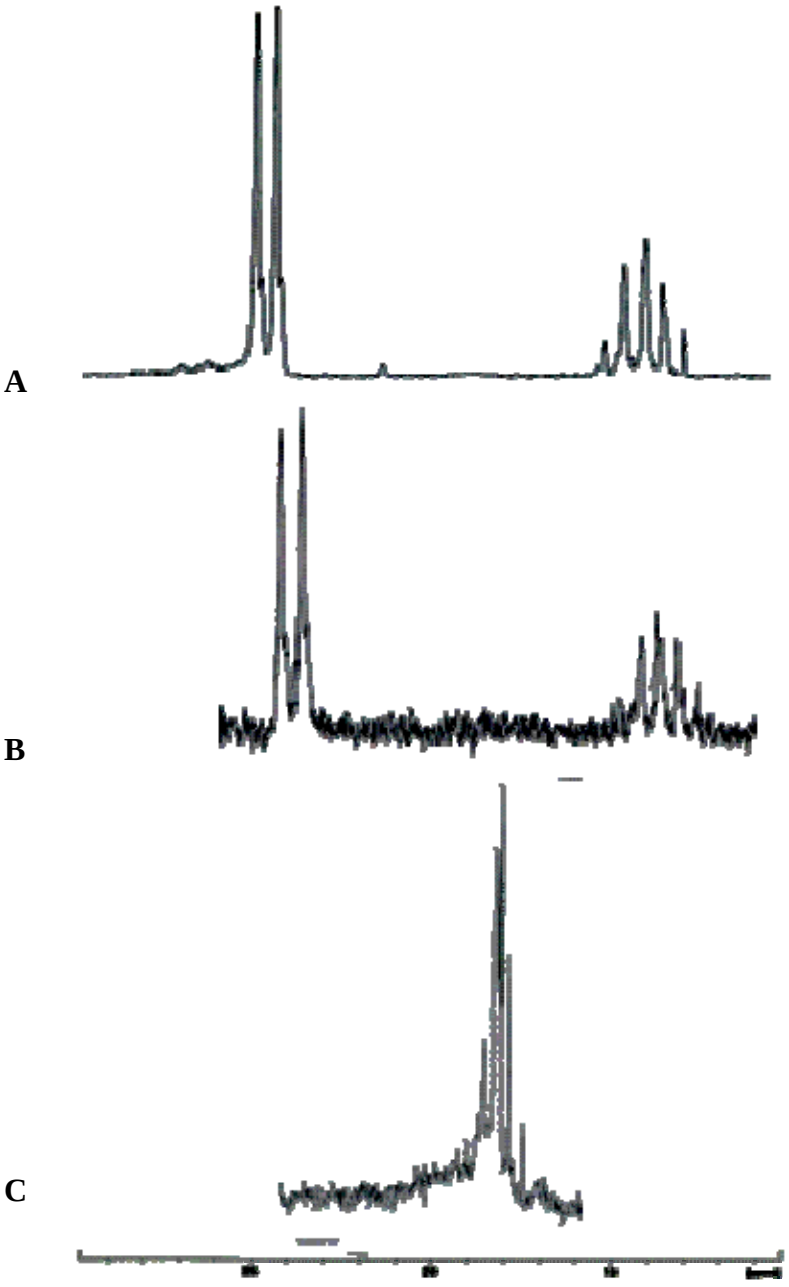

Figure C-1. ^{31}P NMR spectra of (A) the unsubstituted pentachlorocyclophosphazene polymer, (B) 5% sulfonimide substitution, and (C) 5% sulfonimide 95% methoxyethoxyethoxy substituted polymer.

high loading of covalently bound anions (a maximum of five anion units per polymer repeat unit). This allowed the earlier maximum loading of two lithium sulfonimide groups per repeat unit in linear classical polyphosphazenes to be raised, thus increasing the lithium ions available for conductivity. This allowed comparisons to be made with classical linear polyphosphazenes that were doped with unbound lithium sulfonimide salts.[4]

B. Result and Discussion

1. Lithium Ion Conductivity

The conductivity of a polymeric electrolyte is limited by (1) the number of mobile lithium ions in the system and (2) the ease with which the lithium ions can move between the cathode and anode. The ease of cation diffusion depends on the re-orientational freedom of polymer components to which the lithium ions are loosely coordinated. In turn this depends on the glass transition temperature, T_g, and the presence or absence of coordinative solvents. The norbornene backbone probably plays no role in lithium ion solvation. Instead the etheric oxygen atoms in the methoxyethoxyethoxy groups or in a propylene carbonate solvent can serve as electron donors for lithium cation solvation. The immobilized sulfonimide salt used in this work acts as the lithium ion source for the polymer. In this work, the unplasticized polymers with immobilized sulfonimide loadings higher than 20 % showed no ionic conductivity (above 10^{-7} S/cm), because they possess insufficient free volume for lithium ion transport due to the rigidity of the

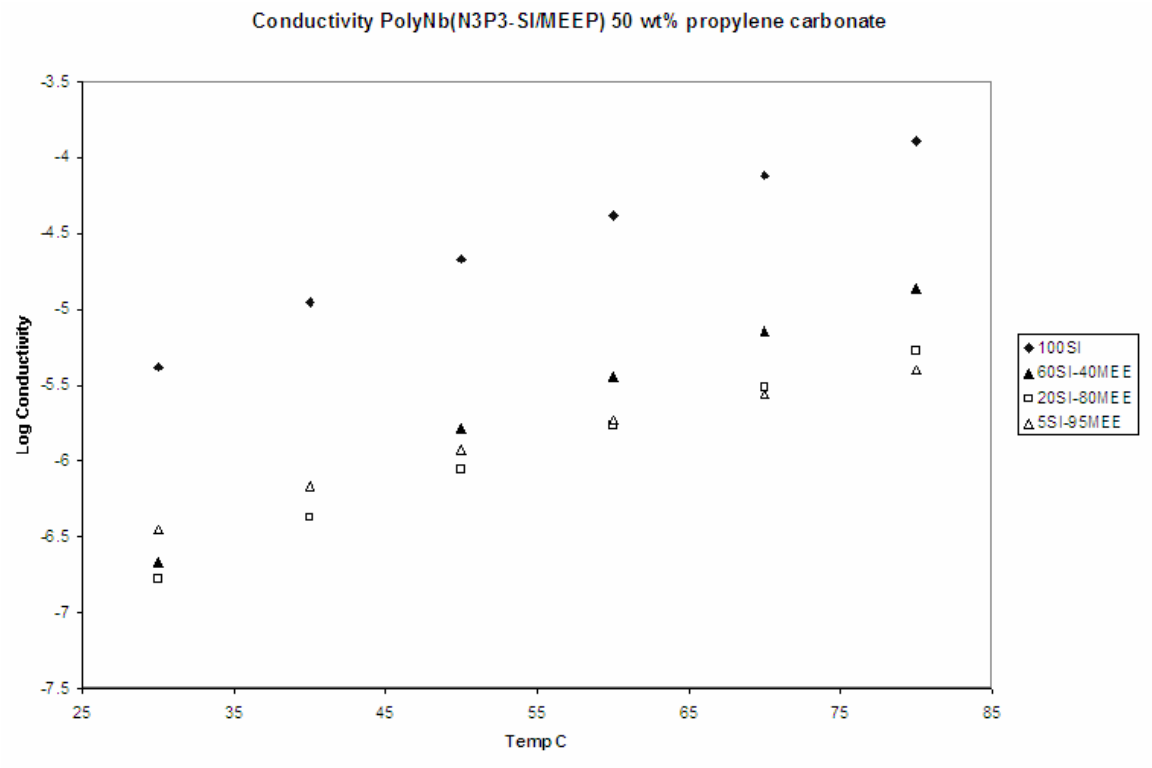

Figure C-2. Conductivity in (S/cm) of polyNb(N_3P_3-SI/MEE) 50 wt% propylene carbonate.

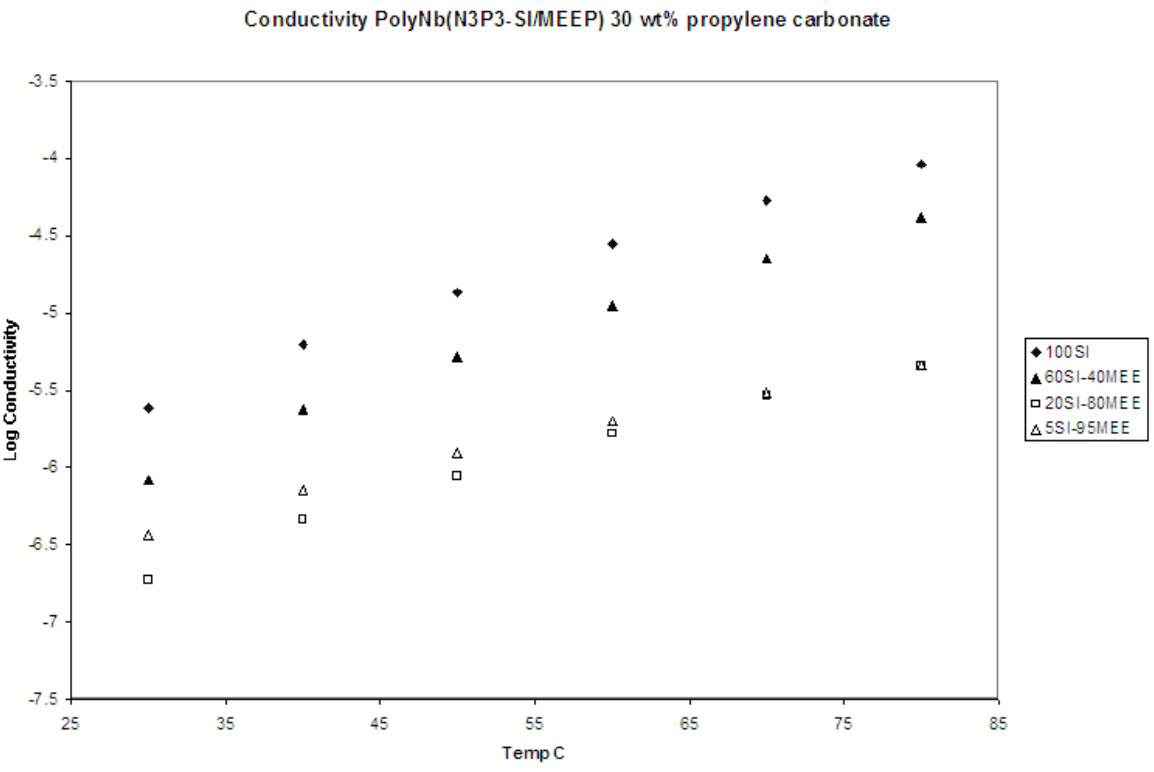

Figure C-3. Conductivity in (S/cm) of polyNb(N_3P_3-SI/MEE) 30 wt% propylene carbonate.

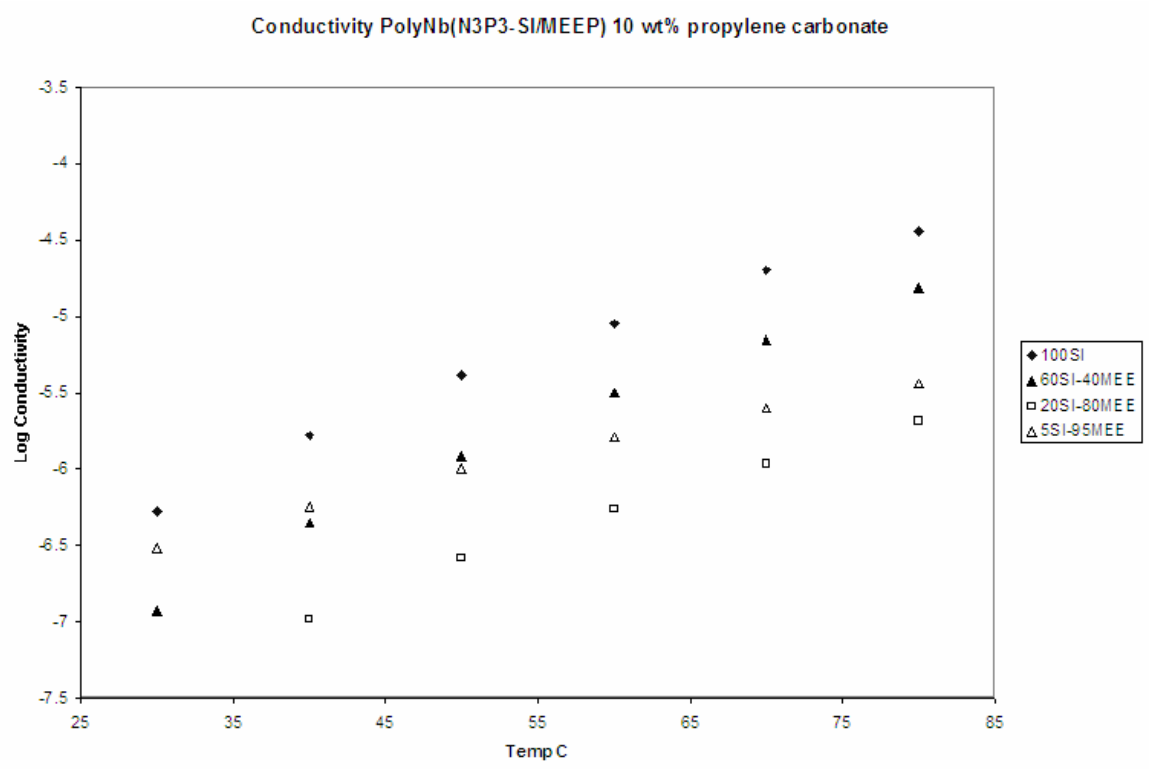

Figure C-4. Conductivity in (S/cm) of polyNb(N_3P_3-SI/MEE) 10 wt% propylene carbonate.

polymeric material (T_gs = -50 to 70 ºC). However, after the addition of the propylene carbonate plasticizer, the materials became flexible and adhesive. Lithium ions can then migrate through the polymer matrices and give rise to increased conductivity.

2. Influences on Conductivity in a Norbornene/Phosphazene Polymer

As illustrated in Figure C-2, the conductivity increases directly with increasing temperature and increased incorporation of lithium via the higher loading of sulfonimide side groups. The polymer with pendent groups containing only bound aryl sulfonimide groups (100SI) produced conductivities an order of magnitude greater than polymer (60SI-40MEE) which produced the second highest conductivity tested. The salt is fully solvated in all the polymers leading to a direct relationship between salt concentration and conductivity. The 5% SI has a slightly higher conductivity at room temperature then the 20 and 60% SI, this is caused by the increased free volume in the system. The 5% SI conductivity is exceeded at higher temperatures when the free volume in the 20 and 60% SI samples increased which allowed the larger amount of lithium ions in these materials to work more efficiently and raise the conductivity. This leads us to believe the number of lithium ions in a polymer to be the key factor in polymer systems with similar levels of ion solvating etheric oxygen atoms.

Figure C-3 shows the increasing levels of conductivity with increasing temperature with the same trends described for Figure C-2. The polymers that contained smaller amounts of plasticizer (30 wt% pc) produced lower conductivities with the exception of the 60% SI which produced the highest conductivity for that lithium ion

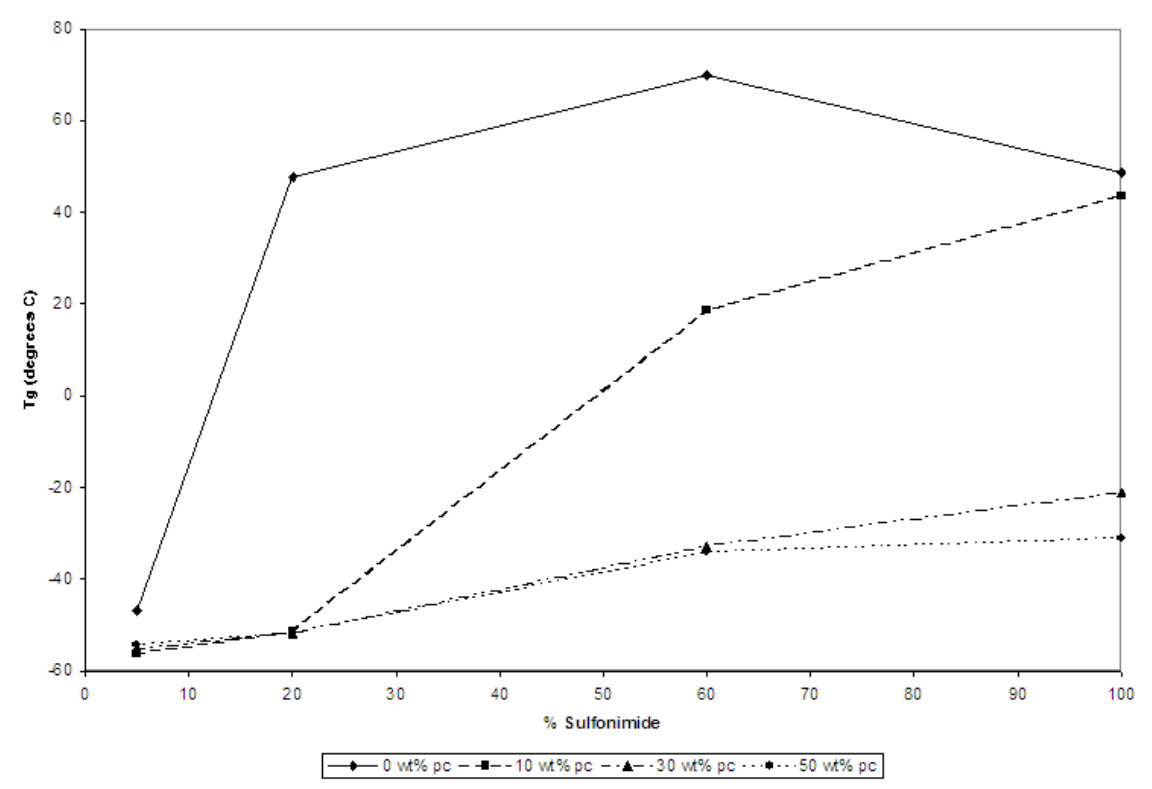

Figure C-5. Graph of glass transition temperatures.

loading level with 30 wt% of propylene carbonate. We attribute this increase to the finding an optimal balance of lithium ions to lithium solvating groups for this material. The 50 wt% propylene carbonate of Figure C-2 only served to dilute the lithium ion loading of this material and the 10 wt% was not sufficiently solvating for that lithium ion loading.

From these data we conclude that the high concentration of lithium, incorporated via the sulfonimide side groups (up to five lithium atoms per repeat unit), is the most important requirement for high conductivity. However, plasticizer additives, self-plasticizing side groups such as methoxyethoxyethoxy units, and higher temperatures increase the free volume in the system and allow lithium ions to migrate through the polymer at an increased rate, thus increasing the conductivity.

3. Role of Glass Transition Temperature

The glass transition temperatures of the unplasticized polymers are near -50 ºC when 5 % of the side groups are sulfonimide units. This probably reflects the internal reorientational mobility of the methoxyethoxyethoxy side groups. Intermediate levels of sulfonimide raise the Tg to ~70 ºC mainly by offsetting the internal-plasticization by the methoxyethoxyethoxy side groups and increasing the interpolymer coordination between sulfonimide groups via the lithium cations. The highest concentrations of sulfonimide groups linked to the polymer (100% SI) reduced the interpolymer coordination and decreased the Tg slightly to around 50 ºC. Increased lithium content leads to increased

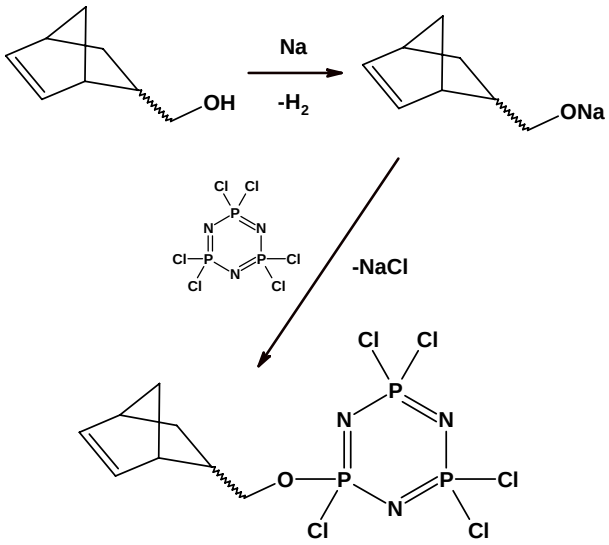

Scheme C-1. Norbornene-pendent-pentachlorocyclotriphosphazene monomer synthesis.

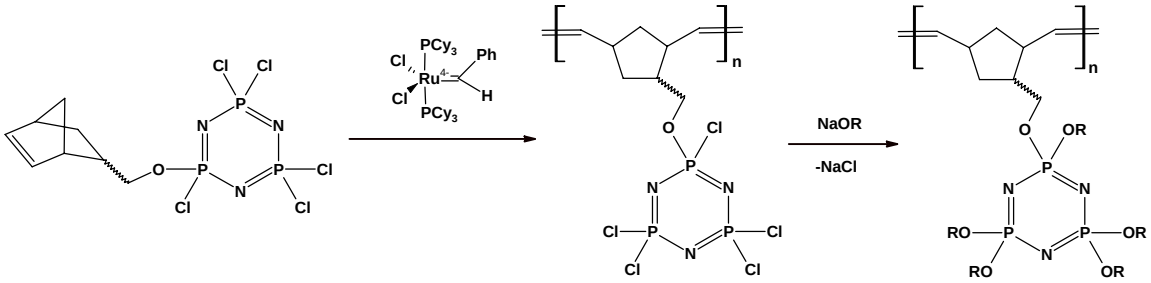

Scheme C-2. Poly(norbornene-pendent-pentachlorocyclotriphosphazene) synthesis.

conductivity as interpolymer coordination is reduced. Further reduction of the glass transition temperatures might be accomplished by the incorporation of more flexible cyclotetraphosphazene pendent groups or linear phosphazene oligomeric pendent units. The polynorbornene backbone serves mainly to provide a flexible, tough film morphology and a good platform for the functional groups.

4. Advantages of a Single-Ion Conductive Polymer

When single-ion conductive polymers are compared to similar polymers that utilize an unbound lithium source of $LiN(SO_2CF_3)_2$ we see that unbound ions offer increased conductivity (Table C-1). No Tg's were observed in the unbound $LiN(SO_2CF_3)_2$ salt poly(norbornene-pendent-phosphazene) analogues reported in literature.[6] Small differences in conductivity were also observed in linear type polyphosphazenes containing bound and unbound lithium sources.[7] We attribute the lower level of conductivity in our materials to increased steric hinderance of the sulfonimide group attached the phosphazene pendent and the absence of a mobile anion source. Our polymer conductivity of 100% SI matched the maximum values of the non-bound anion system described in literature.[6] The ability of the two different salt systems to retain function over an extended use lifetime may favor the system with the most components bound to the backbone. This would minimize the loss of lithium and plasticizing components to phase separation or volatilization from the polymer membrane.

C. Conclusions

Polymers that contain covalently bound anions (like the aryl sulfonimide) can allow higher levels of lithium cation incorporation without precipitation when compared to polymers "doped" with free lithium salts. For the polymers described here, the polynorbornene backbone provided good structural integrity compared to linear polyphosphazenes that bear both sulfonimide and methoxyethoxyethoxy side groups. We believe that the increased structural integrity is directly related to the increased steric hinderance provided by the pendent units along the polynorbornene backbone. Modest levels of plasticization by the addition of propylene carbonate (10 wt %) removed all brittleness and yielded gel-type materials that were adhesive and flexible. The conductivities of 10^{-4} S/cm in this system provide encouragement for the view that the increased free volume provided by other polynorbornene/phosphazene polymers may give useful conductivities without the addition of organic small molecule plasticizers. Bound component polymer systems exhibit reduced conductivities when compared to their non-bound analogues with the same lithium ion loading. However, they are a technological step forward in conductive membrane design because of their increased use of bound components and their increased lithium loadings. Bound components were used to increase free volume and increase salt loadings of our ion conductive polymers. By utilizing bound component systems devises may be produced that have little component loss to phase separation or ion leaching from the polymer membrane.

D. Experimental

1. Characterization Equipment

All manipulations were carried out under an atmosphere of dry nitrogen using standard Schlenk line techniques. ^{31}P and ^{1}H NMR spectra were recorded on a Bruker AMX360 spectrometer operated at 146 and 360 MHz, respectively. Chemical shifts are reported in ppm relative to the deuterated solvent resonances. Gel permeation chromatograms were obtained using a Hewlett-Packard HP 1090 gel permeation chromatograph equipped with two Phenomenex Phenogel linear 10 columns and a Hewlett-Packard 1047A refractive index detector. Data collection and calculations were accomplished with use of a Hewlett-Packard Chemstation equipped with Hewlett-Packard and Polymer Laboratories software. The molecular weights and polydispersities are reported versus monodisperse polystyrene standards. Differential scanning calorimetry was performed using a Perkin-Elmer DSC-7 differential scanning calorimeter controlled by a PE7500 computer. Polymer samples were heated from -100 to 120 °C under an atmosphere of dry nitrogen. Heating rates of 5-10 °C/min and sample sizes of 10-20 mg were used. Conductivity measurements were made using a Hewlett-Packard 4192A LF impedance analyzer at a potential of 0.1 V with an alternating frequency range of 800 Hz to 1 MHz. The samples were placed between platinum electrodes separated by a Teflon spacer. The platinum electrode containing the sample was compressed between aluminum blocks held in a Teflon fixture. Electrical leads were attached between the impedance analyzer and aluminum blocks. All conductivity measurements were carried out at variable temperatures under an atmosphere of dry argon.

Polymer	Ion Source	Li:O:N ratio			Conductivity 10^{-5} S/cm		
					30 ºC	60 ºC	80 ºC
Poly(Nb-PN) MEE (1.0)*	30mol% $LiN(SO_2CF_3)_2$	1.0	17.3	3.5	2.2	11.5	26.3
Poly(Nb-PN) MEE (1.0)*	40mol% $LiN(SO_2CF_3)_2$	1.0	14.0	2.9	2.1	13.6	32.0
Poly(Nb-PN) MEE (0.8) SI (0.2) w/ 50 wt% propylene carbonate	20% -$OPhSO_2N(Li)SO_2CF_3$	1.0	21.0	4.0	0.02	0.2	0.5
Poly(Nb-PN) MEE (0.8) SI (0.2) w/ 30 wt% propylene carbonate	20% -$OPhSO_2N(Li)SO_2CF_3$	1.0	19.3	4.0	0.2	0.2	0.5
Poly(Nb-PN) MEE (0.8) SI (0.2) w/ 10 wt% propylene carbonate	20% -$OPhSO_2N(Li)SO_2CF_3$	1.0	18.3	4.0	n/a	0.1	0.2

*****conductivity data from Allcock et al. *Macromolecules* **2001**, 34, 787-794.

Table C-1. Lithium, oxygen, and nitrogen ratios and conductivity of poly(norbornene-pendent-phosphazene) polymers .

2. Sulfonimide Synthesis

The sulfonimide group was synthesized using standard literature procedures.[4] $MeOPhSO_2Cl$ (25g 0.1209mol) and $CF_3SO_2NH_2$ (20g 0.1526mol) were dissolved in 250mL of acetone. Triethylamine (40mL 0.2870mol) was added drop-wise to this solution while the solution was stirred at 25 ºC for 48 hours. The solid product, $MeOPhSO_2N(Et_3N:)SO_2CF_3$, was isolated by removal of the solvent via distillation. The solid was dissolved in 1M HCl (250 mL) and was extracted with three washes of CH_2Cl_2 (250mL each). The organic layer was isolated and dried over sodium sulfate, then filtered through a glass frit. The solvent was removed by distillation. The solid product, $MeOPhSO_2N(Et_3N:)SO_2CF_3$, was then dissolved in methanol (150 mL) and $LiOCH_3$ (120 mL of 1M in methanol) was added and stirred at 25 ºC for 1 hour. The solid product, $MeOPhSO_2N(Li)SO_2CF_3$, was then isolated by distilling off the solvent. The $MeOPhSO_2N(Li)SO_2CF_3$ was dissolved in DMF (150 mL), and sodium ethanethiol (30g 0.3566mol DMF) was added and the mixture was stirred at reflux for 3 hours. The tan colored solid, $LiOPhSO_2N(Li)SO_2CF_3$, was isolated by distillation of DMF and drying for 3 days in a vacuum oven. This solid was then dissolved in an aqueous sodium chloride solution (250 mL water and 250 mL NaCl), and residual DMF was extracted by two THF washes (500 mL each). The water layer with a pH of 3 was prepared by the addition of HCl (25mL). The sulfonimide was then extracted with three THF washes (250 mL each) and was isolated by distillation of THF from the solid white product.

3. Norbornene-Pendent-Pentachlorocyclotriphosphazene Synthesis

The monomer was prepared using procedures similar to those described recently in the literature.[5] 5-Norbornene-2-methanol (65g 0.5234mol) was added drop-wise to a stirred solution of potassium tert-butoxide (60.55g 0.5234mol) in THF (1200 mL) at -78 ºC (isopropanol/ CO_2 bath) and allowed to warm to 25 ºC over 12 hours. This salt solution was then added drop-wise to a solution of hexachlorocyclotriphosphazene (260g 0.7477mol) in THF (1300 mL) at -78 ºC (isopropanol/ CO_2 bath) and allowed to warm to 25 ºC over 12 hours. The product was isolated by distilling off the THF. The product was dissolved in ether (600 mL) and washed with water (600 mL each) three times. The organic layer was dried over $MgSO_4$, filtered, and concentrated by distillation of the ether. Excess phosphazene cyclic trimer was then removed by sublimation (40 ºC 72 hours) to yield 162.54g (71.3%) of norbornene-pendent-pentachlorocyclotriphosphazene.

4. Catalyzed Polymerization of the Monomer

Mono(5-norbornene-2-methoxy)pentachlorocyclotriphosphazene (60g 0.1378mol), prepared as described in the literature,[5] was dissolved in CH_2Cl_2 (300 mL). The solution was stirred at 25 ºC, as Grubb's catalyst (1.134g 0.0016mol) dissolved in CH_2Cl_2 (30 mL), was injected via syringe as quickly as possible. The monomer was allowed to react for 20 seconds until a visible increase in viscosity had occurred. At that time ethylvinyl ether (1 mL) was injected to terminate the polymerization.

5. Chlorine Replacement Reaction

All the organic-modified polymers were synthesized in the same manner using portions of the same polymerized reactive polymeric intermediate. Only the ratio of aryl sulfonimide to methoxyethoxyethoxy groups was varied. The following procedure was followed for the 5% sulfonimide 95% methoxyethoxyethoxy compound. Potassium tert-butoxide (0.25g 0.002mol) was dissolved in THF (500 mL) and $HOPhSO_2N(Na)SO_2CF_3$ (0.726g 0.0022mol) was added and the mixture was stirred for 12 hours at 25 ºC to yield $KOPhSO_2N(Na)SO_2CF_3$ in solution. Separately, potassium tert-butoxide (4.985g 0.0444mol) was dissolved in THF (500 mL), and methoxyethoxyethanol (5.33g 0.0444mol) was added and the mixture stirred for 12 hours at 25 ºC to yield $KOCH_2CH_2OCH_2CH_2OCH_3$ in solution.

A fraction of the polymer solution containing poly(norbornene-2-methoxy-pendent-pentachlorocyclotriphosphazene) (3.86g) in CH_2Cl_2 (8mL) was diluted in THF (500 mL) and the $KOPhSO_2N(Na)SO_2CF_3$ (0.002mol) reagent solution was added and the mixture was stirred at reflux for 12 hours. At this time a 5% shift of the P-Cl peak in the ^{31}P NMR spectrum of the unsubstituted polymer had occurred to generate a multiplet at 18.5 ppm, which was consistent with previous studies.[5] The $KOCH_2CH_2OCH_2CH_2OCH_3$ (0.0444mol) solution was then added and the mixture was stirred for 48 hours at reflux, by which time full chlorine replacement was confirmed by a ^{31}P NMR shift to a 18.5 ppm multiplet in Figure C-1. The gel permeation chromatogram contained a single peak with a Mn of 129,000 and a Mw of 258,000, and with a polydispersity index of 2.003.

E. References

(1) Allcock, H. R.; Napierala, M. E.; Cameron, C. G.; O'Connor, S. J. M. *Macromolecules* **1996**, *29*(6), 1951-1956.

(2) Allcock, H. R.; Ravikiran, R.; O'Connor, S. J. M. *Macromolecules* **1997**, *30*(11), 3184-3190.

(3) Allcock, H. R.; Laredo, W. R.; Kellam, E. C., III; Morford, R. V. *Macromolecules* **2001**, *34*(4), 787-794.

(4) Hofmann, M. A.; Ambler, C. M.; Maher, A. E.; Chalkova, E.; Zhou, X. Y.; Lvov, S. N.; Allcock, H. R. *Macromolecules* **2002**, *35*(17), 6490-6493.

(5) Stone, D. A.; Allcock, H. R. *Macromolecules* **2006**, 39(15), 4935-4937.

(6) Allcock, H. R.; Laredo, W. R.; Kellam, E. C.; Morford, R. V. *Macromolecules* **2001**, 34, 787-794.

(7) Allcock, H. R.; Welna, D. T.; Maher, A. E. *Solid State Ionics* **2006**, 177, 741-747.

VITA

Lee Brent Steely

Lee Brent Steely, son of Kenneth and Ruth Steely of Fayetteville, PA was born June 2nd, 1979 in Chambersburg, PA. He graduated from the Cumberland Valley Christian School in 1998 as Valedictorian of his class and with membership in the National Honor Society. He then received a Provost scholarship to attended Messiah College in Grantham, PA where he graduated *cum laude* with a Bachelor of Science degree in Chemistry in May 2002 with membership in the Sigma Zeta Honor Society. Lee began his graduate studies at the Pennsylvania State University under the guidance of Professor Harry R. Allcock in August of 2002. While there he received a Roberts graduate fellowship and a travel award from the department of chemistry.